Master Thesis in Geosciences

Basement – cover relationships in the Bodø area

The "basement" rocks in the Heggmovatn and Bodø areas: a Fennoscandian, Laurentian or suspect terrane?

Nana Yaw Agyei - Dwarko

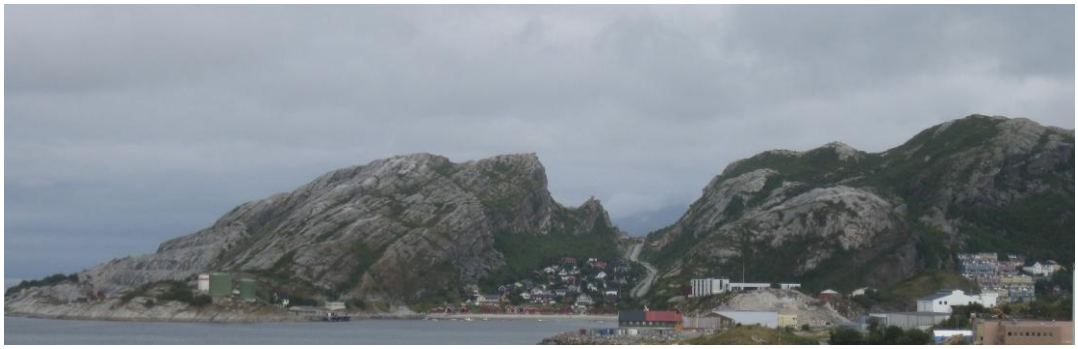

UNIVERSITY OF OSLO

FACULTY OF MATHEMATICS AND NATURAL SCIENCES

Basement – cover relationships in the Bodø area

The "basement" rocks in the Heggmovatn and Bodø areas: a Fennoscandian, Laurentian or suspect terrane?

Nana Yaw Agyei - Dwarko

Master Thesis in Geosciences

Discipline: Tectonics, Petrology and Geochemistry

Department of Geosciences

Faculty of Mathematics and Natural Sciences

UNIVERSITY OF OSLO

1st June 2010

Tutor(s): Professor Arild Andresen

This work is published digitally through DUO – Digitale Utgivelser ved UiO

http://www.duo.uio.no

It is also catalogued in BIBSYS (http://www.bibsys.no/english)

Acknowledgements

This thesis has been supervised by Professor Arild Andresen. Arild took me up to Bodø and went to great lengths to familiarize me to the regional geology before I started independent work for this thesis. We have had several stimulating and exciting talks about the problems (some of which are still unsolved) we have been working on, on this project. His relaxed leadership style has been most beneficial to me as a student. Arild has been of great help to me both academically and socially. There is quite a lot to thank him for.

I am grateful to Lars Augland who took time of his field work to see how I was coping in the field. Lars has also been very helpful and has always been willing to share his knowledge of geochronology with me.

I am also grateful in general to the staff at the institute who helped me with the analytical work at various stages during this thesis particularly, Berit Berg, Siri Simonsen and Muriel Erambert.

I am also heavily indebted to the Ahenkorah family who have made my stay in Oslo these past two years quite pleasant.

And finally, to my wife Gifty, thank you for everything….. You're the best!!

Table of Contents

Abstract

Most maps and publications dealing with the geology of the Bodø-Sulitjelma area have postulated the presence of a major basement culmination, the "Heggmovatnet basement dome", between Bodø and Fauske. Granitic gneisses and orthogneisses which dominate region west of Bodø, have also been considered to be comparable with basement rocks exposed in the Tysfjord and Glomfjord culminations of ~ 1.8 Ga.

Whereas orthogneisses are abundant in the Tysfjord and Glomfjord culminations, the Heggmovatn area dominated by alternating metapsammites and metapelites which are intruded by both pre- and syn/post-tectonic granitoids. U-Pb ages on zircons from the syn/post-tectonic leucogranites indicate a mid-Silurian (~431Ma) emplacement age whiles Neoproterozoic ages (924 – 928 Ma) are recorded in the orthogneisses in both Bodø and Hegmmovatn units indicating Grenvillian/Sveconorwegian magmatic activity which has not been previously recorded in this area. The lithologic differences between the Heggmovatnet supracrustals and related intrusives, and the nearby basement culminations, as well as the marked differences in ages indicate that neither the Bodø gneisses nor the Heggmovatn units are Baltic basement rocks.

In addition to lithologic differences between the Heggmovatn metasediments and Krummedal Sequence of the East Greenland Caledonides, the obtained data constrains the period of deposition of the Heggmovatn metasediments to be between 1138 – 928 Ma which is remarkably similar to the 1100 – 930Ma depositional age of the Krummedal Sequence. The similarities in clastic zircom populations as well as the ages of their associated intrusives suggests very strongly that the Heggmovatn metasediments represent an exotic thrust sheet closely related to the Krummedal Sequence.

The obtained data strengthens the interpretation that the Uppermost Allochthon in the Scandinavian Caledonides represents a fragment of Laurentia crust.

1. Introduction

1.1 Purpose of study

This thesis focuses on basement – cover relationships in the western part of the Bodø – Sulitjelma transect (Fig 1.1). The principal objective is to map and constrain the development of the Caledonian orogen in the area and to compare the geology of this part of the Caledonian orogen with the geology of Northeast Greenland.

Of particular interest is the nature of the basement – cover contact, as well as the relationship between the basement rocks in the western Bodø area and the so called "Heggmovatn basement dome" which has been interpreted in several maps and publications as a major basement culmination.

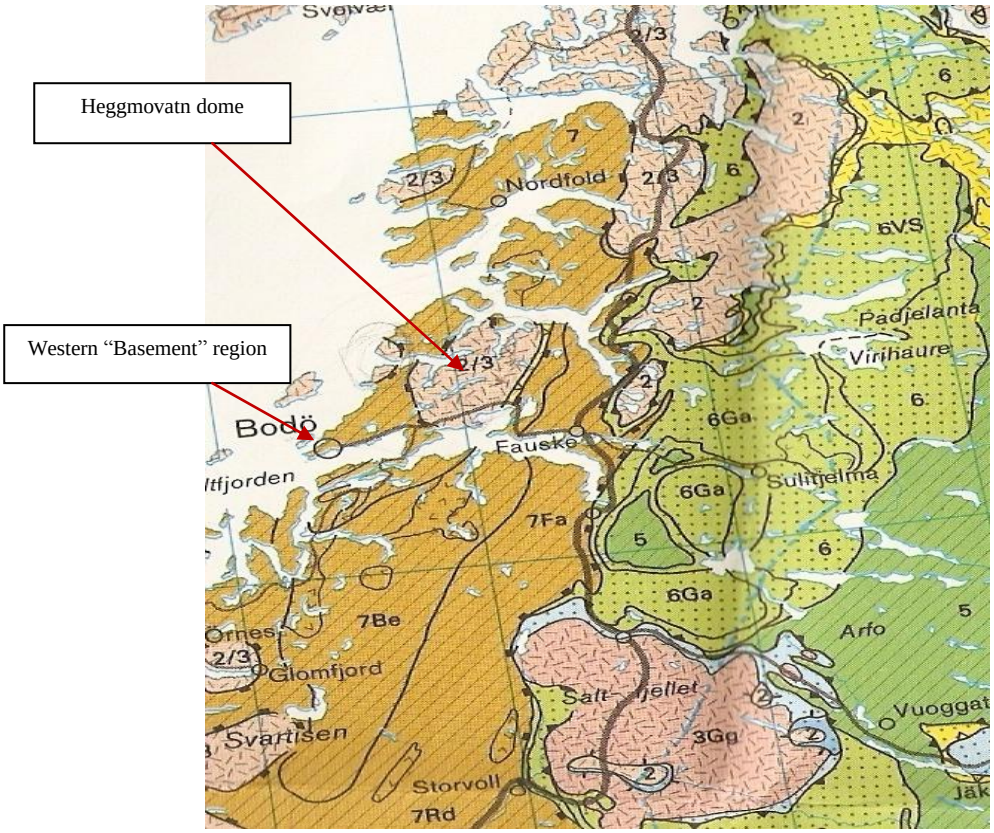

Fig 1.1 Simplified tectonic map of the Central Scandinavian Caledonides showing study area. From Gee and Sturt, 1985

The metamorphic condition of the various lithotectonic units in both the basement and cover sequence will also be examined. Field observations and geochronology of the key lithotectonic units are the main basis for interpreting the geological evolution of the study area.

1.2 Geological setting

The rocks of the Caledonian – Appalachian orogen are exposed today, on opposite sides of the North Atlantic Ocean. They are present on the eastern margin of North America and in the British Isles, eastern Greenland, western Scandinavia and the Svalbard archipelago. The Caledonian fold and thrust belt in Scandinavia extend for almost 2000km along the length of Norway. The Norwegian Caledonides comprise an Archean to Paleoproterozoic autochthonous/parautochthonous basement with a Neoproterozoic to Early Paleozoic sedimentary cover sequence derived from the Baltic shield, and a series of overlying Caledonian thrust sheets comprising Mesoproterozoic, Neoproterozoic and Cambro - Silurian metasediments as well as several intrusive units of variable age into this sequence (Gee and Sturt, 1985). The thrust sheets are subdivided into four major tectonic units; the Lower, Middle, Upper and Uppermost Allochthons. The Upper and Uppermost Allochthons are considered to be exotic with respect to Baltica (Roberts and Gee, 1985).

The rocks in the study area were thought to belong to the autochthonous Baltic basement, and the metasedimentary Bodø Group which is a part of the structurally highest of the thrust sheets, called the Uppermost Allochthon. A detailed description of the geological setting in presented in the next chapter.

1.3 Field area

The field area is located on the Bodø peninsula in central Nordland. Detailed field mapping was conducted between latitudes 67°17’30” and 67°19’30” and between longitudes 14°22’30” and 14°29’30”. Reconnaissance traverses were also taken in the Mjelde – Kjerringøy area north of this as well as the Heggmovatn area.

1.4 Logistics and Support

Field work was conducted in July and August of 2009. The trip from Oslo to Bodø was on 11th July and the return trip to Oslo was on 12th August 2009, totaling 32 days of field work.

The first three days of the field work was conducted from a camp in Geitvagen, after which I was accommodated at Flatvold, a residence on the outskirts of Bodø owned by the Bodø University College for the rest of the time.

Maps used for the fieldwork were copies of the original 1:50000 map by Gustavson, 1991 of Bodø published by the NGU blown up to 1:25000. A 360° Silva compass was used to measure the strike and dip of planar structures and the trend and plunge of linear structures. A GPS was used to record the coordinates and altitudes of geological localities.

1.5 Field Methods

Fieldwork was done using traditional methods. Traverses were taken to cover as much ground as possible and in sufficient detail. Both large and small scale photos were taken for documentation. Samples were taken from several lithological units and for petrographic descriptions and potentially, geochronological and geothermobarometric determinations. Thin sections of the samples were made at the Museum of Natural History in Toyen, Oslo.

1.6 Geochronology and Geothermobarometry

Both ID-TIMS and LA-ICPMS dating techniques available at the Department of Geosciences at the University of Oslo were used to date zircons. Although all samples were crushed and processed for dating by myself, actual ID-TIMS dating was carried out by Lars Augland, a PhD candidate at the University of Oslo whose study area is immediately south of Bodø. LA-ICPMS dating of clastic zircons from the metapsammites was carried out on selected samples to obtain ages of some of the more important lithotectonic units. A detailed description of the methodology is presented in chapter 5.

Thin - sections were studied by use of an optical microscope. Further analysis of selected thin -sections was conducted using an electron microprobe available at the Department of Geosciences.

Metamorphic conditions of selected samples were estimated using the garnet – biotite geothermometer (Holdaway, 2000), the garnet – biotite – plagioclase – quartz geobarometer (Wu et al., 2004) and the hornblende – garnet – plagioclase - quartz geothermobarometer (Dale et al., 2000).

2. Tectonic Setting

2.1 Regional Geology and Geological Setting

The Caledonian orogeny is recorded in the northern parts of the British Isles, eastern Greenland, western Scandinavia and the Svalbard archipelago (Fig 2.1). The orogen is the result of the collision between the Laurentian and Baltica plates in the Early Paleozoic. The collision resulted in Laurentia (as well as oceanic terranes deriving from the Iapetus ocean) being thrust upon the Baltic basement (with its sedimentary cover) and accompanying closure of the Iapetus sea which previously separated them.

The Scandinavian Caledonides consists of numerous thrust sheets of diverse rock associations, produced by broadly southeastward - directed transport (Gee, 1978), and include rock associations derived from island arcs and oceanic crust (ophiolites) from the Iapetus ocean as well as from Laurentia.

Many of these nappes are thrust over high grade gneissic and granitoid rocks of the Baltic shield which are generally considered to be of Precambrian age. The nappes contain diverse rock assemblages of disparate origins that developed during a series of tectonic events generally believed to have occurred in the Early Palaeozoic (Roberts, 2003).

As the data presented in this thesis are interpreted to be derived from Laurentia, a brief overview of the east Greenland Caledonides as well as the Scandinavian Caledonides will be given.

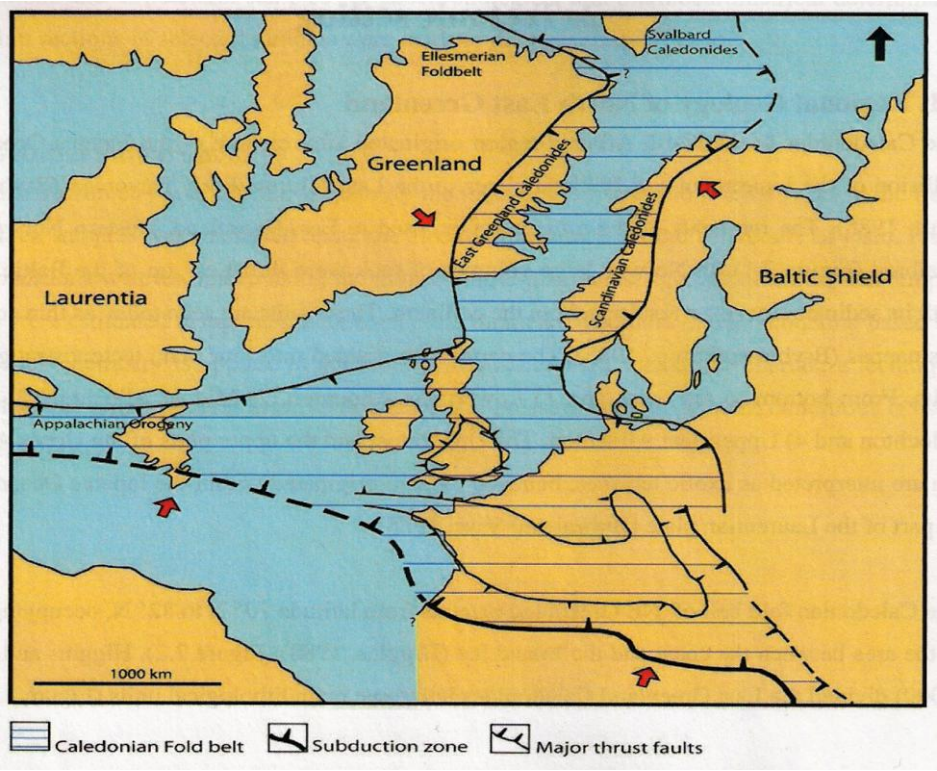

Fig 2.1 Modified reconstruction of the Caledonian – Appalachian orogen prior to the opening of the North Atlantic Ocean. Based on Gee and Sturt (1985) and Cocks and Torsvik (2002).

2.2 Regional Geology of Western Scandinavia

In Scandinavia, the Caledonian mountain chain, with many peaks reaching a little over 2000m, extends for nearly 2000 km along the length of Norway; they include substantial regions of western Sweden and the highest parts of northwestern Finland. (Gee, 2005)

The units which were thrust onto the Baltic shield with its Neoproterozoic to Lower Paleozoic cover deposits are divided into four main tectonostratigraphic units and are bounded by broadly west dipping shear zones (Roberts and Gee, 1985). These are from bottom up;

- Lowermost Allochthon
- Middle Allochthon
- Upper Allochthon
- Uppermost Allochthon

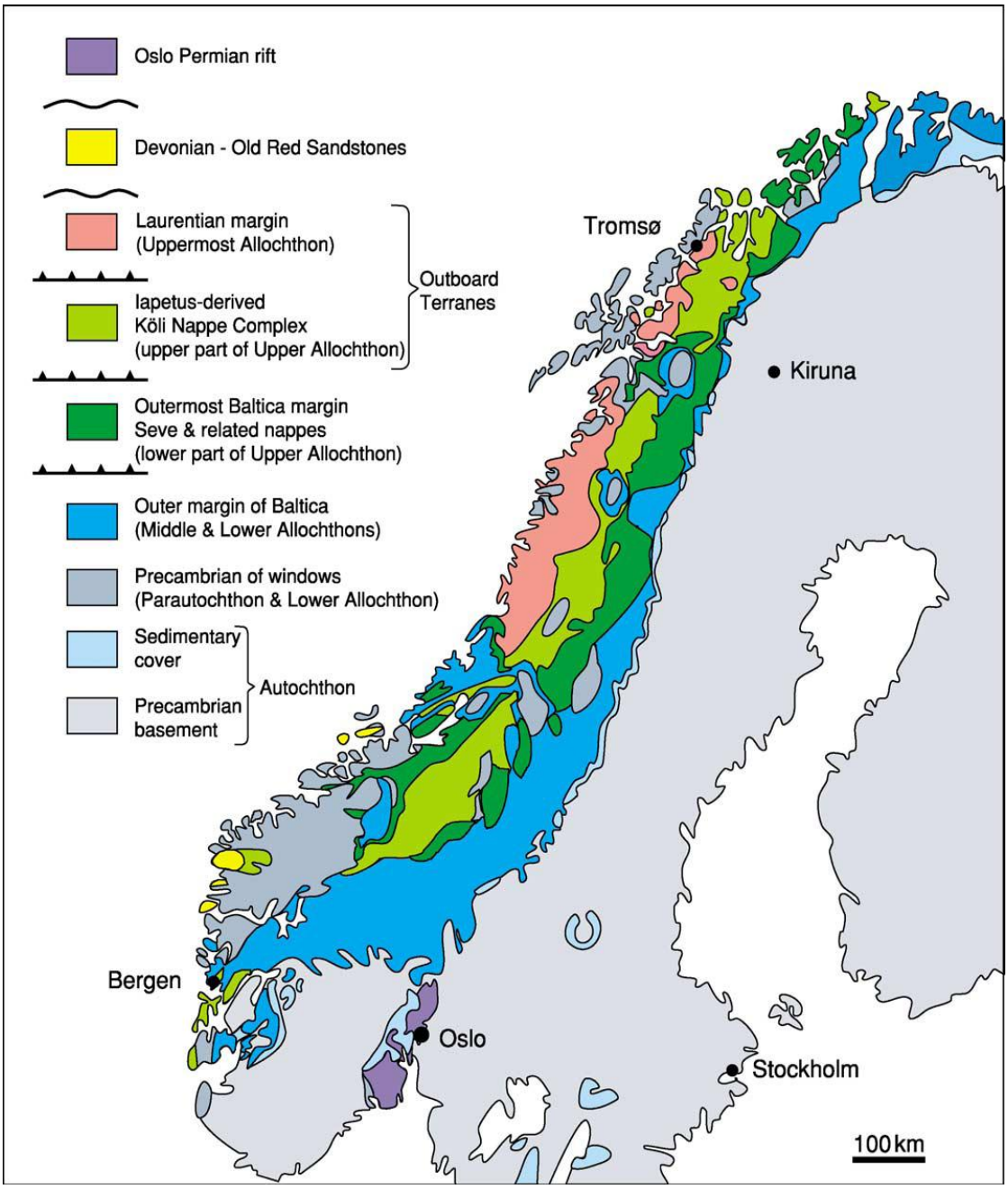

Fig 2.2 The Scandinavian Caledonides. Reproduced from Gee (2005)

2.2.1 The autochthonous/parautochthonous basement

Within the Scandinavian Caledonides, the term basement is issued to refer to the high grade crystalline rocks belonging to the Precambrian crust of the Baltic shield. They structurally underlie a thin autochthonous Neoproterozoic to Lower Paleozoic cover sequence and have several intrusive units within them (Sturt and Austrheim, 1985). The term parautochthon is

used in the western part of the orogen where the rocks beneath the lower Allochthon are disturbed but still comparable to the autochthon.

These rocks form the foreland of the orogen and are well exposed in southwestern Norway. They also outcrop further in the hinterland from the foreland in a series of antiformal windows within the Caledonian nappes and comprise a wide variety of rocks.

In northern Scandinavia, the basement is composed of gradually younger units from the northeast to the southwest. The northeastern part of the Baltic Shield is composed of a Late Archean Domain (3.1–2.6 Ga) and an early Svecofennian supracrustal sequence (2.6–2.1 Ga) (Skår, 2002). Rocks of the Trans-Scandinavia-Igneous Belt (TIB) composed of alkali-calcic, mafic to acid rocks with I- and A-type characteristics intrude the Svecofennian domain (Skår, 2002).

The oldest rocks within the Svecofennian domain are exposed in the Lofoten - Vesteralen area and are dominantly calc- alkaline intermediate volcanic rocks dated at about 2.70 Ga and intruded by granodioritic to granitic rocks at about 2.60 Ga. (Skår, 2002). Supracrustal rocks were deposited in the time interval from 2.10 to 1.83 Ga when the rocks were metamorphosed in amphibolite and granulite facies. After the regional metamorphism, there were emplacement of large volumes of anorthosite, mangerite, charnockite and granite (AMCG) between 1.80 and 1.70 Ga (Griffin et al., 1978). Recent work shows that the AMCG suite was emplaced during two distinct short – lived events at about 1870Ma and 1800 – 1790Ma (Corfu, 2004).

The basement rocks present in southern Scandinavia today are generally deformed and metamorphosed and are largely as a result of two orogenic/magmatic episodes; the Gothian (1700 – 1500Ma) and the Sveconorwegian (1130 – 900Ma). They occur in a large area in southern Norway and the adjacent part of southern Sweden west of the TIB. (Andersen, 2005)

Early workers recognized basement rocks in the Heggmovatn dome and the islands west of the Bodø peninsula, my study area. It is considered as part of the Tysfjord basement and is thought to be autochthonous to parautochthonous (Roberts and Gee 1985; Stephens et al. 1985). Granitic gneisses occurring on Hjartoy, west of Bodø and Bratten on the Bodø peninsula were initially interpreted by Rutland and Nicholson (1965) to be part of the autochthonous basement, and later considered them to be outliers of the Beiarn nappe (which is regarded as part of the Uppermost Allochthon) (Rutland and Nicholson, 1969). These gneisses were later mapped by Gustavson (1991) as belonging to the autochthonous basement. Gustavson (1991)

placed the contact between this basement (and its thin cover) and the thrust sheet to the east, as a thrust fault. These gneisses are intruded by late quartz and pegmatite veins (Rutland and Nicholson, 1965).

2.2.2 The Lower and Middle Allochthons

Rocks of the Lower and Middle Allochthons have clear affinities to the Baltic craton (Gee and Sturt 1985; Roberts and Gee, 1985). They are composed of rocks thought to be shelf and continental rise sediments derived from the Baltoscandian margin in the Neoproterozoic and their associated underlying crystalline basement (Grenne et al., 1999; Roberts, 2003). The Lower Allochthon is dominated by low grade sedimentary successions and minor slices of Precambrian crust. The upper parts of the Middle Allochthon have a similar stratigraphy to the lower part; composed of thick Neoproterozoic siliciclastic and carbonate sediments overlain by tillites and sandstones (Nystuen et al., 2008) However, the upper part of the Middle Allochthon (Sarv nappes) is heavily intruded by ca. 600Ma mafic dykes swarms (Gee, 2005). The Lower and Middle Allochthons are imbricated and metamorphosed to greenschist facies (Roberts and Gee, 1985; Bjorklund, 1987).

2.2.3 The Upper Allochthon

This unit is thought to represent outboard, magmatic arc, ophiolitic and marginal basin deposits derived from locations within or peripheral to, the Iapetus Ocean (Stephens and Gee, 1989; Pedersen et al., 1991). The tectonostratigraphic units of the Upper Allochthon are the Køli Nappe (Gee, 1978), the Narvik nappe complex (Steltenpohl and Andresen, 1991; Andresen and Steltenpohl, 1994) , the Ofoten nappe complex, and a lower nappe known as the Seve Nappe which overlies the Sarv Nappe of the Middle Allochthon. It is dominated by psammites, pelites, and subordinate marbles, with numerous amphibolitized dolerites and gabbros and occasional dunites and serpentinites. However, it is usually considered as a suspect terrane which was most likely derived from the outermost edge of Baltica, where the extensive mafic magmatism and solitary ultramafites were concentrated in the transition zone between continental and oceanic crust (Gee, 2005).

2.2.4 The Uppermost Allochthon

This is the most relevant allochthon for the study area and is therefore reviewed in more detail than the preceding thrust sheets. It is structurally highest in the nappe pile and is exposed along the western coast of central Norway and in Troms. It is composed of the most exotic units of the nappe stacks and postulated to be of Laurentian affinity (Stephens and Gee, 1985). It is almost entirely confined to north – central Norway in the counties of Troms, Nordland and part of Nord – Trondelag covering six degrees of latitude over a strike length of more than 700km (Roberts et al.,2007). South of the Tysfjord basement window, it is dominated by two major tectonic units; the Rodingsfjallet Nappe Complex and the overlying Helgeland Nappe Complex (Ramberg, 1967), each of which is composed of several thrust sheets of diverse rock units. The Beiarn Nappe which outcrops north of Mo i Rana was previously thought to be a correlative of parts of the Helgeland Nappe Complex though geographically separated from it (Rutland and Nicholson, 1965) but has been shown by later workers to be more likely, a structurally higher unit within the Rodingsfjallet Nappe Complex (Gustavson and Gjelle, 1991; Gustavson, 1996)

2.2.4.1 Lithostratigraphic successions in the Uppermost Allochthon

The Uppermost Allochthon in Central Norway (Nordland) is dominated by several granitoid batholiths which are intruded into amphibolite facies sedimentary successions of continental affinity (Gee, 2005) and exotic carbonate shelf, slope/rise and evolved magmatic arc assemblages of Laurentian or peri - Laurentian ancestry (Roberts, 2003).

It can be lithologically divided into; abundant supracrustal successions, isolated gneissic basement-like slices and plutonic bodies which are particularly well developed in the Helgeland Nappe Complex (Barnes et al., 1992; Nordgulen et al., 1993).

Melezhik et al., (2002a) report depositional ages of the metasedimentary units to range from Riphean to Early Silurian. The supracrustals are of Late Riphean to Cambrian age and are generally composed of diverse psammitic, pelitic and calcareous schists of medium to high grade, marbles and amphibolites with subordinate quartzites, conglomerates and diamictites as

well as stratabound iron ore formations (Gustavson, 1966; Nicholson and Rutland, 1969; Steltenpohl et al., 1990).

Although metamorphosed carbonate formations (marbles) are not uncommon in most of the major nappes of the Scandinavian Caledonides, they are particularly abundant in the Uppermost Allochthon (Roberts et al., 2007). The carbonate formations are dominated by calcite marbles with dolomite marbles being subordinate (Roberts et al., 2007). Several different age groups based on isotope chemostratigraphy for Neo- and Mesoproterozoic, Late Ordovician – Early Silurian and Cambrian time (Melezhik et al.,2001a; Melezhik et al.,2002b; Sandoy, 2003; Melezhik et al.,2003). Metasedimentary iron ores, some of which are manganiferous, are numerous in the Uppermost Allochthon from the Mosjen area of Nordland to the Tromso district (Roberts et al., 2007). They are most abundant in the Mo i Rana where they are hosted by calcareous mica schists and marbles of the Dunderland Group (Bugge, 1948). The ores vary in P and Mn content although the host rock lithology is fairly uniform and are divided into a lower horizon of magnetite - apatite - carbonate – amphibole with high P content, and an upper horizon of magnetite – hematite – quartz horizon with a lower P content (Bugge, 1948). Grenne et al. (1999) suggest a volcanogenic origin for the P – rich ores due to the presence of amphibole minerals although Bugge (1948) originally a suggested a sedimentary origin for both ore types.

Fragmented ophiolites are present in some of the thrust sheets of the Helgeland Nappe Complex (Nordgulen et al., 1993; Heldal, 2001). The Leka Ophiolite is considered to lie within the lowest structural unit of the Helgeland Nappe Complex (Yoshinobu et al., 2002). A minor felsic sheet within the sheeted dyke unit yielded a U – Pb age of 497 ± 2 Ma (Dunning and Pedersen, 1989). The ophiolite complex is deformed, metamorphosed and unconformably overlain by mafic breccias and conglomerates (Gustavson, 1981).

In the far north, east of Tromso, the lower parts of the Lyngsfjell nappe are dominated by the Lyngen Magmatic Complex and is the largest dismembered ophiolite in the Norwegian Caledonides (Furnes et al., 1985). It is divided into western and eastern suites which are separated by a ductile oceanic shear zone (Furnes and Pedersen, 1995). Based on their geochemical signatures, the western suite is believed to be derived from tholeiites of back – arc basin origin whiles the eastern suite are cumulates crystallized from undepleted, high Ca boninitic magmas similar to those of forearcs (Furnes and Pedersen, 1995). A tonalite body in the eastern suite has yielded a U – Pb zircon age of 469 ± 5 Ma (Oliver and Krogh, 1995).

Granitoid batholiths are abundant in the Uppermost Allochthon. In the Helgeland Nappe Complex, the compositionally varied (Nordgulen et al., 1993) Bindal Batholith includes several plutons and composite intrusive complexes ranging in age from 477 – 430 Ma (Roberts et al., 2007). A regional migmatization event affected rocks in the western part of the nappe complex during which 477 – 468 Ma peraluminous granites were intruded (Yoshinobu et al., 2002). These older plutons (477 – 468 Ma) have isotopic compositions indicating crustal sources (Birkelund et al., 1993). A younger group of plutons was emplaced from 448 to 430 Ma (Nordgulen et al., 1993) and range in composition from olivine gabbros to leucogranites. Another batholithic intrusion is present on large parts of the islands of Smola, Hitra and Froya (about 25km SW of the Bindal Batholith) (Tucker et al., 2004) and is probably correlative to the Bindal Batholith (Roberts et al., 2007).

In the Rodingsfjallet Nappe Complex, granitoids do not occur as batholiths but as dyke swarms that cross – cut the foliation of host rocks, which consist mainly of metasedimentary units interlayered with minor metavolcanic rocks (Bjerkgard et al., 1997). Stephens et al. (1993a) report an age of 447 ± 7 Ma for the dykes based on an Rb – Sr whole rock isochron. Age determinations on granitoid intrusions in the Beiarn Nappe include Rb – Sr whole rock dates of 440 ± 30 for the Hogtind Granite (Torudbakken and Brattli, 1985) and 495 ± 14 Ma for a quartz - monzonitic gneiss at Harefjell (Cribb, 1981). Bingen et al. (2002) report U – Pb ages in the range of 432 – 429 Ma from a granite on an island ~ 5km south of Bodø.

In the northern parts of the Uppermost Allochthon, S- and I- type granitoids are present in the Ofotfjorden area whiles A- type granitoids outcrop in the Snaufjell area (Steltenpohl et al., 2003).

Corfu et al. (2003b) and Selbekk et al. (2000) have described eclogites, eclogitized gneisses and diverse migmatized rocks from the Tromso Nappe.

2.2.5 The Bodø – Sulitjelma Transect

Rocks in this transect have been generally considered to consist of several metasedimentary structural units overlying a region – wide Baltic granitic gneiss basement (Rutland and Nicholson, 1969). Relatively very little recent work involving structural geology, metamorphic petrology and geochronology has been done in this area as compared to other parts of the north Norwegian Caledonides.

Rutland and Nicholson (1969) presented a cross section spanning 100km from Landegode in the west to the Norwegian – Sweden border to the east in which supposed basement granitic gneisses were overlain successively from the top downward, by the Beiarn Nappe complex, the Rodingsfjallet Nappe Complex and the Seve – Kolli Nappe Complex. In this section, both the Heggmovatn and Rishaugfjell are considered to be basement domes.

The description in this section of the thesis is subdivided into western, central and eastern units and largely follows the subdivisions of Rutland and Nicholson (1969). The western unit is of most relevance to the study area and is discussed in more detail than the central and eastern units.

2.2.5.1 Western units

The term western is used here to refer to rocks between Landegode and Fauske (Fig. 2.3A, 2.3B). This unit was described by Rutland and Nicholson (1969) to be composed of basement granitic gneisses on Landegode and Mjelde, outliers of the Beiarn Nappe on Hjartøya and Bratten, the metasedimentary Bodø, Saura and Vagen Groups and the Heggmovatn basement dome.

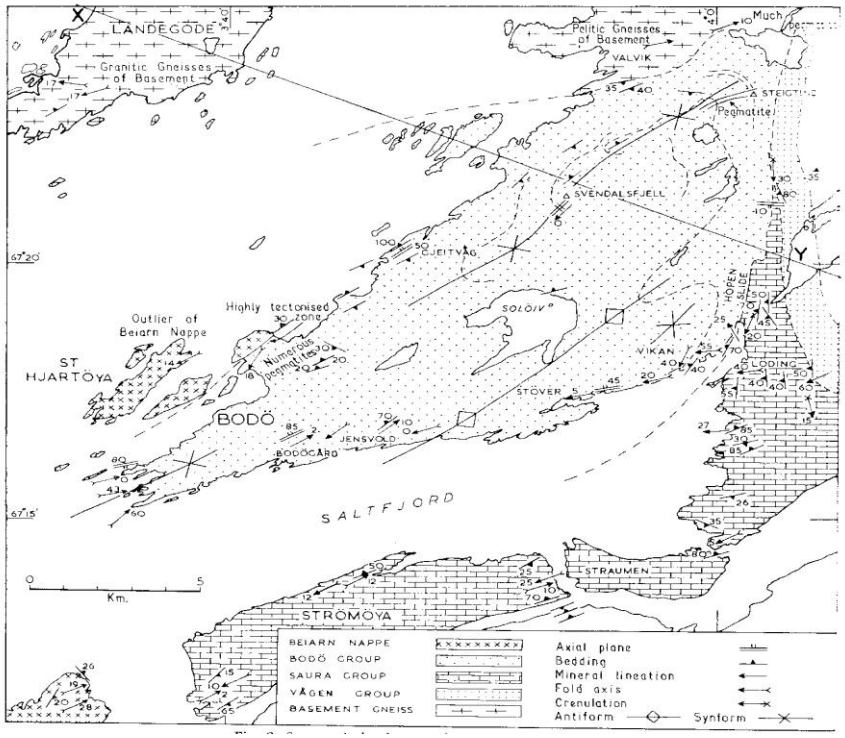

Fig 2. 3A Structural sketch map of the Bodø Group. Reproduced from Rutland and Nicholson (1969)

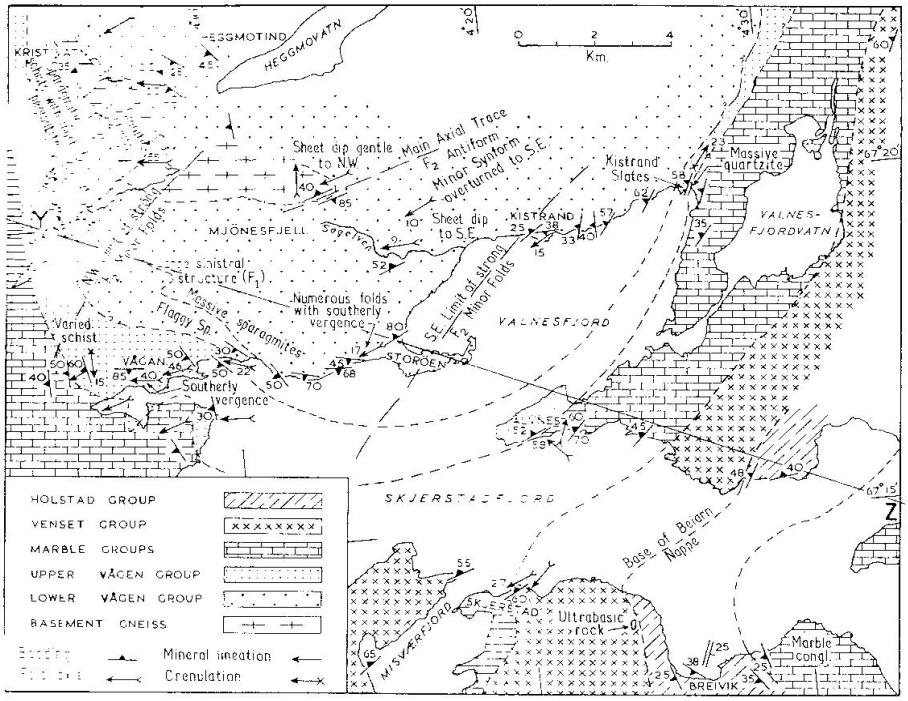

Fig 2. 3B. Structural sketch map of the Heggmovatn antiform. Reproduced from Rutland and Nicholson (1969)

Gustavson (1991) also considered the rocks on Mjelde and the Heggmovatn to be basement rocks and mapped the rocks on Hjartøya and Bratten also as part of the autochthonous basement. More recently, Solli and Nordgulen (2008) interpreted the Heggmovatn dome to be part of the allochthonous sheets although no evidence is presented in support of this change. New data will be presented in subsequent chapters in support of this new interpretation; however, the present discussion is based on previous interpretations.

The Bodø Group is dominated by quartzofeldspathic and micaceous schists which grade with increasing calcite content to the impure marbles of the Saura Group and occupy the Steigtind synform between Bodø and Hopen (Rutland and Nicholson, 1969). Gustavson (1991) more specifically distinguished the group to be composed of mica schists, calcareous mica - schists, calcsilicate – bearing schists, garnet – mica schists, amphibole – biotite schists and calcite marbles of assumed Cambro – Silurian age which were deformed and thrust during the Caledonian orogeny. Biotite is the dominant mafic mineral. Primary bedding is indistinct due to well developed secondary schistosity resulting from an earlier minor folding phase prior to the main tectonometamorphic event (Rutland and Nicholson, 1965).

The Saura Group is separated from the Bodø Group by the Hopen slide (Rutland and Nicholson, 1969). Gustavson and Blystad (1995) consider the Hopen slide to separate the Bodø group from the underlying Rodingsfjallet complex.

Along the section, the Rodingsfjallet complex consists of the calcite and dolomitic marbles of the Sokumfjell Group and mica gneisses of the Holstad Group (Gustavson and Blystad, 1995). These mica schists were subdivided by Rutland and Nicholson (1965) into Lower Vagen Sparagmitic Group which consists of typical sparagmitic metasediments found in this part of Nordland and an Upper Vagen Schist Group which displays alternations of a wide variety of lithologies with epidote and diopside, present in the more calcareous members (Rutland and Nicholson, 1969). These authors considered the sparagmites to be autochthonous.

Both Rutland and Nicholson (1969) and, Gustavson and Blystad (1995) place a thrust between the mica schists and the rocks of the supposed Heggmovatn basement dome. The Heggmovatn dome was first described by Holmqvist (1900). Following Kautsky (1953),

Rutland and Nicholson (1965) interpreted the dome as an antiformal culmination with a core of basement rocks like those of the Glomfjord area to the south (Rutland, 1959).

Rutland and Nicholson (1969) further described them as gneissic complex composed of coarse grained garnetiferous quartzofeldspathic rocks with a prominent schistosity and considered them to be the product of granitization of pelitic or semi-pelitic sediments. It is important to note that the Lower Vagen group outcrops all around the supposed Heggmovatn dome (Rutland and Nicholson, 1969).

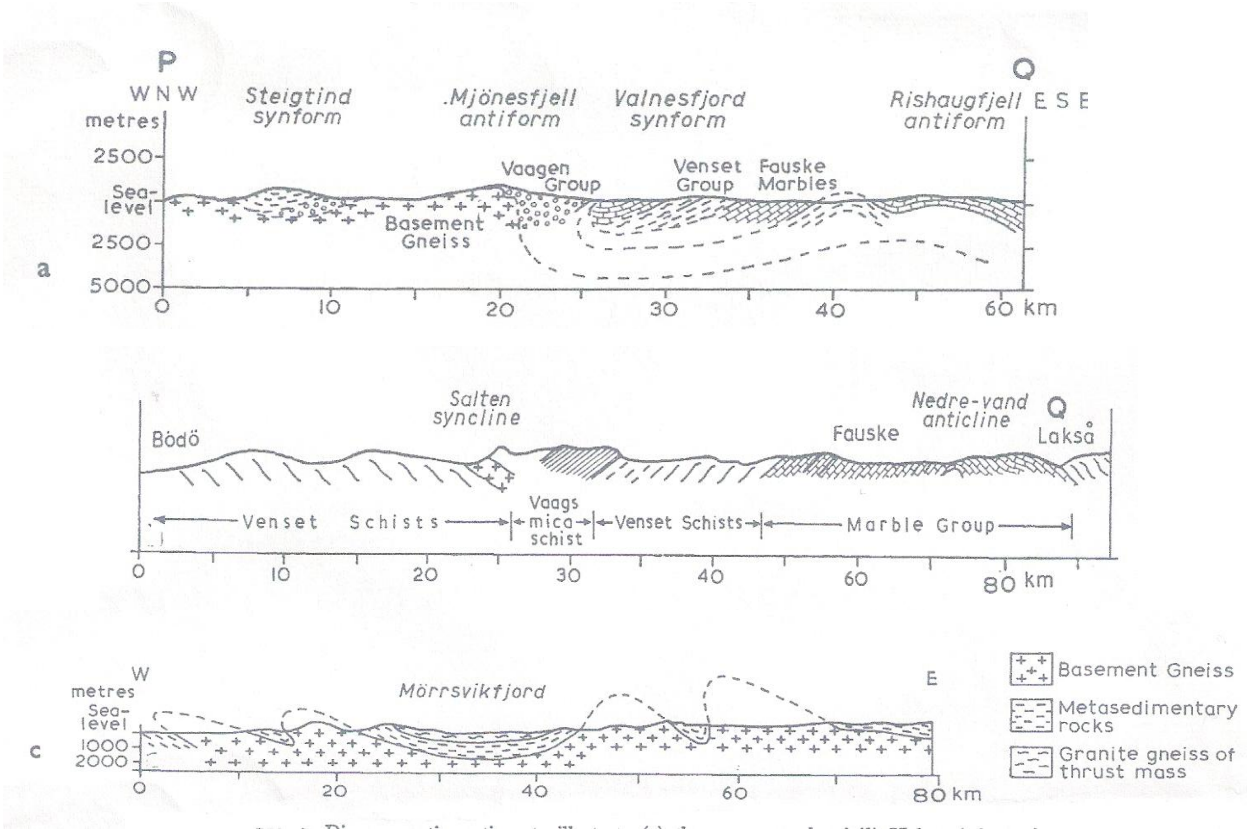

Fig 2.4 Diagrammatic sections illustrating interpretations of (a) Rutland and Nicholson (1965), (b) Holmqvist (1900) and (c) Kautsky (1953)
From Rutland and Nicholson (1965)

Solli and Nordgulen (2008) have interpreted the Heggmovatn dome as part of the Uppermost Allochthon. It is therefore considered as part of the allochthonous sheets and not the basement

units as previously thought. New data and observations will be presented in detail in subsequent chapters to support this new interpretation.

2.2.5.2 Central Units

This refers to rock units between Fauske and Hellarmo (pictured in Fig 2.5A below). The structurally lowest lithological units of this area are the granitic gneisses of the Rishaugfjell antiform which is correlated to the Tysfjord culmination to the north (Rutland and Nicholson, 1969).

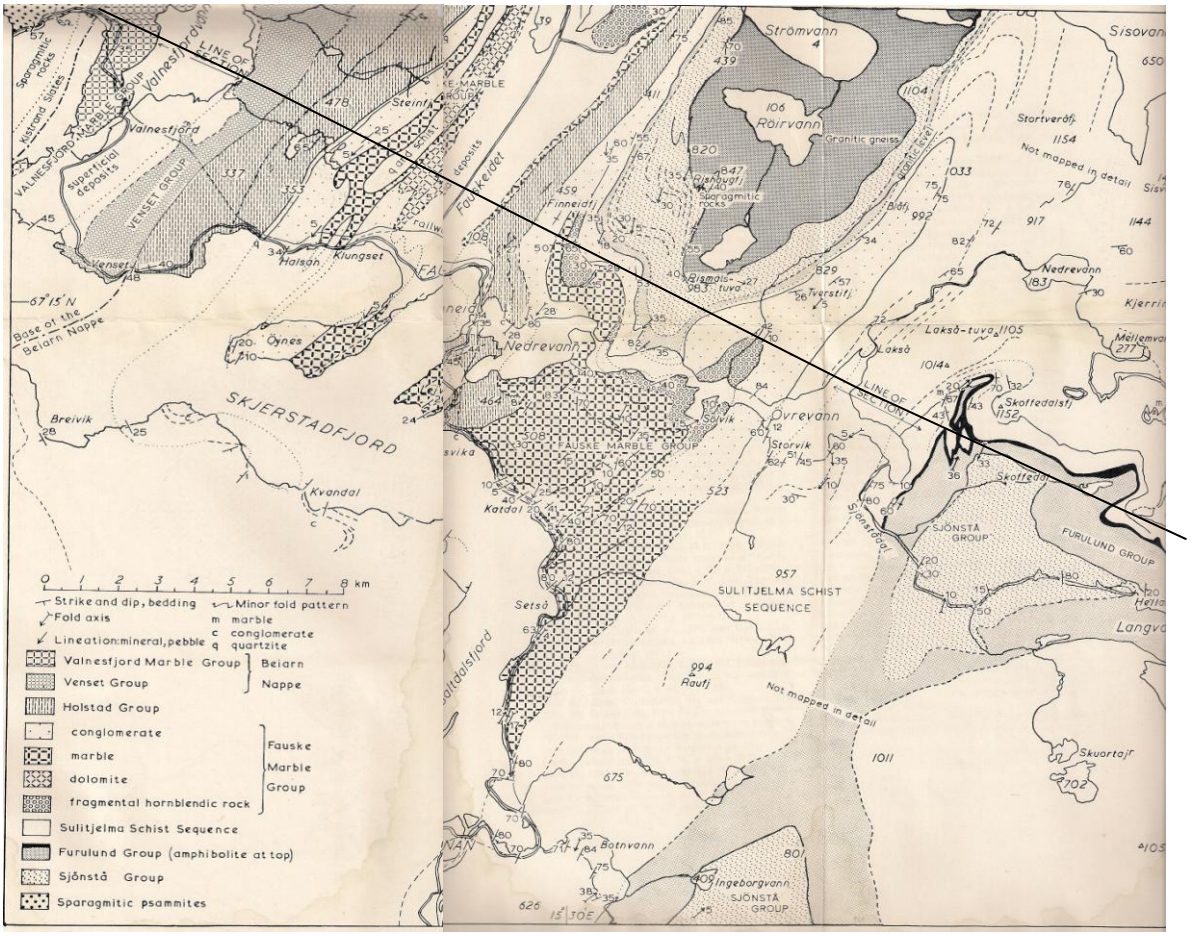

Fig 2.5 A Geological map of the area between Fauske and Hellarmo, reproduced from Rutland and Nicholson (1969)

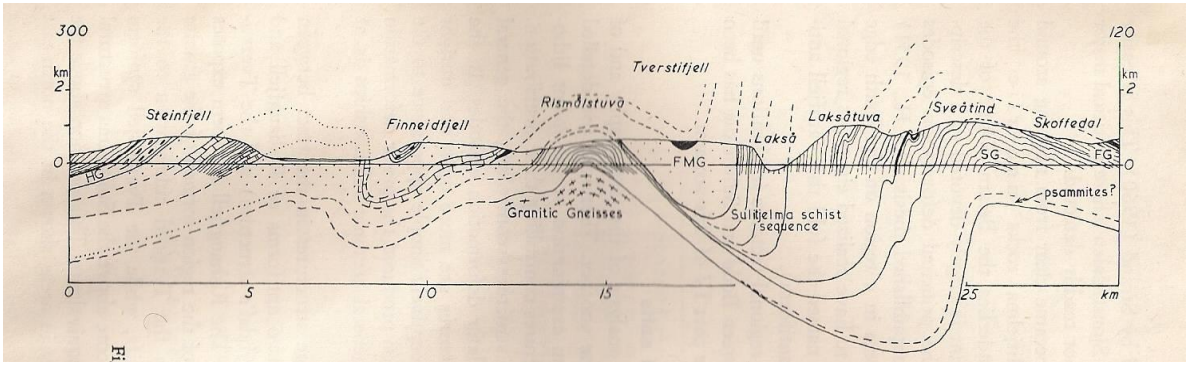

FMG – Fauske Marble Group, FG – Furulund Group, SG – Sjonsta Group

Fig 2.5 B Cross section along the line shown in Fig 2.5A, reproduced from Rutland and Nicholson (1969)

The structural successions above these basement culminations were summarized by Rutland and Nicholson (1969) to be as follows;

Table 1 Comparison of Rishaugfjell and Vatnetfjell antiforms

Rishaugfjell Antiform	**Vatnetfjell Antiform**
4. Fauske Marble Group	4. Fauske Marble Group
3. Thin succession of schists b. Hornblende pelites and marble (Furulund group) a. Semi – pelitic schists characteristic of the Sjonsta Group	3. f. Mica schists with marble and amphibolites e. Muscovite schist group d. Mixed group including marble c. Mixed group including calc – psammites b. Furulund group (pelites, amphibolites, schist, phyllites) a. Sjonsta group (dominated by psammitic schists)
2. Psammites	2. (Possible) Psammites
1. Granitic Gneiss	1. (Possible) Granitic Gneiss

Gustavson (1996) placed the rocks above the Rishaugfjell basement into the Seve – Kolli complex comprising the Sulitjelma, Furulund, Sjonsta and Peiski Groups, and the Gasak

(Rodingsfjallet) complex comprising metavolcanics and metasediments of the Joknacorr, Blamanns, Stormfjell, Smasorju and Sorjus Groups of Cambro – Silurian age.

2.2.5.3 Eastern Units

This refers to those units between Hellarmo and the Norwegian– Swedish border. The major structure of this area is the Sulitjelma tectonic depression lying between the Tysfjord and the Nasafjell basement culminations (Rutland and Nicholson, 1969). Rutland and Nicholson (1969) divided the rocks within this depression into a lower part comprising basement granitic gneisses, sparagmites, Peiske Group marbles, Sjonsta Group, Furulund Group and the Sulitjelma amphibolites, and an upper part comprising the Furulund Group, Sulitjelma Amphibolites, Sorjus Marble Group, a fragmental group (of graphitic schists and gneissic material), a thin unit of amphibolites and pelitic schists, and the Fauske Marble Group.
It is important to note that one of the first absolute ages published in this area was by Wilson (1971) who reported an Rb - Sr age of 413 ± 34 Ma for the Furulund granite.

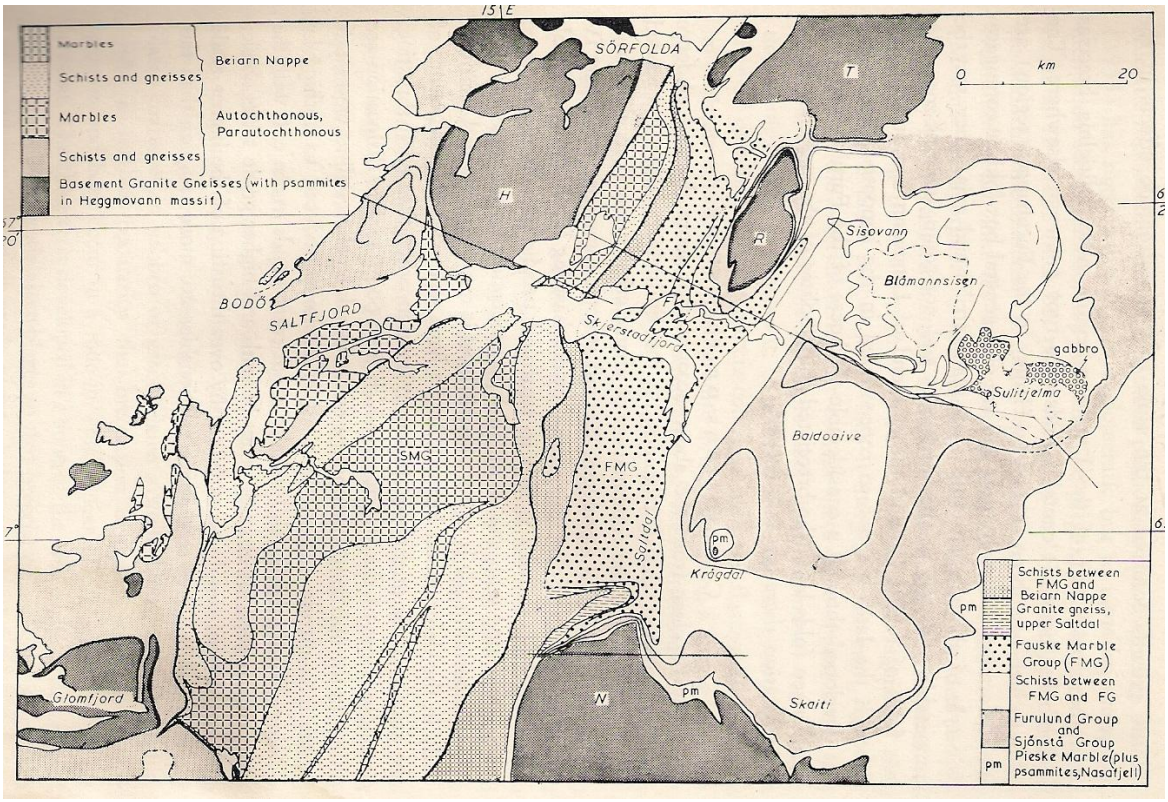

Fig 2.6A Map of Bodø – Sulitjelma tract showing major lithological units. Reproduced from Rutland and Nicholson (1969)

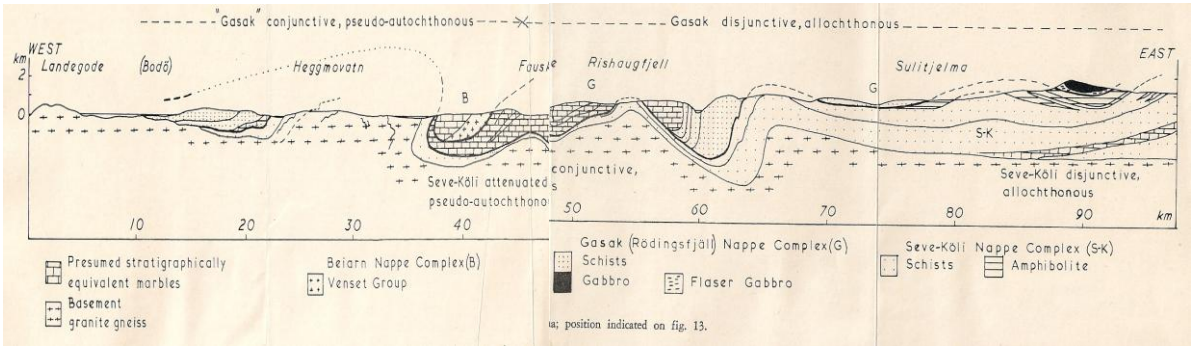

Fig 2.6B Cross section of Fig 2.6A Reproduced from Rutland and Nicholson (1969)

2.2.6 Purpose of investigations the Bodø and Heggmovatn areas

The primary purpose of the detailed mapping in the Bodø area were primarily to work out the supposed basement – cover relationships in the western part of the Bodø – Sulitjelma transect. Samples from the supposed basement rocks were to be dated to determine whether the granitic gneisses were emplaced during the 1870–1860 Ma magmatic episode corresponding to contraction, amalgamation of arcs, and regional deformation or the 1800–1790 Ma magmatic episode which was characterized by major shifts in plate convergence, intraplate deformation, and by a diversity of magmatic associations including suites derived from the subcontinental mantle and widespread granitoid rocks extracted from the continental crust (Corfu, 2004).

The rocks from the supposed basement in the Bodø was also to be compared to those from the Heggmovatn dome, as those rocks were atypical of basement rocks described elsewhere in Nordland as basement domes. Finally, the metamorphic condition of the rocks in the supposed basement and the supracrustal thrust sheet (Bodø group) were to be studied. This data forms the basis for a model for the geological evolution of the area.

2.3 Regional Geology of North East Greenland

A brief review of the East Greenland Caledonides is important because most authors consider the Uppermost Allochthon to be derived from Laurentia (East Greenland margin).

The Caledonian mountains of NE Greenland extend from latitude 70˚N- 82˚N and occupy the eastern edge of the Greenland ice dome.

The entire Caledonian belt of North East Greenland consists of rocks derived from the Laurentian margin, including both Archean and Paleoproterozoic crystalline and younger shallow marine sedimentary successions. (Gee, 2005). Unlike the Scandinavian Caledonides, there is a distinct absence of outboard and exotic terranes in the North East Greenland Caledonides, possibly with the exception of the Liverpool Land Eclogite province (Augland, 2010).

Higgins et al. (2004) divided the East Greenland Caledonides into three main lithological units: an autochthonous Early to Mid-Proterozoic basement complex and three thrust sheets; the Niggli Spids Thrust Sheet, the Hagar Thrust Sheet and the Franz Joseph Allochthon.

More recently, Andresen et al. (2007) argue for one thrust sheet citing the repetition or ortho- and paragneisses and the Krummedal sequence as being the result of large scale recumbent folding as originally interpreted by Haller (1971). The tectonostratigraphy presented here is based largely on that presented by Andresen et al. (2007).

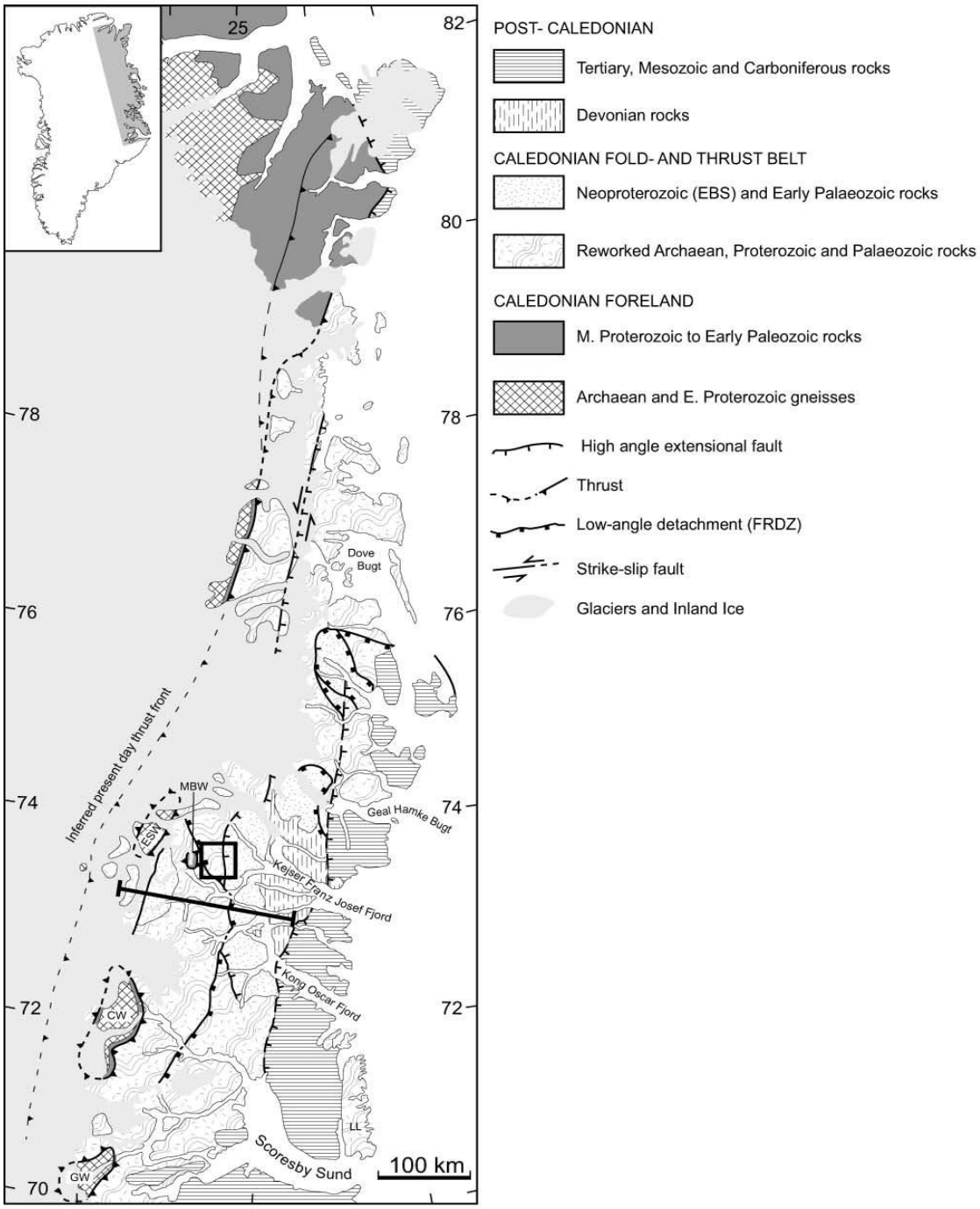

Fig 2.7 The East Greenland Caledonides CW, Charcot Land Window; MBW, Malebjerg Window; ESW, Eleonor Sø Window; GW, Gletscherland Window; EBS, Eleonore Bay Supergroup; FRDZ, Fjord Region Detachment Zone

(Reproduced from Andresen et al., 2007)

2.3.1 The autochthonous basement

The autochthonous basement is exposed in the north and northeastern parts of Greenland and in tectonic windows in the southern part of the thrust belt (Henriksen, 2003) and is composed of Archean to Paleoproterozoic orthogneisses and paragneisses. This autochthonous basement is overlain by a thin veneer of Vendian to Early Palaeozoic low grade cover sediments (Fig. 2.7).

Autochthonous foreland sediments are poorly exposed in this part of the orogen because of the Inland Ice, but appear in several tectonic windows (Charcot Window, Malebjerg Window, Eleonore Sø Window) in the southern part of the thrust belt (Escher, 2001; Henriksen, 2003)

Zircon crystallization ages in granites and K – Ar age of hornblende in a crosscutting amphibolite dyke set an upper age constraint of 2520Ma for the autochthonous basement (Steiger et al., 1979). So far, limited Caledonian deformation has been recorded in the autochthonous basement.

2.3.2 The Niggli - Hagar thrust sheet

The Niggli - Hagar thrust sheet, according to Andresen et al., 2007, consists of three distinct lithotectonic units in ascending structural order;

- Archean – Neoproterozoic ortho- and paragneisses
- the Late Mesoproterozoic to early Neoproterozoic metasedimentary Krummedal Sequence
- The Neoproterozoic metasedimentary Eleonore Bay Supergroup with the overlying Tillite Group and early Palaeozoic sediments.

2.3.2.1 Archean – Neoproterozoic ortho- and paragneisses

This unit is lithologically similar to the basement. It is interpreted to be parautochthonous basement which was sliced of and reworked during the Caledonian orogeny. It however preserves pre – Caledonian structures (Friderichsen et al., 1994). Ages reported from this unit range from Archean to Neoproterozoic (Kalsbeek et al., 2000). Escher (2001) reports a depositional contact between this unit and the overlying Krummedal sequence.

Table 2 Ages of Parautochthonous – Allochthonous basement

Rock type and locality	Technique	Age (Ma)	Reference
Banded Gneiss, Danmarkshvan	U – Pb, zircon Rb – Sr, whole rock	~ 3000	Steiger et al., 1976
Granites, 72ºN - 74ºN	Rb – Sr, whole rock	ca. 1950	Rex and Gledhill, 1981
Orthogneisses, 74ºN - 76ºN	Sm – Nd, Rb – Sr, whole rock	2110 - 2330	Kalsbeek et al., 1993
Gneiss, 76ºN - 77ºN	U – Pb, zircon	1974 – 1739	Kalsbeek et al., 1993
Orthogneisses, Dronningen av Louises Land	U – Pb, zircon	1909	Friderichsen et al., 1994

2.3.2.2 The Krummedal / Smallefjord Sequence

This unit is called the Krummedal Sequence south of 74˚N and Smallefjord Sequence north of 74˚N. It is composed of psammites, pelites and mica schists with subordinate quartzites and amphibolites, and is about 8000m thick (Higgins, 1988). The Krummedal Sequence overlies the allochthonous basement but is generally isoclinally folded with it. The unit is variably migmatized and intruded by two generations of leucogranitic plutons and dykes dated to c. 940–910 Ma (Kalsbeek et al. 2000; Watt et al. 2000; Higgins et al. 2004), and around 435–420 Ma (Andresen et al. 1998b; Hartz et al., 2001). The unit is generally accepted to have been deposited between 1100 – 930Ma (Kalsbeek et al., 2000).

Ages of 445 – 420Ma which have been reported by several workers (e.g. Watt et al., 2000; Leslie and Nutman, 2003; Andresen et al., 2007; Kalsbeek et al., 2008) and are accepted as recording Caledonian deformation, metamorphism and magmatism along Laurentia's eastern margin.

2.3.2.3 The Eleonore Bay Supergroup

The Eleonore Bay Supergroup is widely exposed in the fjord region between 72ºN and 76ºN and outcrops mainly in the Central Fjord zone (Sønderholm and Tirsgaard, 1993). The Supergroup has been divided by Sønderholm and Tirsgaard (1993) into three main units; a lower siliciclastic unit, a mixed carbonate and siliciclastic middle unit and an upper carbonate unit.

The supergroup is overlain by the Tillite group, interpreted to be of Vendian age (Sønderholm and Tirsgaard, 1993) and the Paleozoic Kong Oscar Fjord group. The lower c. 200 m of the Kong Oscar Fjord Group is dominated by a siliciclastic succession that fines upwards, whereas the remainder of the group comprises carbonate sediments of Early Cambrian to Mid-Ordovician age. The group reaches a thickness of about 4 km, and is unconformably truncated by post-Caledonian Devonian continental molasse deposits (Smith and Bjerreskov 1994). The Kong Oscar Fjord Group and Tillite Group sediments are generally non-metamorphic.

All of the above units are interpreted to have been deposited in shallow marine to fluvio - deltaic environments on a subsiding shelf along the eastern margin of Laurentia (Hambrey and Spencer, 1987). The Eleonore Bay Supergroup is thought to have been deposited between 950 – 610Ma (Sønderholm and Tirsgaard, 1993).

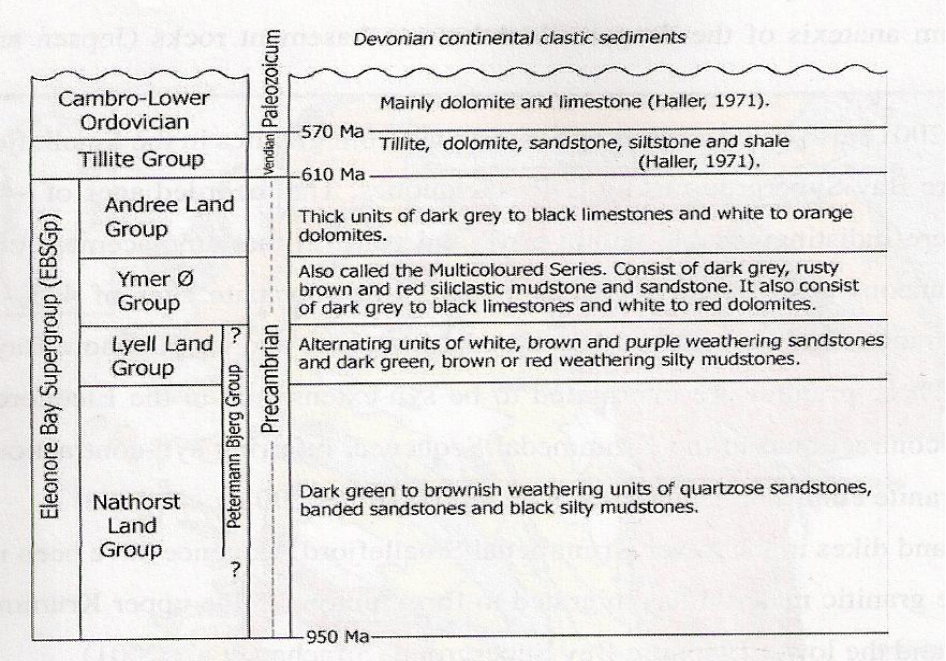

Fig 2.8 Stratigraphic column showing the different units of the Eleonore Bay Supergroup. From Sønderholm and Tirsgaard (1993).

3. Geology of the Study Area

3.1 Introduction

The study area represents a section from the supposed autochthonous basement gneisses in the extreme west (Bodø) across the Bodø supracrustal sequence into the Heggmovatn thrust sheet. The rock units in this transect are divided into three main lithotectonic units;

1. The Pre - Caledonian allochthonous rocks and its intrusive units
    a. Megacrystic granite (oldest)
    b. Diorite intrusive
    c. Mafic intrusive
    d. Orthogneiss
    e. Cover sequence
    f. Granitoid intrusives (youngest)

2. The Allochthonous Caledonian supracrustal cover (Bodø Group) (as observed in the study area)
    a. Dark mica schist (oldest)
    b. Amphibole – biotite schist
    c. Garnetiferous schist
    d. Calcsilicate bearing schist
    e. Mica schist (youngest)

3. The Allochthonous Heggmovatn sequence and its intrusive unit.
    a. Metapsammites and metapelites (oldest)
    b. Coarse grained deformed orthogneisses
    c. Undeformed leucocratic granitic dykes

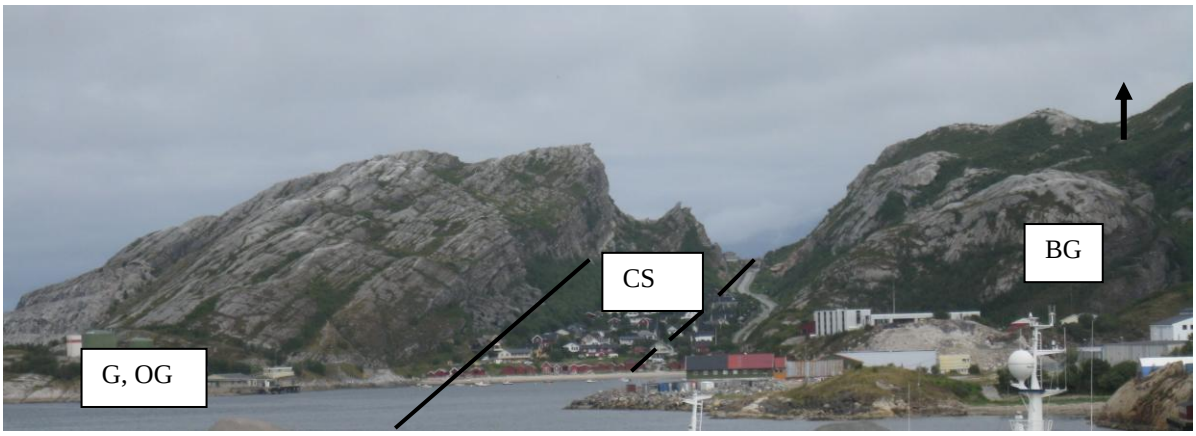

G – Granite OG – Orthogneiss CS – Cover sequence BG – Bodø Group

Fig 3.1 General orientation of rocks in Bodø area showing general orientation of rocks in study area, as well as overturned contact between orthogneisses and "cover sequence", and the Bodø Group. Picture taken from Buroya facing due north.

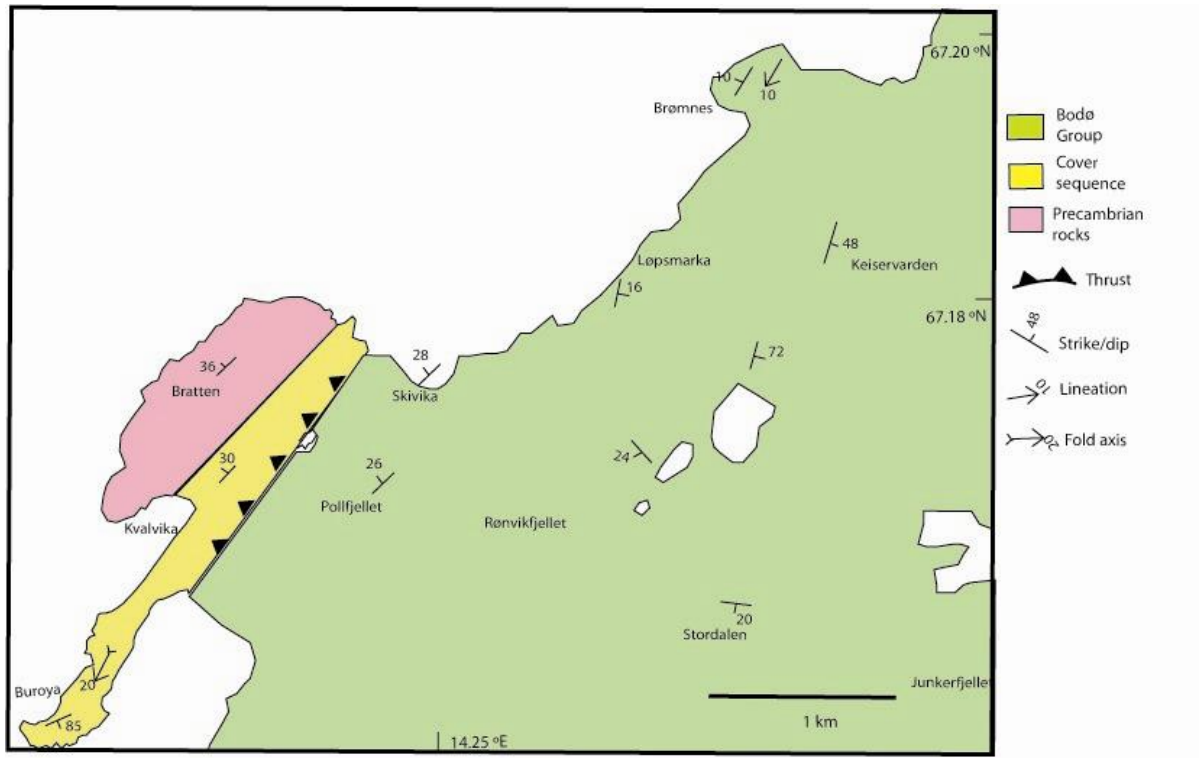

Fig 3.2 Simplified geological map of the study area showing the main lithotectonic units

3.2 The Pre - Caledonian allochthonous rocks and cover

The rocks outcropping on Hjartøya and other islands west of the Bodø peninsula as well the southwestern part of Bodø in the Bratten quarry have been mapped as autochthonous basement by Gustavson (1991). It is composed of granites, gneisses and intrusive units. However, age determinations of the granites on Bratten to be presented in later chapters indicate that these do not belong to the Baltic basement.

3.2.1 Megacrystic granite and Orthogneiss

The megacrystic granite is present within the Bratten quarry area. It is coarse grained, massive and has large feldspar phenocrysts. The groundmass is dominated by feldspar and quartz with minor muscovite and biotite. Very small garnet crystals are also interspersed within the rock. Most of the feldspar phenocrysts are large and deformed as can be clearly seen in Fig. 3.3. Some of the larger phenocrysts measure up to 3.5cm across.

Fig 3.3 Megacrystic granite with large phenocrysts of feldspar

This granite is deformed into augen gneiss and orthogneiss towards the east where the contact with the "cover sequence" is exposed. The transition between the megacrystic granite and the augen gneiss is gradual but that between the augen gneiss and orthogneiss is very sharp and marked by a shear zone (work by previous workers in the area do not mention this shear zone). This shear zone is inferred to be older than the metasedimentary cover of the gneisses. It is considered to be a thrust as the hanging wall (orthogneiss) has moved upwards relative to the footwall (augen gneiss). The shear zone is roughly sub – parallel to the dominant foliation and most likely marks a transition of metamorphic grade in the unit. The P – T conditions in the augen gneiss could not however, be determined to prove this due to its mineral assemblage.

In the augen gneiss, the feldspar augens are slightly smaller than the phenocrysts in the granite. They are generally symmetrical and do not indicate a distinct sense of shear. Most of the larger feldspar augens are Θ-type objects and some appear to be zoned with a plagioclase mantle a k – feldspar core.

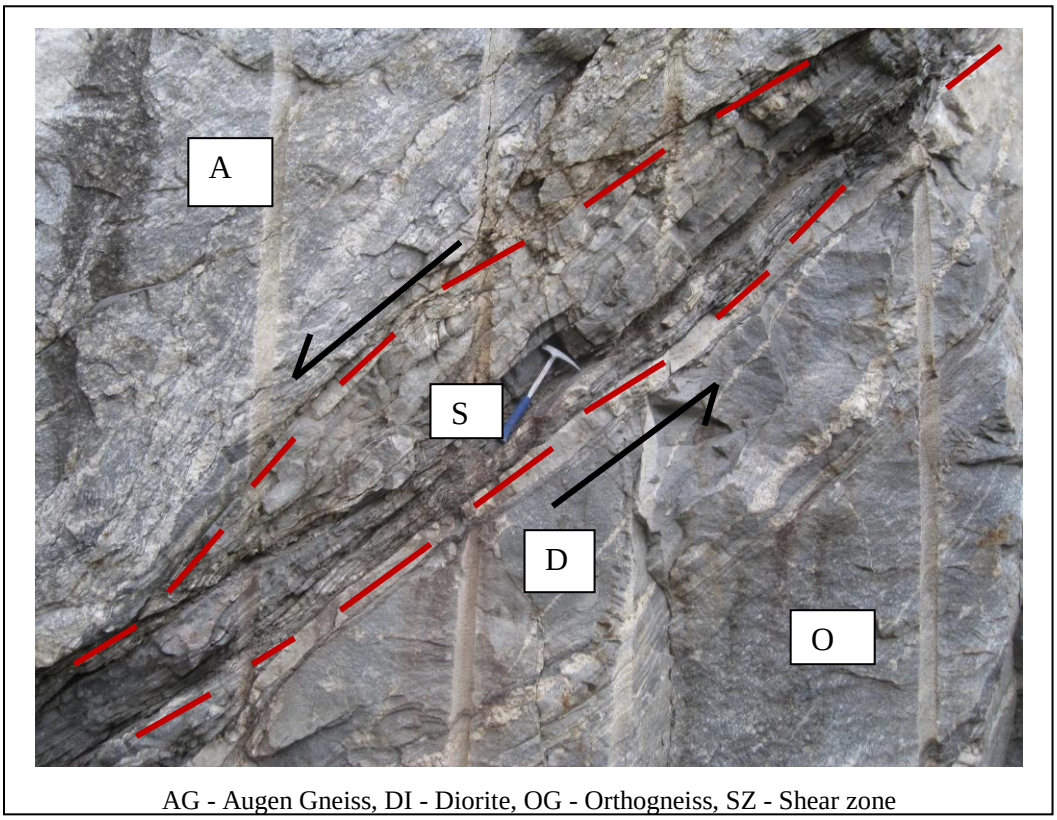

AG - Augen Gneiss, DI - Diorite, OG - Orthogneiss, SZ - Shear zone

Fig 3.4 Sharp transition from augen gneiss to orthogneiss marked by shear zone

The orthogneiss is the most deformed version of the original granitic protolith. It has a well developed foliation derived from alternating bands of quartzofeldspathic minerals and mafic minerals. Biotite is much more abundant than in the nearby granite.

The amount of garnet present appears to increase with increasing deformation as it is progressively more abundant in the augen gneiss and the orthogneiss as compared to the granite. The dominant foliation in the gneisses is deformed.

The contact of the orthogneiss with the "cover sequence" is well exposed a few metres from the shear zone in Fig 3.3 and can be traced about 200m to the Bratten amusement park and is intruded by a pegmatite along the entire stretch of the contact. As such, it is quite difficult to tell whether it was originally a depositional contact or a tectonic contact. At the contact, just outside the quarry, the orthogneisses is seen to overlie a metasedimentary unit which is interpreted to be the cover sequence. This implies an overturning of the contact.

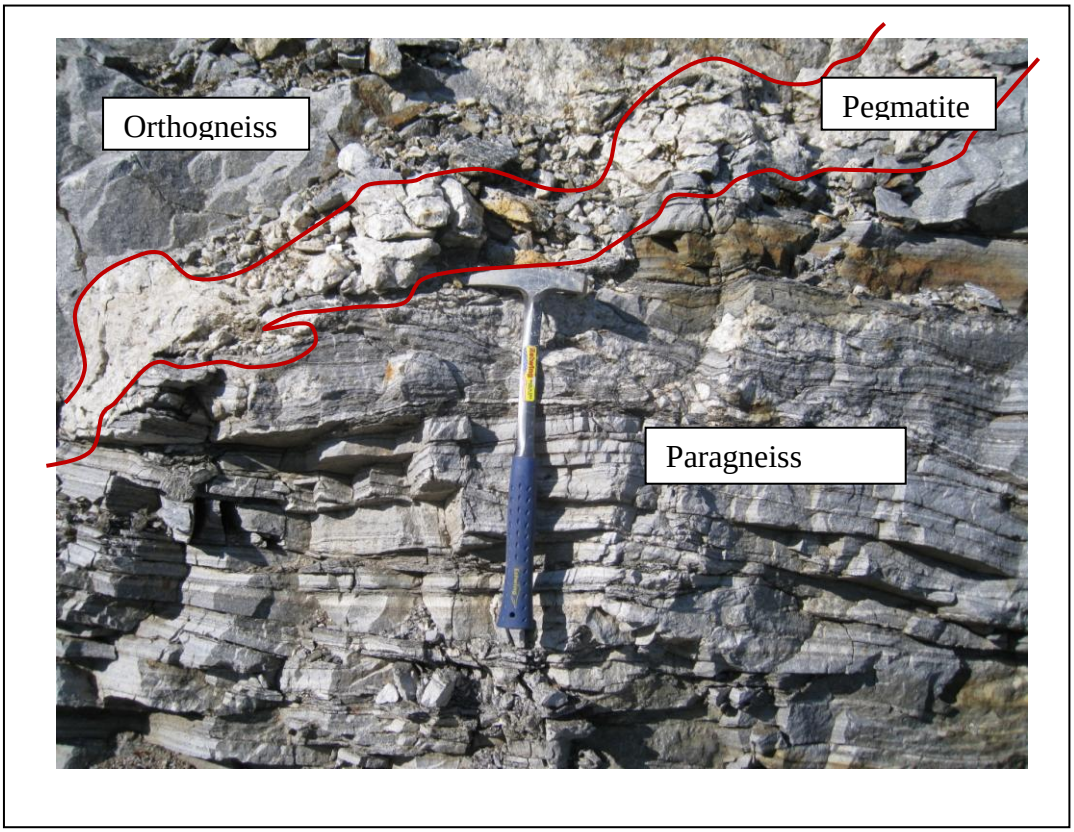

Fig 3.5 The overturned contact between the orthogneisses and the "cover sequence" at the Bratten amusement park (picture taking facing northwest).

Petrography of megacrystic granite

The observed texture is porphyritic and the main minerals present are microcline (55%), quartz (15%), plagioclase (10%), muscovite (8%) and biotite (7%) The accessory minerals present are epidote, apatite and zircon, and together, constitute the remaining 3% of the thin section. The high percentage of microcline is due to the fact that it forms the large phenocrysts as well as part of the groundmass. The microcline phenocrysts show well formed crystals and are undergoing moderate alteration to muscovite and epidote. The large microcline phenocrysts contain "regular" sized (as found in the groundmass) crystals of plagioclase which in themselves contain epidote and biotite. Some of the plagioclase crystals within the larger microcline grains are undergoing the same alteration, albeit to a lesser degree. The groundmass is composed of plagioclase, microcline, quartz and mica. Most of the plagioclase crystals in the groundmass are subhedral to anhedral but those within the microcline phenocrysts (with the epidotes) show euhedral forms. Some of the plagioclase crystals also contain inclusions of quartz and dissolution lamellas are also common.

Quartz occurs as subhedral grains within the groundmass and shows high strain evidenced by undulose extinction. Muscovite and biotite are approximately equal in abundance and show a very weak preferred orientation suggesting some degree of deformation.

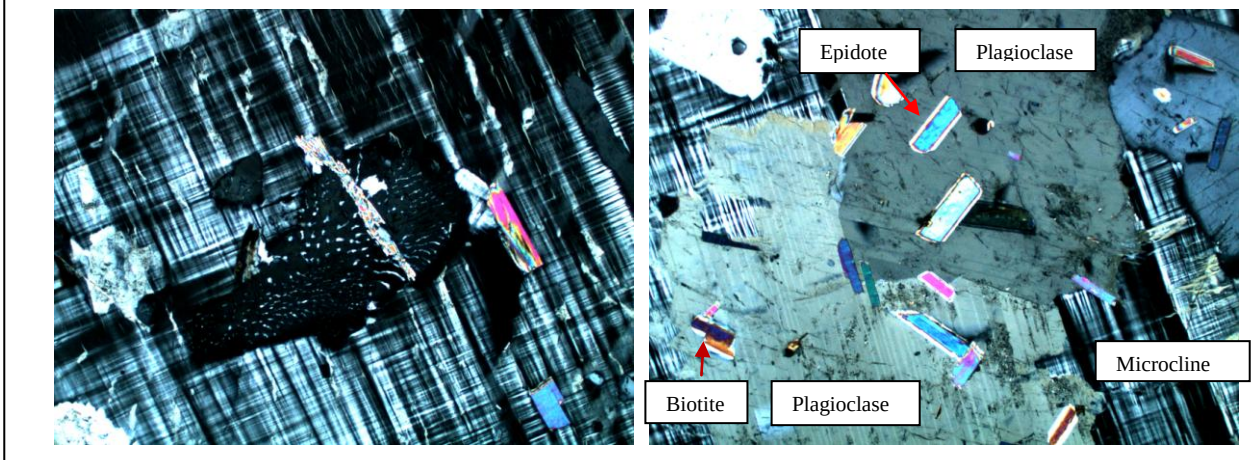

A B

Fig 3.6 A Myrmekites in plagioclase within a larger microcline crystal (Image is 3mm across, magnification is 5X)

B. Epidote and biotite as inclusions in plagioclase which is itself an inclusion in a large microcline porphyroclast (Images are 3mm across).

Petrography of deformed orthogneiss

The texture is porphyroblastic and the primary minerals present are biotite (35%), plagioclase (25%), quartz (15%), garnet (12%) and microcline (10%). Accessory minerals present include zircon, apatite, titanite and unidentified opaque minerals. Unlike the megacrystic granite, muscovite is absent.

Biotite is abundant. The crystals are euhedral to subhedral and appear to be of two populations; population I is composed of large crystals which show a clear preferred orientation. They appear to be slightly bent suggesting them to be deformed. Population II occurs in considerably smaller sizes than those of population I but is approximately subparallel to population I. Pleochroic halos of zircons are abundant in the both biotite populations.

Both plagioclase and microcline are present and form subhedral to anhedral grains. Both of them show dissolution lamella. Myrmekites which are formed by a graphic intergrowth of plagioclase with quartz to produce worm-like structures are also observed.

Quartz occurs mostly as small sub rounded crystals and are closely associated with both feldspars. They also occur as inclusions within the garnets. The quartz crystals are highly strained and some appear to be fractured. Some of the quartz is recyrstallized and is closely associated with biotite.

Garnet is common in the section and appears to be in isolated clusters separated by quartz, feldspar and biotite. Some of the garnets seem to be undergoing some reaction with plagioclase and biotite. Generally, the grain boundaries are sharp.

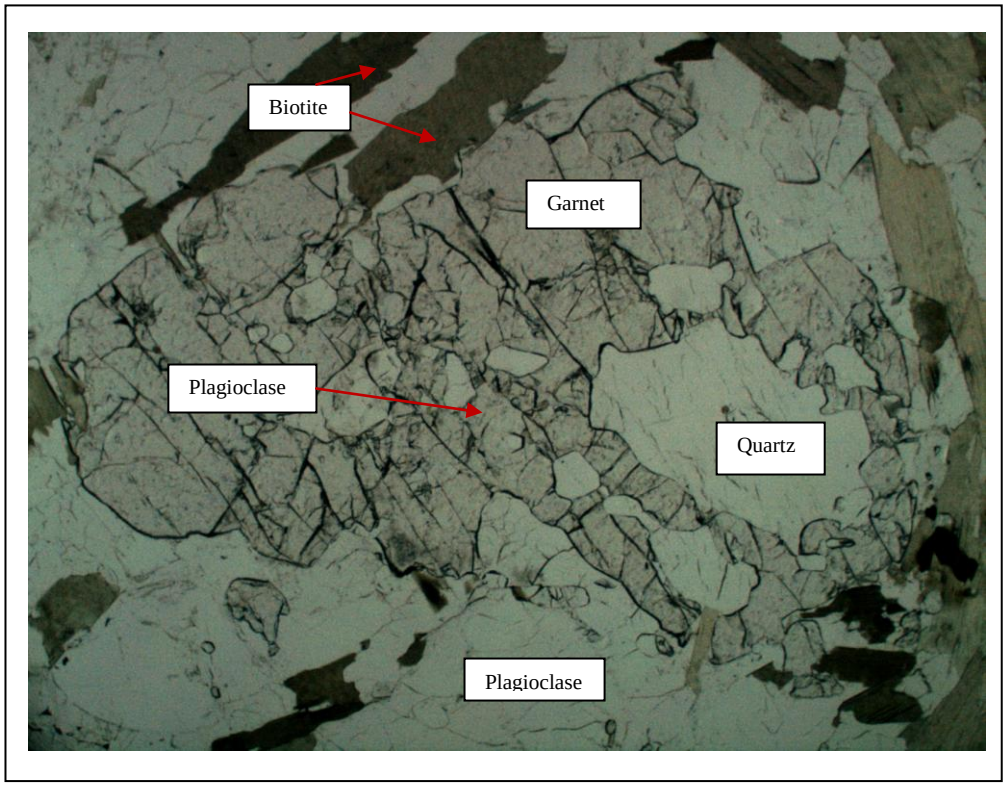

Fig 3.7 Subhedral garnet porphyroblast containing inclusions of quartz and plagioclase (Image is 3mm across) (Image taken in plane polarized light)

3.2.2 Pre – Caledonian Intrusives

The rocks observed in the Bratten area are heavily intruded by several units. These range in composition from mafic to felsic.

3.2.2.1 Intermediate intrusive / Diorite

This unit intrudes the augen gneiss as dykes. At the coast on the west, about 30m from the quarry, large volumes of this intrusive are present. It has a very weak fabric that is roughly subparallel to the gneissic foliation. It has a fine grained massive texture. Quartz, feldspar and biotite are observed in the hand specimen. It is classified as a diorite based on the modal composition (most feldspar is plagioclase) composition in thin section. From the cross - cutting relationships, it is inferred to be the first intrusive, as it is intruded by the mafic dyke and the pegmatite

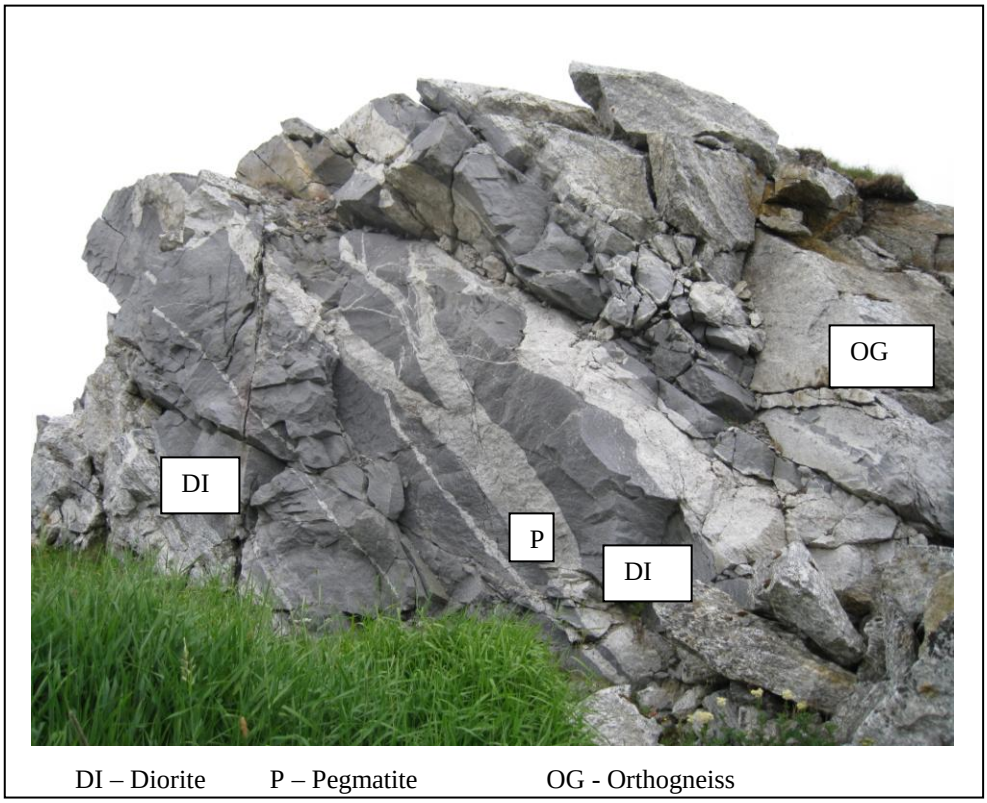

Fig 3.8 Diorite (itself intruded by pegmatite) intruding orthogneiss

Petrography of Diorite

Main minerals are biotite (50%), plagioclase (35%) and hornblende (10%), quartz (3%) and the texture is intergranular. Microcline occurs in very small quantities whiles apatite and titanite occur as accessory minerals.

Most of the biotite crystals are subhedral and show a preferred orientation. Plagioclase forms euhedral to subhedral crystals and is much more abundant than microcline which forms in only minor amounts. Some of the plagioclase crystals contain inclusions of biotite and quartz. Quartz is minor and shows high straining and dissolution structures.

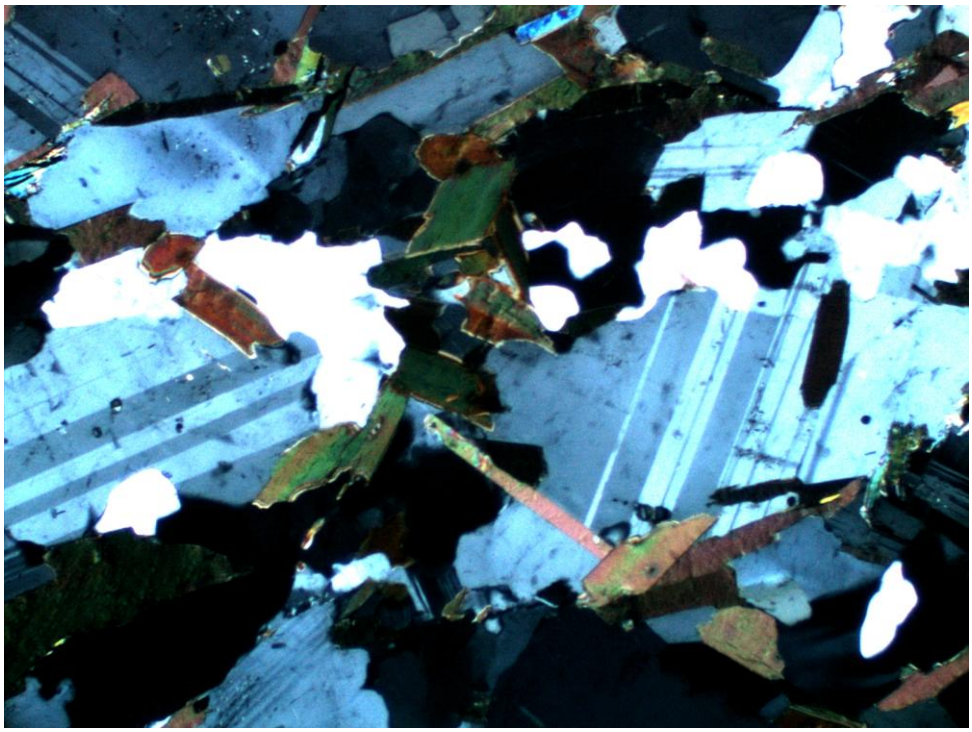

Fig 3.9 Photo micrograph (taken with cross nicols) of diorite showing main minerals (plagioclase with interstitial biotite) and interlocking textures (Image is 3mm across).

3.2.2.2 Mafic intrusive/Amphibolite

This unit is minor in volume and in hand specimen, appears to be dominated by biotite. It is very fine grained and intrudes the gneisses and diorite. They have a foliation that is subparallel to the surrounding rock suggesting that they intruded prior to the main deformational event that formed the dominant foliation.. They are generally thin and are no thicker than 25cm in the quarry. In the more deformed sections of the quarry, these mafic intrusives have been transformed into amphibolites and biotite schists by post – emplacement deformation and retrogression, including introduction of water. Its fabric is subparallel to the gneissic foliation Most of the contacts along which they intrude the gneiss have been reactivated as slip surfaces.

Fig 3.10 Original mafic dyke intruding granite and transformed into amphibolite and augen gneiss respectively

Petrography of mafic intrusive/Amphibolite

The sample shows a strongly pronounced schistose texture in thin section and is composed almost entirely of hornblende (80%) and some plagioclase (11%). Small amounts of biotite and muscovite (6%) are present whiles quartz (2%) is very minor. Clinozoisite is the main accessory mineral present.

Hornblende is the dominant amphibole and shows well formed euhedral crystals, most of which show simple twinning. There is a very strong preferred orientation of the minerals in the section. Plagioclase shows exsolution lamella.

Biotite and muscovite are present but in small quantities and forms euhedral crystals. Clinozoisite is present as an accessory and shows simple twins.

The inter grain boundaries are very sharp. The sample is clearly distinguished as an amphibolite.

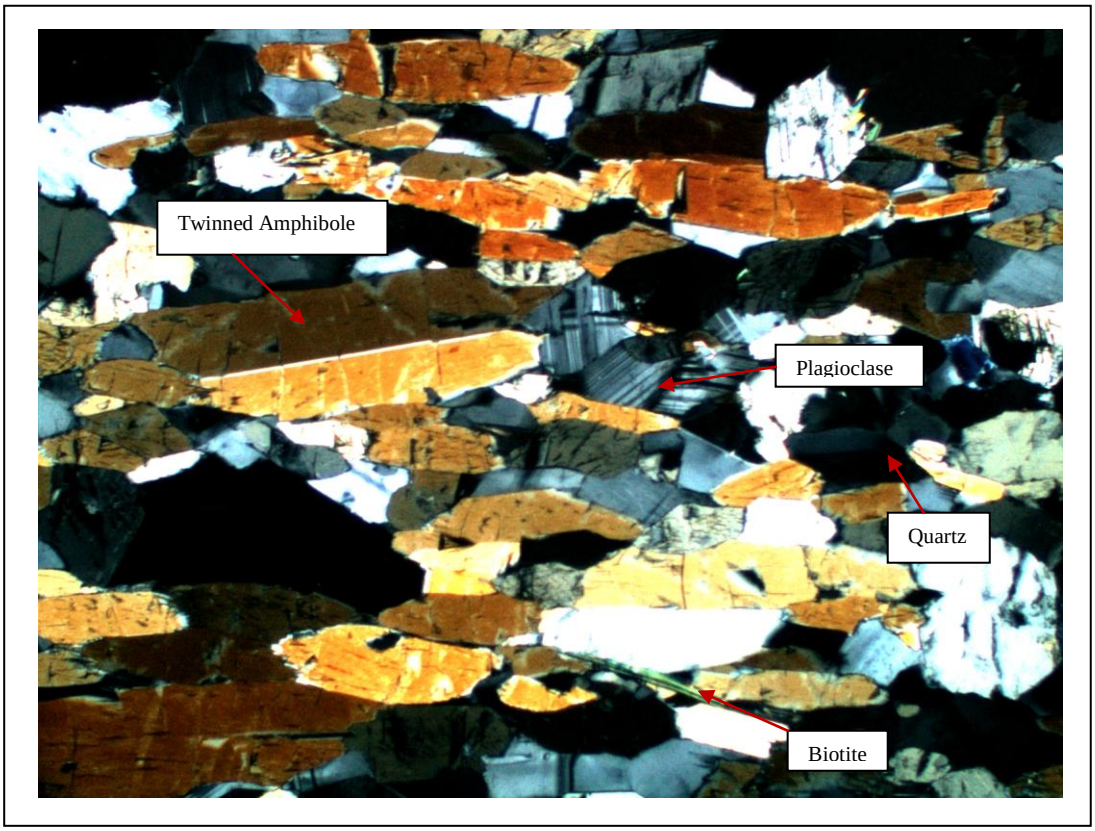

Fig 3.11 Photo micrograph (taken with cross nicols) of amphibolite showing strong preferred orientation of amphibole crystals, some of which show simple twins and main minerals (Image is 3mm across)

3.2.2.3 Granitoids

There are two types of granitoids intruding the augen gneiss, foliated granite and the diorite units. The first is an aplite which occurs only in the vicinity of the shear zone shown in Fig 3.2 at the tunnel entrance to the quarry. It intrudes orthogneiss and is itself intruded by a pegmatite.

The pegmatite intrudes all units within the basement; the granitic protolith and gneisses, as well as the other intrusives discussed above. It is very coarse grained and is composed of quartz, plagioclase, K-feldspar and muscovite. Small grains of garnet are present in the pegmatite. In the quarry, where it intrudes the granite, augen gneiss, intermediate and mafic intrusives, it is generally deformed and cuts across the dominant foliation of the gneisses indicating at least two separate episodes of folding . Some of the pegmatites are composite in nature showing aplitic textures in their inner portions. Most of the pegmatites show boudinage structures as well as ptygmatic folds. There appear to be two generations of pegmatites; an

older deformed generation intruding the granites and gneisses, and a younger generation of less deformed pegmatites which intrude the Bodø group metasediments.

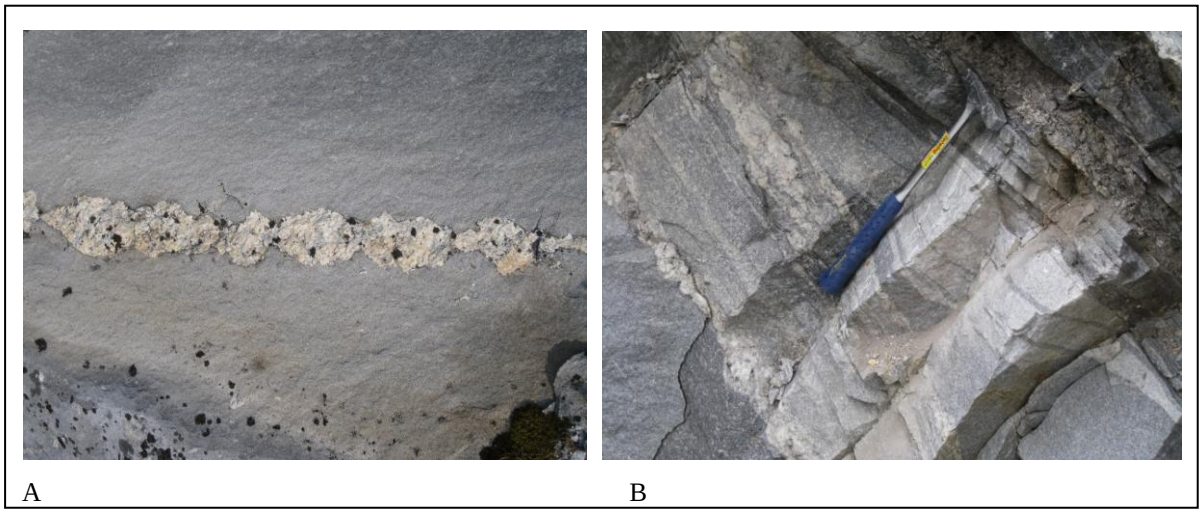

A B

Fig 3.12 A. Pegmatite showing boudinage structures and intruding the intermediate intrusive
B. Aplite and pegmatite intruding diorite

From the cross-cutting relationships observed, it is inferred that the intermediate intrusive was the first to be emplaced after the megacrystic granite as it does not intrude any other units. It was followed by the mafic intrusive, the aplitic granitoids and the pegmatite in that order.

Petrography of pegmatite

The texture is porphyritic and plagioclase, microcline, quartz, muscovite and biotite form the main minerals. The accessory mineral seen is apatite. It is difficult to estimate the proportions of the individual components due to the very large sizes of plagioclase and microcline.
Plagioclase and microcline are the dominant minerals; they have a euhedral to subhedral form and contain several dissolution lamella. There is heavy alteration of the large plagioclase to muscovite at their edges but it is more difficult to tell the nature of the alteration within the crystals (possibly epidote). The large microcline crystals and the smaller plagioclase crystals are also altered but to a much lesser extent than the large plagioclase. The alteration of the plagioclase appears to be from the rim towards the core as some of them have cores that are unaltered.

Biotite and muscovite are approximately equal in abundance and relatively minor. They do not show a distinctly preferred orientation although some of them are bent (indicative of deformation).

Some quartz crystals occur in the plagioclase and are very well formed. Where they occur outside the large plagioclase crystals, they are subhedral and poorly formed.

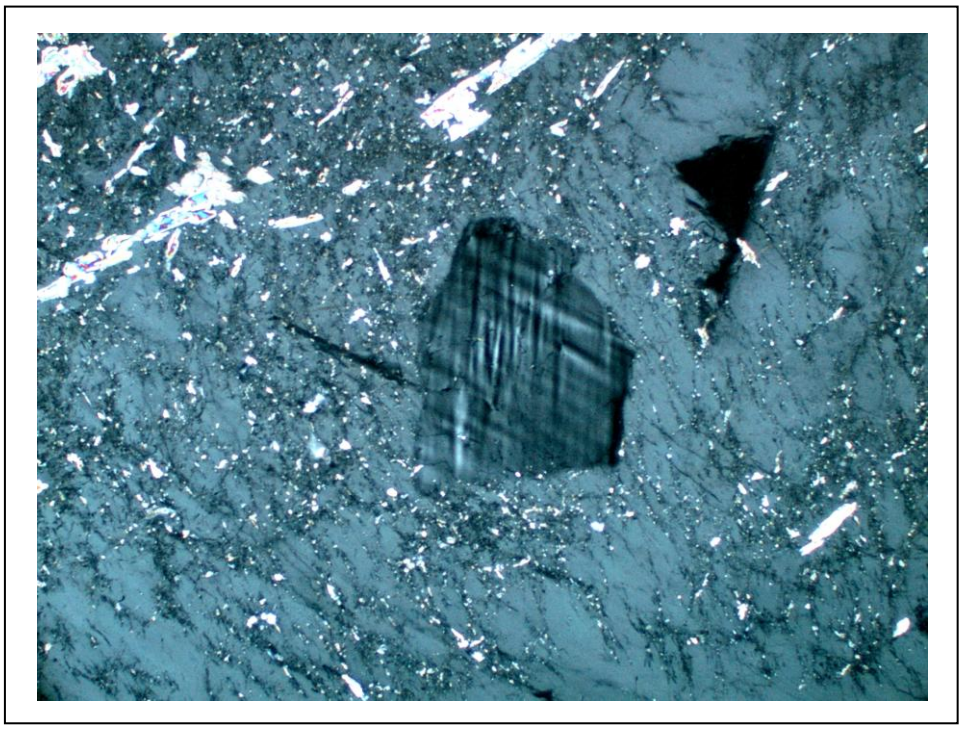

Fig 3.13 Plagioclase undergoing alteration to sericite with an unaltered core: alteration is from the rim towards the core. (Image is 3mm across) (Image taken with cross nicols)

Petrography of aplite

The texture is intergranular and the major minerals observed are quartz (40%), plagioclase (40%), microcline (10%), muscovite (6%) and biotite (4%). Quartz forms subhedral to anhedral crystals, some of which are recyrstallized.

Plagioclase also forms subhedral crystals and contain inclusions of quartz. Dissolution lamellas are common in the plagioclase. Some plagioclase crystals display simple twins. Minor alteration to chlorite is present as a re myrmekites. Microcline forms crystals of considerably smaller size than those of plagioclase and do not show any alterations.

Biotite and muscovite are minor and show a preferred orientation.

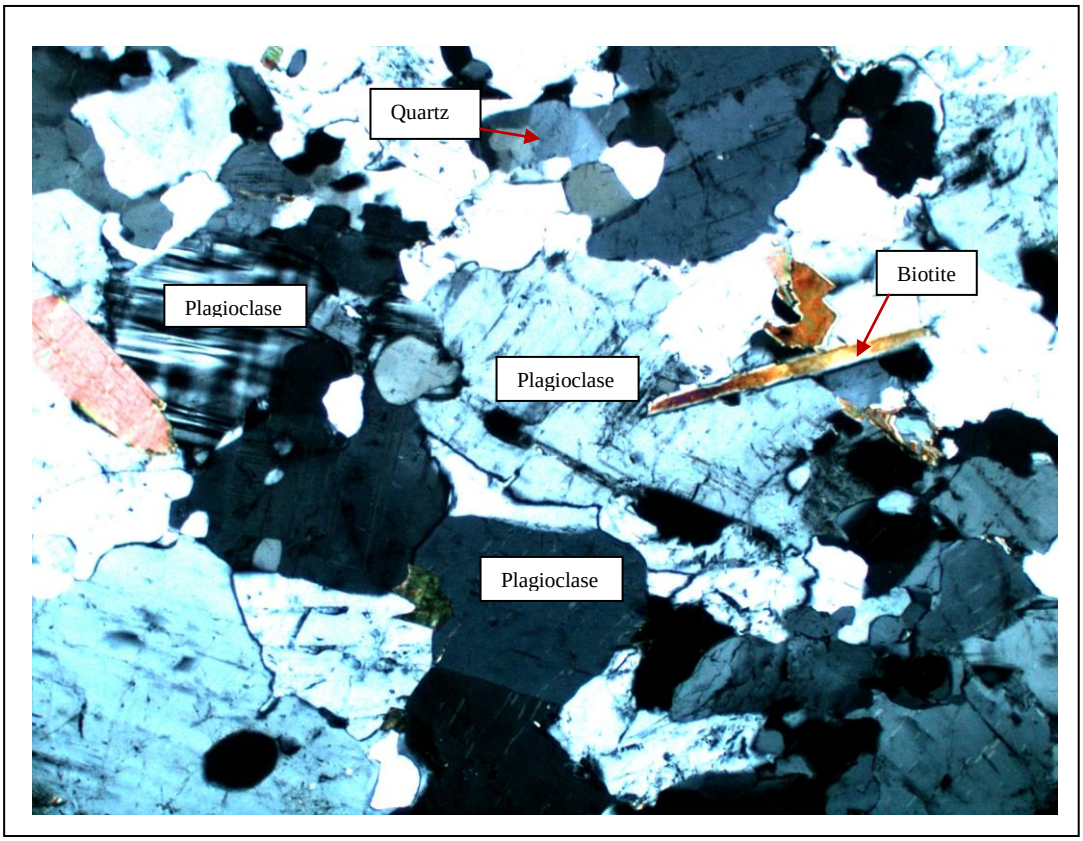

Fig 3.14 Photo micrograph (taken with cross nicols) of aplitic intrusion showing main mineral assemblage (Image is 3mm across)

3.2.3 "Cover sequence" (Paragneiss)

This unit was mapped by Nicholson and Rutland (1969) to be part of the Beiarn Nappe while Gustavson (1991) considered it to be parautochthonous mica gneiss of assumed Proterozoic age. It is therefore considered to be separate from the allochthonous Bodø Group metasediments. Both of them marked the contact with the overlying metasedimentary sequence of the Bodø Group to the east, to be a thrust. However, no physical evidence of this thrust was observed.

The orthogneiss overlies the cover unit as shown in Fig 3.3. The nature of this contact could not be easily determined in the field; as it was intruded by the pegmatite. The contact could therefore be a primary depositional contact, tectonic or an intrusive contact. If the assumption of Gustavson (1991) that the "cover sequence" is of Proterozoic age is correct, then a thrust between that unit and the presumed Caledonian Bodø Group is reasonable. Furthermore, an

inversion of the contact between the orthogneiss and cover sequence would be necessary. An inferred metasediment from this unit was sampled to collect zircons for provenance studies to obtain more information about the nature of this contact, as well as to test the validity of various interpretations by Rutland and Nicholson (1969) and Gustavson (1991). However, no zircons were found in the sample after crushing and mineral separation methods had been applied. This paragneiss is compositionally banded and dominated by quartz, feldspar and biotite. The thickest compositional layer observed was 6cm thick. The biotite forms very thin layers separating the more quartzofeldspathic layers. It is fine to medium grained and contains few isolated thin lenses of marbles and calc-silicates within this unit near the Bratten amusement park. The paragneiss is also intruded by pegmatites and hydrothermal quartz pods. This unit is not uniform as it is schistose in appearance in the Bratten quarry and to the SW at Burøya (where it has garnet porphyroblasts which measure between 1 and 2mm in diameter) but psammitic at the amusement park (about a hundred metres north of the quarry). The unit is intruded by pegmatites near Kvalvika. Intrusions of hydrothermal quartz pods are common. The unit is folded at almost all the localities where it outcrops with the contact locality being a notable exception.

A B

Fig 3.15 A. Cylindrical folds in the cover sequence near Burøya

B. Hydrothermal quartz vein folded together with dominant foliation

Petrography of cover sequence

Major minerals observed are quartz (50%), microcline (25%), biotite (15%), plagioclase (6%) and muscovite (4%). Biotite and muscovite form euhedral crystals which show a strong

preferred orientation. Microcline and plagioclase form subhedral crystals and show dissolution lamella. Almost all the quartz crystals are sub rounded. Other thin sections of the same unit show the same mineral assemblage but with a much higher (60%) of biotite and less quartz with few garnets.

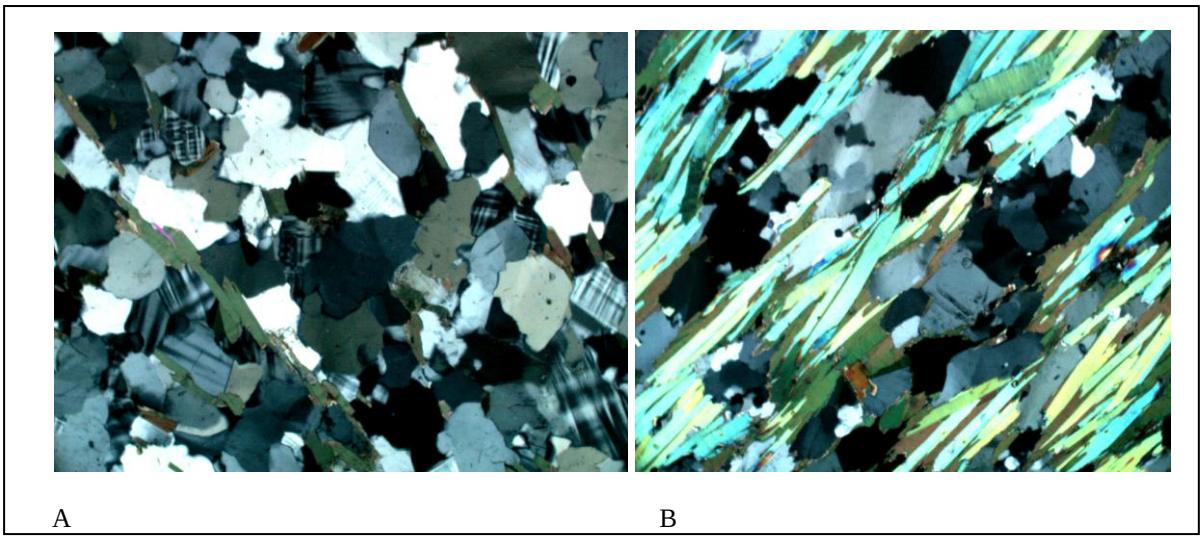

A B

Fig 3.16 A Psammitic paragneiss at Bratten amusement park showing interlocking texture

B. The same unit further south at the Bratten quarry showing schistose texture and strong preferred orientation of biotite "sandwiched" around quartz grains (Images are 3mm across)

3.3 The Allochthonous Caledonian supracrustal cover (Bodø Group)

The Bodø Group is dominated by is dominated by quartzofeldspathic and micaceous schists and occuppies the Steigtind synform between Bodø and Hopen (Rutland and Nicholson, 1969). Gustavson (1991) more described the group to be composed of mica schists, calcareous mica schists, calcsilicate – bearing schists, garnet – mica schists, amphibole – biotite schists and calcite marbles. The Bodø Group underlies the paragneiss unit described above. It is composed of a series of schists which generally strike in a northeasterly direction and dip to the northwest. The Bodø Group is also intruded pegmatites and late granites. Gustavson (1991) reports a thin calcite marble unit outcroping just east of Skivika and a calcareous mica schist in the vicinity of Junkerfjellet. These units were not observed in the field and are not included in the descriptions.

3.3.1 Dark mica schist

This first outcrops just to the east of the Bratten amusement park on the 834 road. The contact with the overlying paragneiss has been marked by Gustavson (1991) as a major thrust. This contact was, however, not observed. If it exists, it is most likely buried beneath the amusement park. The contact is possibly exposed in the cliff face at Skivika beach but, however, the steep nature of the cliff does not permit a direct observation.

The fresh rock has a very dark colour (supposedly derived from the presence of sulphide minerals (Gustavson, 1991)) and is intruded by pegmatites and hydrothermal quartz pods. It is fine to medium grained and dominated by hornblende. Biotite, quartz and plagioclase are also identified in the hand specimen.

The primary bedding is generally indistinct. Foliation is weak and defined by thin layers of light coloured minerals; plagioclase and quartz. It is moderately weathered and shows a brown colour on weathering. The unit also outcrops at the Skivika beach where it is heavily weathered. It shows a bright yellow colouration which is inferred to be due to the presence of weathered sulphides. Here, there are lenses of garnet – mica schist (large garnet porphyroblasts) akin to those at Brømnes.

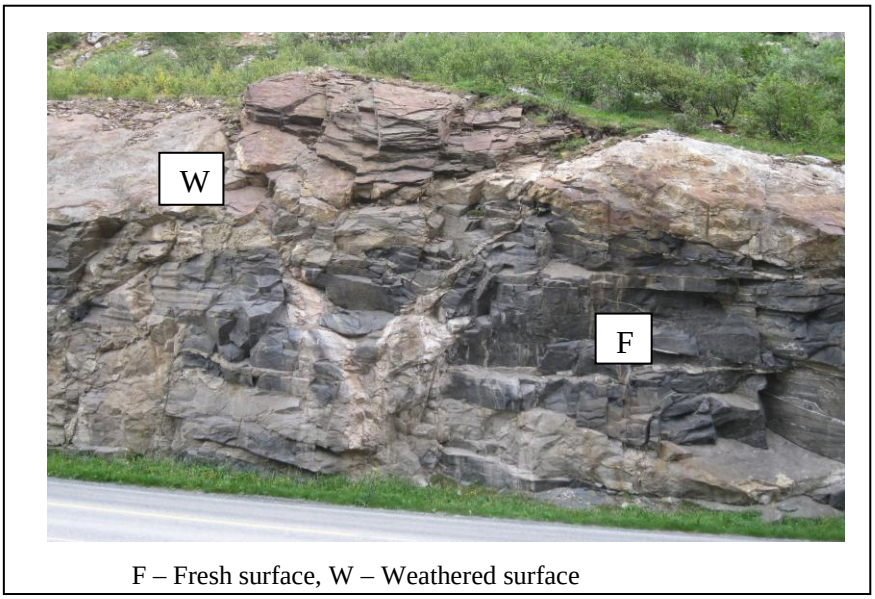

F – Fresh surface, W – Weathered surface

Fig 3.17 Dark mica schist from the Bodø Group showing fresh and weathered surfaces (Locality is near Bratten amusement park)

Petrography of Dark mica schist

The major minerals are hornblende (45%), plagioclase (19%), biotite (15%), quartz (15%), microcline (5%) and zircon, apatite and opaque minerals forming the remaining 1%. Amphibole occurs as hornblende and show the distinctive 120º cleavage. They form subhedral (elongated) to anhedral crystals and appear to be heavily fractured. Plagioclase forms euhedral to subhedral crystals with few showing simple twins.

Dissolution lamellas are common as well as quartz inclusions. Biotite shows a strongly preferred orientation. Quartz forms subhedral grains and shows undulose extinction suggesting high strain. Microcline is minor. Intergrain boundaries are generally sharp.

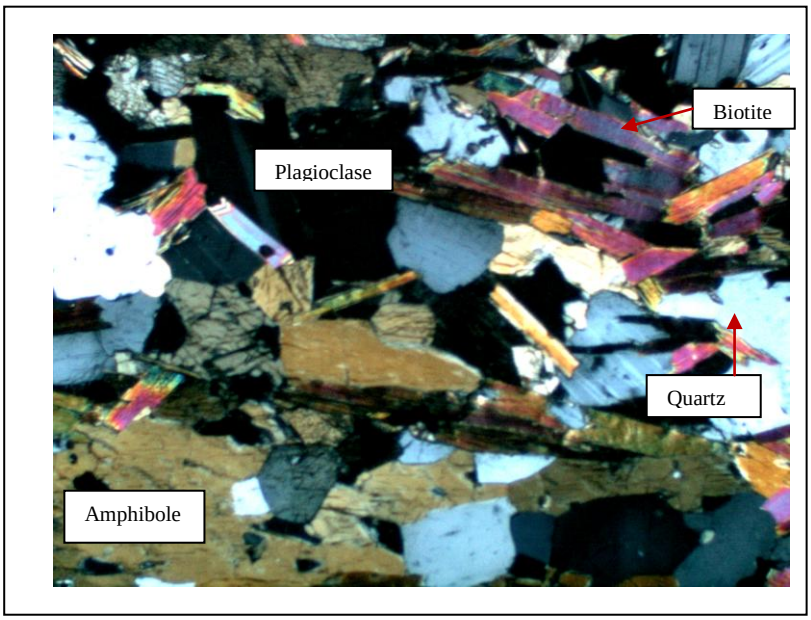

Fig 3.18 Photo micrograph (taken with cross nicols) of dark mica schist showing main mineral assemblage (Image is 3mm across)

3.3.2 Amphibole – biotite schist

This unit outcrops at the Skivika beach over a very small area. It has a distinct green colour and is composed mainly of hornblende and biotite. It has a well developed schistosity defined by thin quartzofeldspathic bands. Folding within this unit is not as severe as in the paragneisses of the Pre – Caledonian cover. It is also intruded by some late granitoids.

The contact between this unit and the overlying Dark micas schist is inferred to be a sharp depositional contact although it was not observed. It is most likely exposed in the cliff face pointing out to sea at the beach. The steep nature of the cliff makes it quite impossible to observe this.

Fig 3.19 Hand specimen of the amphibole biotite schist (with quartz vein)

Petrography of amphibole – biotite schist

This is composed of hornblende (55%), biotite (20%), quartz (20%) and plagioclase (5%). Hornblende forms euhedral crystals which show simple twins. Biotite is euhedral to subhedral, elongated and shows a preferred orientation. Quartz shows undulose extinction and is subrounded.

The composition is very similar to the dark mica schist except for the slightly higher amount of amphibole. It also shows a much stronger preferred orientation of the amphibole and biotite minerals than the dark mica schist. The texture is schistose.

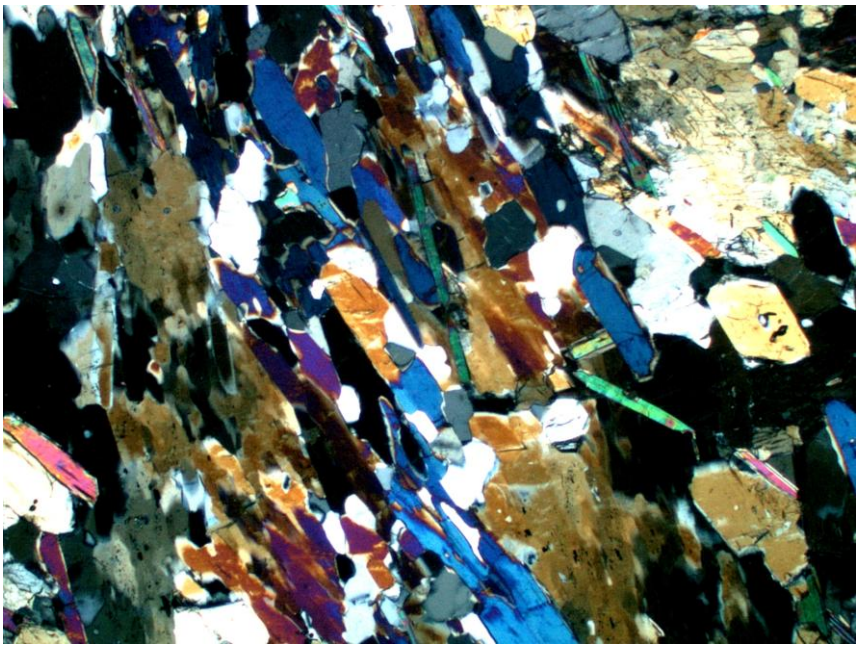

Fig 3.20 Photo micrograph of amphibole-biotite schist showing preferred orientation of biotite (Image is3mm across)

3.3.3 Garnetiferous schist

This unit outcrops at Brømnes. It is a medium grained micaceous schist with garnet porphyroblasts. It is distinguished from the garnet bearing schistose rocks of the Pre – Caledonian cover by the size of the garnet porphyroblasts. Whiles the garnets in the Pre – Caledonian cover are small in size (1- 3mm), those in the garnet – mica schist are large (1 – 4cm) and abundant. It has a well developed foliation, is heavily weathered, and interlayered with a calcsilicate bearing schist. There are few isolated hydrothermal quartz pods intruding the unit.

Fig 3.21 Large garnet porphyroblasts in garnet – mica schist. (Locality is Brømnes)

Petrography of Garnetiferous schist

The major minerals are garnet (25%), amphibole (30%), scapolite (25%), quartz (15%), plagioclase and microcline (8%). Zircon is an accessory. Garnet is subhedral and occurs in isolated clusters and is heavily altered. Inclusions of quartz and muscovite are present in the garnet porphyroblasts. Amphibole occurs both as hornblende and tremolite in approximately equal proportions. They show a preferred orientation (although this is not very pronounced). Quartz forms small subrounded grains and appears to be recyrstallized. Feldspars are minor and show few dissolution lamella.

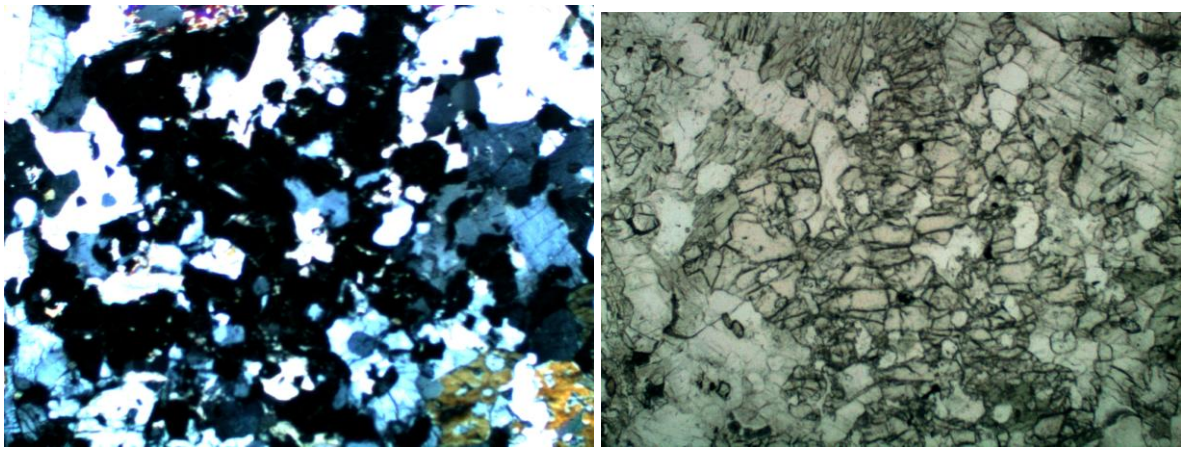

A. Cross nicols B. Plane polarized light

Fig 3.22 Heavily altered garnet with inclusions of quartz and plagioclase (Image is 3mm)

3.3.4 Calc - silicate bearing schist

Fresh outcrops of this unit are generally dark in colour (though not as dark as the dark mica schist) and composed of biotite, quartz, plagioclase and pyroxene. The dark colour is attributed to the presence of the pyroxenes.

It is fine grained and has a foliation defined by alternating greenish (dominated by pyroxene), dark (dominated by biotite) and light (dominated by quartzofeldspathic minerals) coloured areas.

Weathered outcrops of this unit display a more pronounced banding and a brown colour most likely due to the breakdown of the pyroxene minerals. It is the most dominant unit in the study area.

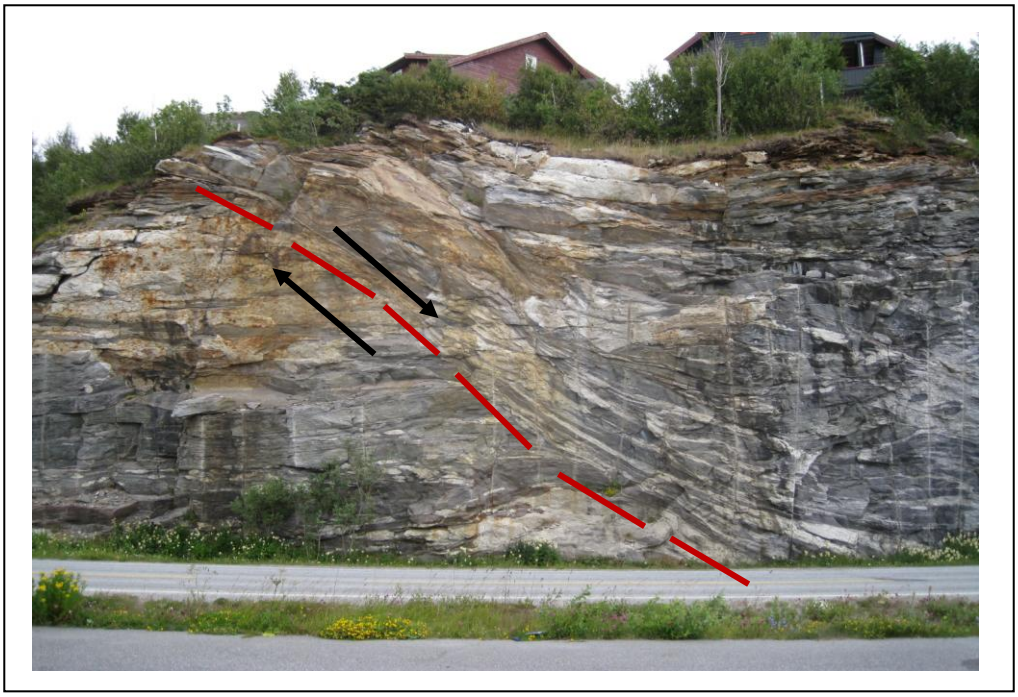

Fig 3.23 Late shear zone in an outcrop of calc-silicate bearing schist with hydrothermal quartz (Locality is near Lopsmarka on 834- road)

Fig 3.24 Hand specimen of calc-silicate bearing schist showing compositional layering of pyroxene (greenish layers) and quartzofeldspathic dominated areas

Petrography of Calcsilicate schist

This is composed of clinopyroxene (50%), plagioclase (15%), quartz (15%), biotite (10%) and microcline (10%). Clinopyroxene forms euhedral to subhedral crystals and display the distinct 90º cleavage. Plagioclase shows dissolution textures while microcline is minor and forms small subrounded grains. Intergrain boundaries are generally sharp.

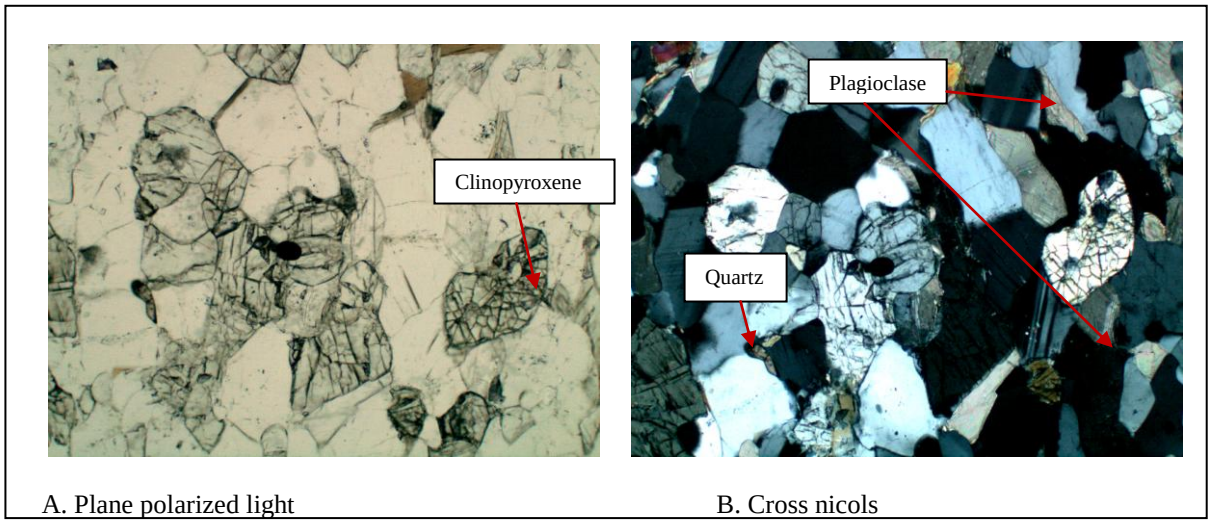

Fig 3.25 Photo micrograph of calcsilicate bearing schist showing main minerals and hypidiomorphic texture (Images are 3mm across)

3.3.5 Mica Schist

This unit occurs as an "enclave" within the calcsilicate bearing schist where it outcrops between Keiservarden and Ramnfloget, and eastwards near Maskiniset. It is medium grained, heavily weathered and has a weak foliation defined by alternating layers of dark coloured areas (dominated by biotite) and light coloured feldspathic layers. Some portions of the unit have garnets which are very small in size (≤ 1mm). Although it is essentially schistose, it appears to be more psammitic than the other units. Near Keiservarden, the rocks have very steep dips of about 70º unlike the other members of the group which have dips of ~ 10º.

Petrography of Mica schist

This is composed of plagioclase (35%), amphibole (30%), microcline (15%), quartz (15%) and biotite (5%). Most of the grains are subhedral; whiles quartz forms small subrounded grains which appear to be recyrstallized. Plagioclase shows exsolution lamella. Biotite is minor and forms anhedral grains

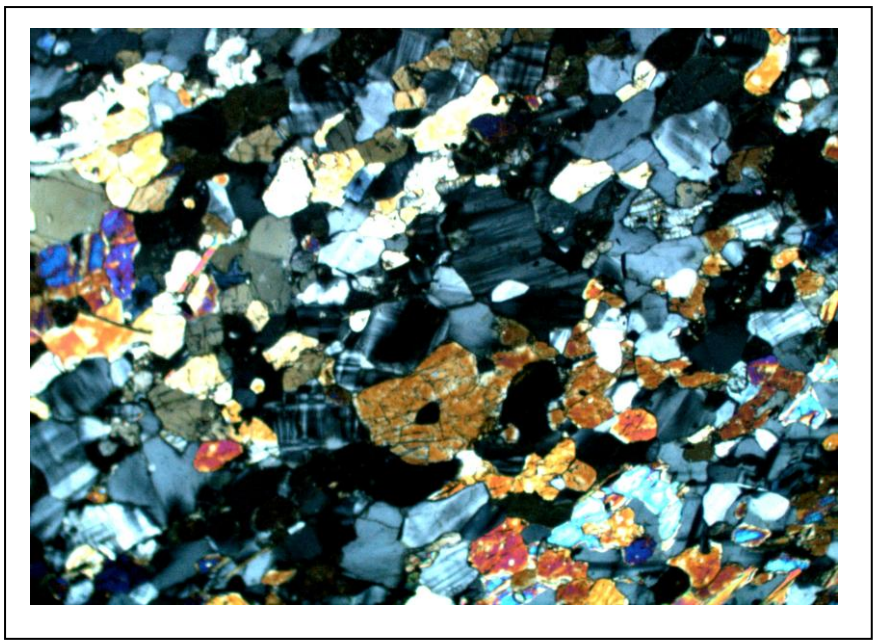

Fig 3.26 Photo micrograph of mica schist showing main mineral assemblage (Image is 3mm and magnification is 5X)

3.4 Structural Geology

3.4.1 The deformation history

From the observed field relationships, three different deformational events are inferred to have occurred. There are also late faults and joint which are considered to be post – Caledonian. These late structures are not discussed here.

3.4.1.1 The D1 event

This is the first deformational event that transformed the megacrystic granite into augen gneiss and orthogneiss, the mafic dyke into amphibolite, and produced the dominant foliation of both the Pre – Caledonian units and the Bodø Group rocks.

3.4.1.2 The D2 event

The second deformational event affected both the Pre – Caledonian and Bodø Group rocks. It was a deformational event which caused the folding of the dominant foliation developed by the first event. The folds which developed as a result of this event are generally tight isoclinal folds (with fold axes having trends between 200º - 206º) observed in the schists and ptygmatic folding of pegmatite intrusions in the gneisses. Where this event has not been overprinted by D3 (e.g. in Fig 3.26B below), the sense of shear appears to be top to the WNW.

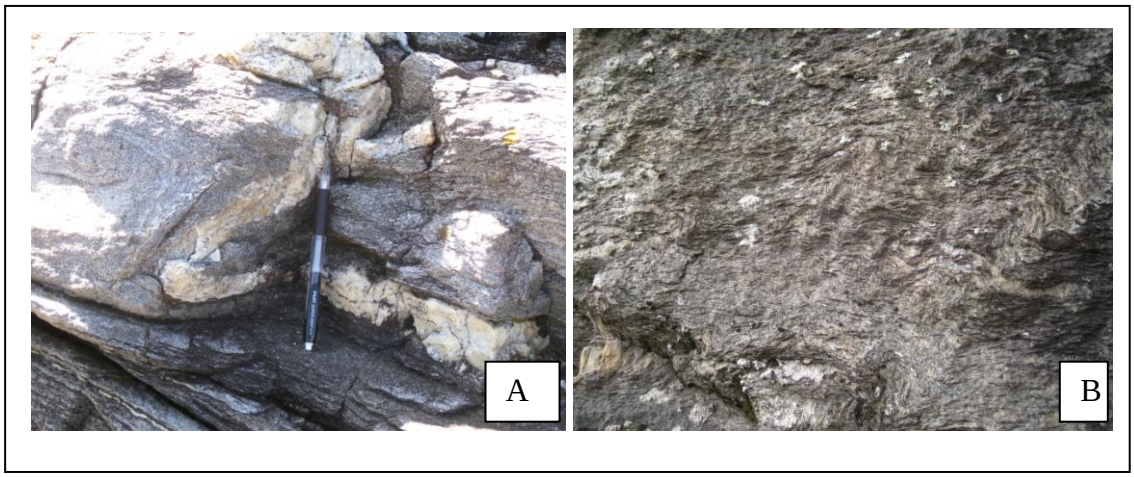

Fig 3.27 A tight isoclinally folded hydrothermal quartz vein in schist from the "cover sequence"

B Deformation of dominant foliation in schist from the "cover sequence"

3.4.1.3 The D3 event

A younger deformational event (D3) is identified by structures superimposed on the D2 folds. This is event affected the rocks to varying extents, most likely due to their compositional variations. In both the "cover sequence" and the Bodø Group, especially in the Burøya area, the folds are complex and tightly appressed, with an axial plane schistosity which dips steeply to the south but with enveloping surfaces having gentle dips. Large non – cylindrical folds plunging SSW are also present in this area. Generally though, the folds have a SW plunge. At Burøya, the rocks dip more steeply to the west and those at the extreme south of the peninsula dip to the south east, suggesting a large folded structure. Lineations are also common, most of which are stretching lineations defined by growth of micaceous minerals.

Where they are present in the D3 folds, the lineations are approximately parallel to the axial plane of the D3 folds.

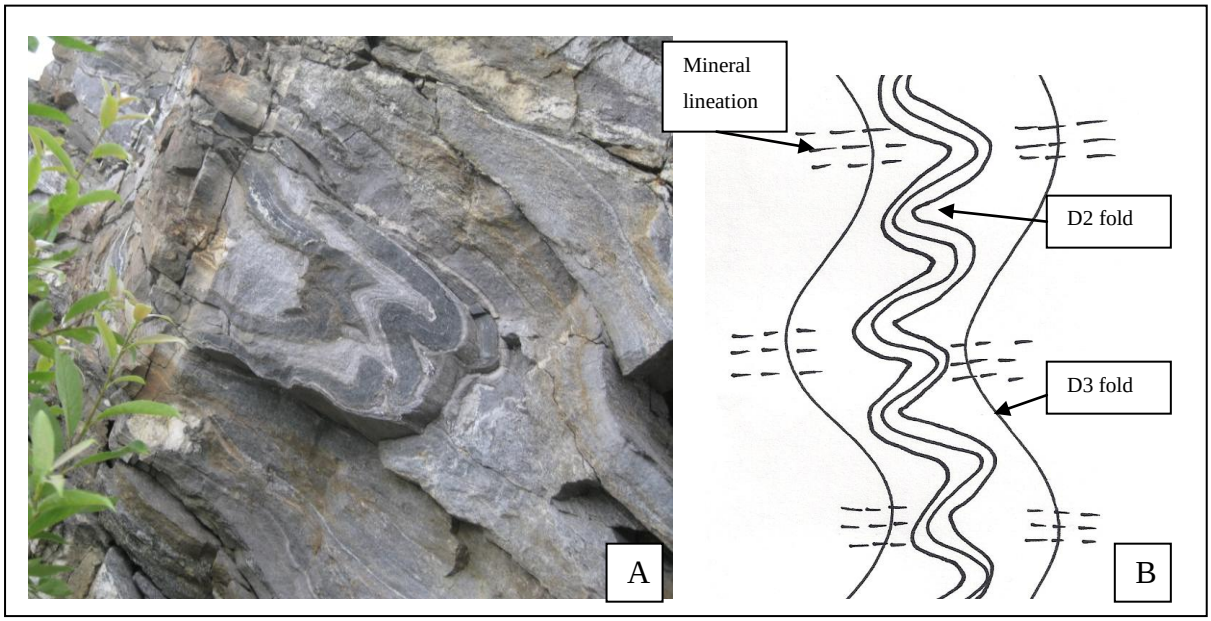

Fig 3.28 A Isoclinal fold related to D2 refolded by D3 event

B Sketch showing mineral lineation related to D3

3.4.2 Structural Trends

In the Pre – Caledonian rocks, the angle of dip of the dominant foliation is roughly uniform and is has a similar orientation to its cover sequence (striking NE and dipping ca. 30˚ to the NW), except in the Buroya area near the southwestern part of the Bodø peninsula (see Fig 3.28A). In the Buroya area, the rocks have dips which are considerably steeper (up to 85˚) than those in the Bratten area. The Caledonian supracrustal Bodø group, however, has a wider range of orientations and dip angles as can be seen in Fig 3.29B

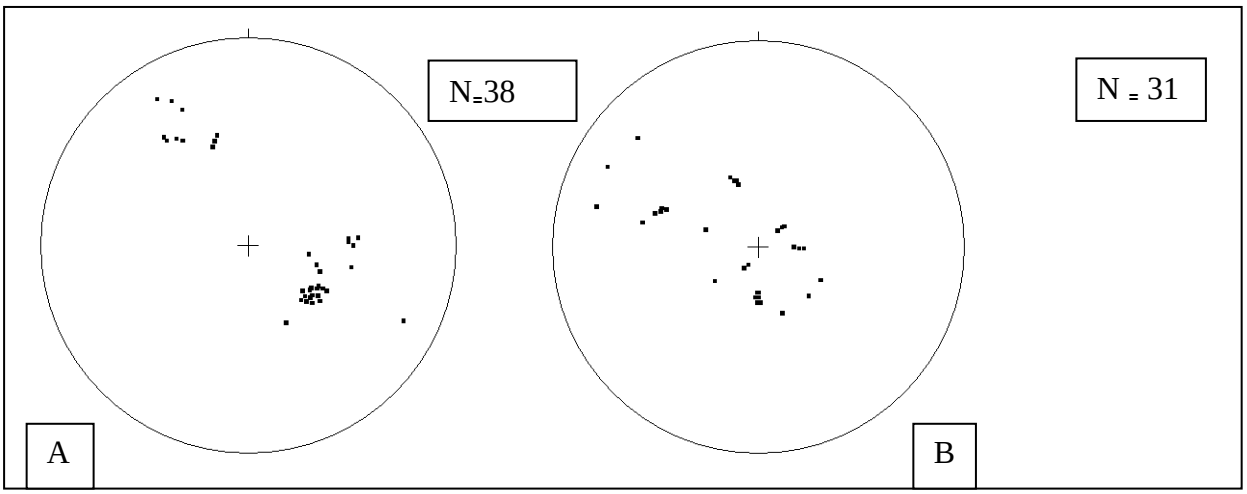

Fig 3.29 Stereographic presentation of structural data (Schmidt net, Lower hemisphere) A Poles of dominant foliation of gneisses and cover (Cluster to the NW is cover unit in Buroya, whiles cluster to the SE is gneissic foliation and cover in Bratten area)

B Poles of foliations in the Bodø Group

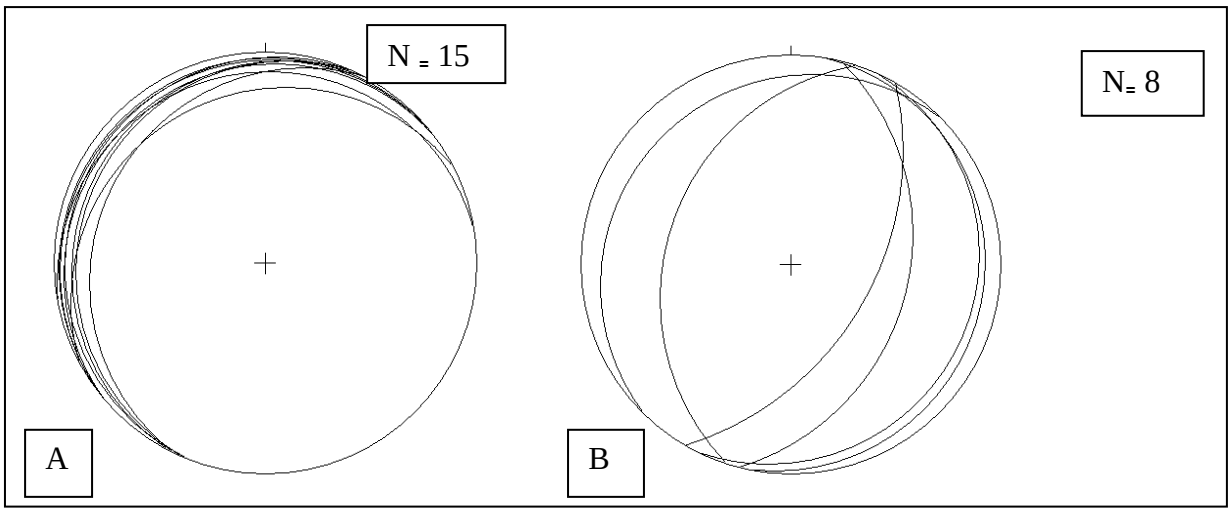

Fig 3.30 A. Stereographic presentation of fold axes from cover sequence

B. Fold axes from Bodø Group

4. Metamorphic Petrology

4.1 Introduction

Two main lithotectonic units are exposed in the Bodø area; Pre – Caledonian rocks (with cover sequence) and the Caledonian Bodø Group. The Pre – Caledonian rocks comprises megacrystic granite, progressively deformed to augen gneiss and orthogneiss (and the thin metasedimentary "cover sequence"), whiles the Bodø Group is mainly composed of metapelites. These units are proposed to be tectonically separated by a thrust (Rutland and Nicholson, 1969; Gustavson, 1991). No evidence for this thrust fault was observed. However, within thin the Pre – Caledonian rocks, a fault is observed to mark the transition between the augen gneiss and the orthogneiss.

To obtain information about the metamorphic condition of the area, two thin sections were made from rocks of useful composition for P – T studies. These were collected from both sides of the tectonic boundary proposed by Rutland and Nicholson (1969), and Gustavson (1991):

- NA 09 -3 is an orthogneiss from the Pre – Caledonian lithotectonic unit outcropping at the entrance to the Bratten quarry
- NA 09-15 is a garnetiferous schist from the Bodø Group outcropping at Brømnes.

Ideally, more than one sample should have been analyzed for P –T determinations, however, the mineral compositions of the rocks severely restrict the application of several geothermobarometers and quantitative results could be obtained only from the selected samples above.

Techniques in geothermobarometry are applied to chart P – T evolution of the selected samples. Geothermobarometry is a useful tool for quantitatively estimating the pressure and temperature of formation of an equilibrium mineral assemblage in a rock.

Whole rock modeling based on bulk rock chemical data was applied to constrain P-T paths due to the limited information obtained from traditional geothermobarometry. However, this could not be completed due to time constraints. The results are not included in this thesis.

4.2 Methodology

Pressure and temperature conditions of the selected samples were estimated based on element distribution in different minerals present in equilibrium in the rocks.

Chemical data of the important minerals were obtained by use of the Cameca SX – 100 electron microprobe at the University of Oslo. The microprobe is equipped with 5 crystal spectrometers and supporting software by Cameca. It was calibrated by using well characterized natural and synthetic standards. It was operated with an accelerating voltage of 15kV, a beam current of 10nA and a focused beam spot size of effectively, 1 µm. The beam spot size was changed to 10µm to cover a wider area and hence, disturb the mineral less strongly when feldspars were analyzed as plagioclase can be partially destroyed by the electron beam. Data reduction was done with a PAP – type correction and all iron present was assumed to be ferric iron.

4.3 Geothermobarometry

Geothermobarometry is the calculation of metamorphic pressures and temperatures of equilibration using the temperature and pressure dependence of the equilibrium constant as a benchmark (Spear, 1993). Stable mineral assemblages are dynamic and change in response to variations in temperature and pressure by chemical diffusion and/or reactions. Some mineral pairs are temperature sensitive (geobarometers) whiles others are temperature sensitive (geothermometers). Different calibrations are used for different geothermobarometers; some based on naturally occurring rocks, whiles others are based on empirical models (Spear, 1993). Net transfer reactions and exchange reactions are the two types of reactions employed by geothermobarometry.

4.3.1 Geothermometry

Most geothermometers are controlled by exchange reactions involving exchange of cations between silicates. Exchange reactions are excellent as geothermometers because of the very

small changes in volume associated with them. There are several exchange geothermometers, some of which have several calibrations. Holdaway's (2000) calibration of the garnet – biotite exchange geothermometer is applied in this work.

4.3.1.1 The Fe – Mg garnet – biotite exchange thermometer

A series of experiments were performed by Ferry and Spear (1978) on the Fe – Mg exchange reaction between biotite and Ca – free garnet. The equilibrium equation for the reaction was written as follows:

$$Fe_3A1_2Si_3O_{12} + KMg_3A1Si_3O_{l0}(OH)_2 \leftrightarrow Mg_3Al_2Si_3O_{12} + KFe_3A1Si_3O_{l0}(OH)_2$$

Almandine phlogopite pyrope annite

The above reaction can also be written as a cation exchange reaction between garnet and biotite:

$$Fe\ Mg^{Grt}_{-1} \leftrightarrow Fe\ Mg^{Bt}_{-1}$$

Perchuk and Laurent'eva (1983) also calibrated the thermometer and calculated temperature based on the following equation:

$$T\ (C) = \frac{7843.7 + \Delta V\ (P - 600)}{1.987\ \ln K_D + 5.699} - 273$$

Where V = a volume constant, P= pressure (bars), T = temperature (ºC), K_D = equilibrium constant

Holdaway's (2000) equation for calculating the temperature is used in this work, and is as follows:

$$T\,(K) = \frac{40198 + 0.295P + G + B}{7.802 - 3R\ln K_D}$$

Where R = molar gas constant, P = pressure (bar), T= temperature (Kelvin), K_D =equilibrium constant

G and B are evaluated based on Margules parameters for garnet and biotite respectively (Holdaway, 2000).

4.3.1.2 History of the garnet – biotite thermometer

Frost (1962) first used the Fe – Mg distribution between garnet and biotite to qualitatively determine the metamorphic grade of metamorphic rocks. Kretz (1964) suggested that the Fe – Mg distribution between garnet and biotite may be dependent on temperature and pressure but did not provide any formula for this. Perchuk (1967) had made an empirical calibration of the thermometer but this work was largely ignored by workers outside the then USSR. Subsequently, a K_D-T relationship was reported by several workers (Sen and Chakraborty (1968); Dahl (1969); Hietanen (1969); Lyons and Morse (1970) and Dallmeyer (1974). Saxena (1969) gave an empirical graphic presentation, while Perchuk (1970) proposed another empirical calibration. Later, empirical calibrations were proposed by several workers.

The first experimental calibration was introduced by Ferry and Spear (1978), involving a KFMASH system with a low Al biotite and equilibrated the phases at 600–800 °C at 2.07 kbar using the graphite–methane buffer. From then, this thermometer has been continuously revised by petrologists. Hodges and Spear (1982) mixed an assumed ideal biotite in the Ferry and Spear (1978) calibration with the Newton et al. (1977) Ca - Mg garnet Margules parameters and the garnet solution model by Ganguly and Kennedy (1974). Perchuk and Laurent'eva (1983) made an experimental calibration using pelites with garnet, high Al biotite and cordierite in the temperature range of 575–950 °C at 6.0 kbar by assuming no ferric iron in the product phases and also assuming ideal mixing for the phases. The non ideal mixing properties of quaternary biotite have not been addressed until Indares and Martignole (1985) first considered the effects of Ti and Al^{VI} in biotite as well as Ca and Mn in garnet. Almost all the later calibrations consider the non ideal, symmetric quaternary biotite and non ideal,

symmetric or even asymmetric quaternary garnet. Berman and Aranovich (1996) used mathematical programming methods and estimated entropy, enthalpy and volume Margules parameters for the FeMgCa garnets, with the added advantage of providing error values whiles Ganguly et al. (1996) estimated enthalpy and entropy Margules parameters for the FeMgCaMn garnets.

In the revision of the GB thermometer, most authors argued that ferric iron contents in garnet and biotite may be neglected. Williams and Grambling (1990) first considered Fe^{3+} in biotite; later Fe^{3+} was taken into account in several calibrations. Holdaway (2000) compares experimental datasets and garnet Margules parameters, and produces an average garnet model. Holdaway's (2000) calibration of the garnet – biotite geothermometer is considered one of the most accurate because it yields the smallest yields the smallest absolute error (±25ºC) in reproducing the experimental temperatures of Ferry & Spear (1978) and Perchuk & Laurent'eva (1983), in the wide temperature range 550 – 950ºC (Wu et al.,2004).

4.3.2 Geobarometry

Geobarometers are based on net transfer reactions that produce and consume phases. Net transfer reactions usually result in a significant change of volume and hence have a low slope on a P – T diagram. The equilibrium constant is thus, pressure sensitive (Spear, 1993). There are several geobarometers that are currently in use. One geobarometer that is very widely used and well calibrated is the garnet – aluminium silicate – plagioclase – quartz (GASP).

The garnet – biotite – plagioclase – quartz (GBPQ) geobarometer is based on the GASP geobarometer and is applicable to rocks which are depleted in/lack aluminium silicates, muscovites or both. This geobarometer is used in this study because no aluminosilicates were found in the samples, making the more popular GASP inapplicable.

4.3.2.1 The GBPQ geobarometer

The garnet – biotite geothermometer (Holdaway, 2000) and the GASP geobarometer (Holdaway, 2001) yield very close estimates for both experimental charges and natural rock

assemblages that are more precise than those obtained using alternative calibrations and are therefore used for the calibration of the GBPQ geobarometer (WU et al.,2004). In calibrating the GBPQ geobarometer, Wu et al. (2004) used the following steps:

- data for 224 aluminosilicate - bearing metapelites was collected from the literature to calibrate the GBPQ barometer
- an additional 89 aluminosilicate-bearing metapelites not included in the calibration, were used to test the validity of the GBPQ barometer
- the GBPQ barometer was applied to aluminosilicate-bearing and/or aluminosilicate-absent metapelites within thermal contact aureoles, and those within a limited geographical area without post-metamorphic structural discontinuity, to test the applicability of the GBPQ barometer.

From their results, they concluded that the GBPQ geobarometer may be applied to either aluminosilicate-bearing or aluminosilicate-free, medium- to high-grade metapelites.

The GBPQ geobarometer is based on the following Mg- and Fe- model equilibria by Hoisch (1991):

pyrope + grossular + eastonite + quartz ↔ anorthite + phlogopite

almandine + grossular + siderophyllite + quartz ↔ anorthite + annite

Chemical formulae for the minerals are shown below;

Pyrope = $Mg_3Al_2Si_3O_{12}$ Grossular = $2Ca_3Al_2Si_3O_{12}$

Eastonite = $K(Mg_2Al)(Si_2Al_2)O_{10}(OH)_2$ Almandine = $Fe_3Al_2Si_3O_{12}$

Siderophyllite = $K(Fe_2Al)(Si_2Al_2)O_{10}(OH)_2$ Annite = $KFe_3(AlSi_3)\ O_{10}(OH)_2$

Wu et al. (2004) used the Al avoidance model for plagioclase (Fuhrman and Lindsley, 1988), the biotite model from Holdaway (2000) and the average garnet model of Holdaway (2000) to derive two pressure dependant regression models. The formulae are as follows;

P (1) (bars)

$[1 - 0.081(-6Fb + Mgb + 2Cab)] = -24450.7 + 40.283T(K) + 59256.2X^{bio}_{Fe} + 0.081T(K)[-RlnK^{ideal}_{(1)} - 6Fa + 2Mga + 2Caa - 788.7X^{bio}_{Fe} - 6Fc + Mgc + 2Cac]$

and

P (2) (bars)

$[1 - 0.081(-6Fb + Feb + 2Cab)] = -19871.0 + 30.75T(K) + 66622.5(X^{bio}_{Fe} - X^{bio}_{Al}) +$

$1363.1X^{bio}_{Mg} - 74704.2X^{bio}_{Ti} + 0.081T(K)[(-RlnK^{ideal}_{(2)} - 6Fa + 2Caa - 840.9X^{bio}_{Fe} + 52.2 X^{bio}_{Mg} + 840.9 X^{bio}_{Al} + 1111.2 X^{bio}_{Ti}) - 6Fc + Fec + 2Cac]$.

Where Fa, Fb and Fc are polynomial expressions for the end members of plagioclase, and Caa, Cab, Cac, Fea, Feb, Fec, Mga, Mgb and Mgc are polynomial expressions for the end members of garnet. $K_{(1)}$ and $K_{(2)}$are equilibrium constants.

Wu et al. (2004) report that the calculated pressures P(1) and P(2) are fairly equal and use an average value.

4.3.2.2 The hornblende – garnet – plagioclase - quartz geothermobarometer

Calibration of this geothermobarometer by Dale et al. (2000) is mainly based on the calibrations of the garnet – hornblende thermometer by Graham and Powell (1984), the hornblende – plagioclase thermometer by Holland and Blundy (1994) and the garnet – hornblende – plagioclase – quartz barometers by Kohn and Spear (1989, 1990).

It is important to note that the lack of adequate mixing properties for amphibole and the poor correspondence between empirical constants used in thermodynamics and known entropies and enthalpies of reaction, make the application of geothermobarometry to amphibole bearing assemblages unsatisfactory (Dale et al.,2000). To resolve this problem, Dale at al. (2000) employ the internally consistent thermodynamic dataset of Holland and Powell (1998) as a basis for the derivation of parameters for a macroscopic non ideal mixing model of amphibole. Since this data set is consistent with a wide range of well constrained thermodynamic data, it allows greater confidence in the use of these geothermobarometers. In addition to this, Dale et

al. (2000) used a dataset derived from 74 naturally coexisting garnet – amphibole – plagioclase assemblage whose pressures and temperatures are well constrained to calibrate four independent equilibria for amphibole bearing assemblages based on the following reactions:

Eqn. 1 $ts + 4/3\ gr + 2/3\ py + 4\ q \leftrightarrow tr + 4\ an$

Eqn. 2 $parg + 2/3\ gr + 1/3\ py + 6\ q \leftrightarrow tr + 2\ an + ab$

Eqn. 3 $gl + 4/3\ gr + 2/3\ py + 4\ q \leftrightarrow tr + 2\ an + 2\ ab$

Eqn. 4 $fact + 5/3\ py \leftrightarrow tr + 5/3\ alm$

Where

Ts – Tschermakite $Ca_2Mg_3Al_4Si_6O_{22}(OH)_2$

Ab – Albite $NaAlSi_3O_8$

Tr - Tremolite $Ca_2Mg_5Si_8O_{22}(OH)_2$

An – Anorthite $CaAl_2Si_2O_8$

Gl - Glaucophane $Na_2(Mg, Fe)_3Al_2Si_8O_{22}(OH)_2$

Py - Pyrope: $Mg_3Al_2(SiO_4)_3$

Parg - Pargasite $NaCa_2Mg_3Fe^{2+}Si_6Al_3O_{22}(OH)_2$

Gr - Grossular: $Ca_3Al_2(SiO_4)_3$

Alm - Almandine: $Fe_3Al_2(SiO_4)_3$

Kpa – K- Pargasite $K\ NaCa_2Mg_3Fe^{2+}Si_6Al_3O_{22}(OH)_2$

Q – Quartz SiO_2

Fact – Ferro-actinolite $Ca_2Fe_5(Si_8O_{22})(OH)_2$

The first three reactions are net transfer equilibria involving garnet, hornblende, plagioclase and quartz whiles the fourth is a Fe – Mg exchange reaction between hornblende and garnet.

These thermometers and barometers are calibrated by fitting the natural data into the equilibrium relationship:

$\Delta G^o + RT\ln K_{id} + RT\ln K_{\gamma} = a + bT + cP + RT\ln K_{id} = 0$

where;

- a, b and c are constants in the Gibbs free energy of reaction calculated from the dataset of Holland and Powell (1998)
- K_{id} is the part of the equilibrium constant made up of ideal activities of the end members
- K_{γ} is the part of the equilibrium constant made up of the activity coefficients of end members and contains the mixing model parameters found by regression.

This result in the following calibrated equilibria can be directly applied to rocks to determine temperature and pressure (Dale et al., 2000);

Tschermakite – Tremolite

$$-12.25 - 0.1225T + 7.082P + RTlnK_{id} + 4\ RTlnK\gamma_{an} - 2/3\ RTln\ \gamma_{py} - 4/3\ RTln\ \gamma_{gr} + 20.3\ (P_{ts} - P_{tr}) - 20.3\ P_{gl} + 11.4P_{fact} + 11.1P_{parg} + 88.3P_{fts} + 35.8P_{kpa} = 0$$

Pargasite – Tremolite

$$-6.41 - 0.454T + 4.189P + RTlnK_{id} + 2\ RTlnK\gamma_{an} + RTln\ \gamma_{ab} - 1/3\ RTln\ \gamma_{py} - 2/3\ RTln\ \gamma_{gr} +$$

$$29.3\ (P_{parg} - P_{tr}) + 2.6\ P_{ts} - 49.2P_{gl} = 0$$

Glaucophane – Tremolite

$$26.17 - 0.1729T + 7.89\ P + RTlnK_{id} + 2\ RTlnK\gamma_{an} + 2\ RTlnK\gamma_{ab} - 2/3\ RTln\ \gamma_{py} - 4/3\ RTln\ \gamma_{gr}$$

$$+ 35.3\ (P_{gl} - P_{tr}) + 58P_{ts} - 55.2P_{parg} - 3.6P_{fact} - 38.8\ P_{kpa} = 0$$

Ferro-actinolite – Tremolite

$$-117.78 + 0.0578T - 0.722P + RTlnK_{id} + 5/3\ RTlnK\gamma_{py} - 5/3\ RTlnK\gamma_{alm} + 11.4\ (P_{fact} - P_{tr}) + 20.8P_{ts} + 17.9P_{parg} + 20.3P_{gl} + 49.8P_{kpa} = 0$$

4.4 Challenges in geothermobarometry and mineral selection criteria

It is necessary that any mineral assemblages used in geothermobarometry are in equilibrium. Where they are not equilibrated, the estimated temperatures and pressures will be erroneous. The textural relationships of the mineral assemblage must be considered in order to decide on which assemblage is in equilibrium.

During peak metamorphic conditions, crystals assumed to be in equilibrium are;

- Cores from large garnets. This is because they are less likely to be affected on the retrograde path due to slow intra-crystal diffusion
- Relatively large plagioclase porphyroblasts which grew prograde and are not recyrstallized
- Biotite crystals isolated in ribbon quartz are considered to be equilibrated at peak metamorphism due to their inability to react with the matrix along the retrograde path.

During post – peak metamorphic conditions, crystals assumed to be in equilibrium are;

- Garnet rims and adjacent plagioclase and biotite crystals. Garnet and biotite will equilibrate along the retrograde path through exchange reactions
- Plagioclase recyrstallizes adjacent to garnet on the retrograde path through net – transfer reactions

The estimation of peak metamorphic pressures and temperatures of a high grade rock are likely to be obscured by disequilibrium in the post – peak metamorphic mineral assemblage due to retrogression (Spear and Florence, 1992). The most important processes for this are phase reactions and intracrystalline diffusion (Spear and Florence, 1992). It is therefore, necessary that mineral compositions which are characteristic of the peak equilibrium conditions are identified, as well as their associated exchange reactions and/or net – transfer reactions.

4.4.1 Diffusion and net –transfer reactions

Fickian (volume) diffusion is mainly controlled by the diffusion porosity of a mineral, the size of the diffusing species, the thermodynamic stability of the species in the crystal lattice, and the temperature.

Spear and Florence (1992) conducted an experiment in coexisting garnet and biotite to study variations in (Fe/Fe + Mg) ratio when cooling from peak metamorphic conditions, to document the effect(s) diffusion may have on a geothermometer. This is illustrated in Fig 4.1 a – d. Their results are summarized below;

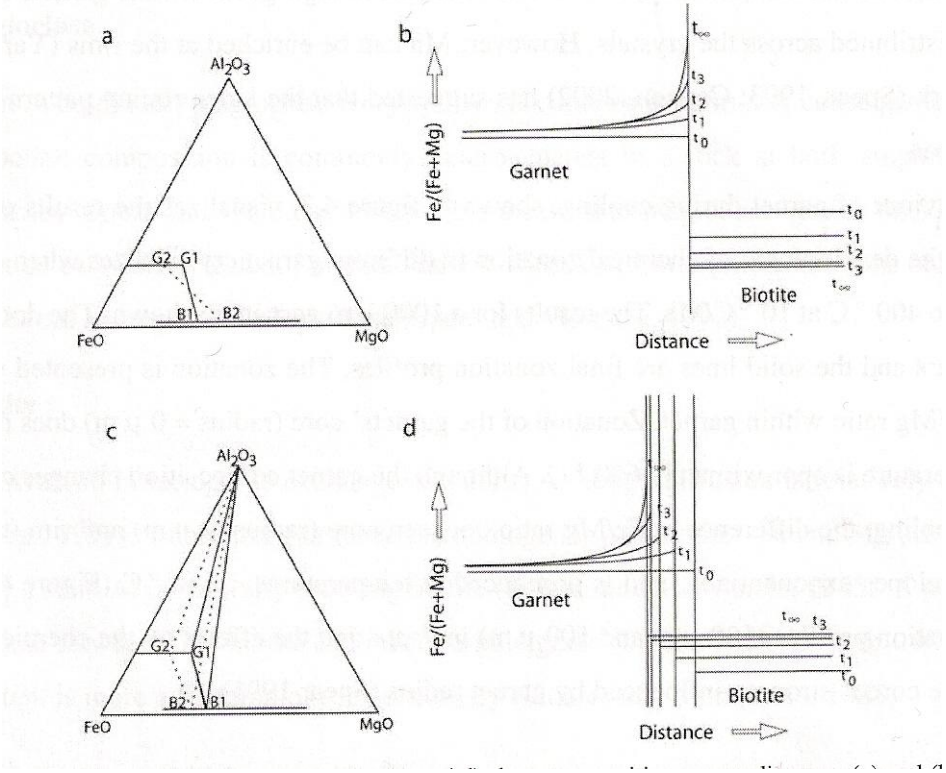

Fig 4.1 (a) and (c) are AFM diagrams. (b) and (d) show composition versus distance. (a) and (b) show the results of Fe – Mg exchange between garnet and biotite at different time steps. (c) and (d) show development of the same exchange reaction as (a) and (b) plus the net transfer reaction; garnet + k-feldspar + water ↔ sillimanite + biotite + quartz. Reproduced from Spear and Florence (1992)

During cooling, the Fe/Fe+Mg ratio increases as opposed to the Fe/Mg content in the biotite rim. Due to the higher intracrystalline diffusion in biotite, its composition is homogeneous; whiles garnet develops a heterogeneous chemistry and displays chemical zoning because of the inefficiency of intracrystalline diffusion at temperatures lower than 675˚C. Spear (1991) shows by numerical modeling that diffusion rates are high enough to homogenize a garnet at temperatures between 650˚C and 700˚C due to a greater velocity of diffusion. Spear (1991) further shows that the degree of homogenization is also partially controlled by the radius of garnet (Fig 4.2).

In biotite, temperatures above 500˚C are enough to homogenize biotite irrespective of cooling rate and crystal size (Spear, 1991; Spear and Florence, 1992)

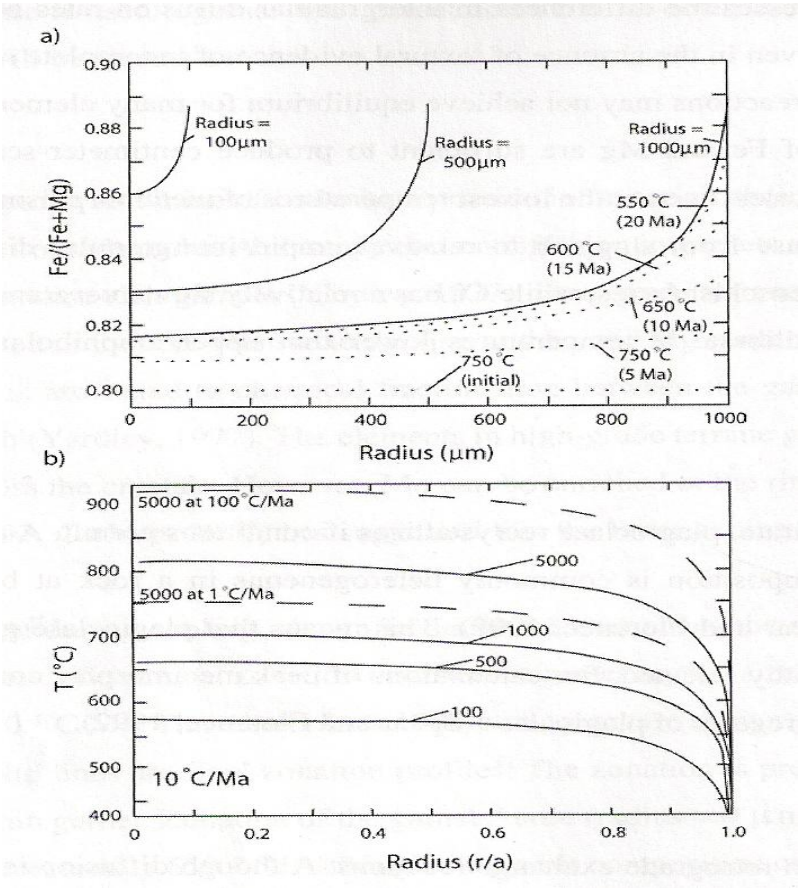

Fig 4.2 (a) Plots from Spear (1991)/ Fe/Fe+Mg vs. radius for garnets cooled from 750˚C to 400˚C. The cooling rate is 10˚C/Ma. The solid lines show final zonation profiles whiles the dashed lines show evolution of diffusion zoning for garnets of radius 1mm. (b) Calculated temperatures vs. normalized radius for garnets of different sizes when the cooling rate is 10˚C/Ma.

If a net – transfer reaction occurs concurrently with Fe- Mg exchange during cooling, the Fe/Mg ratio in both garnet and biotite will increase (Fig 4.1c). Where garnet is the product and biotite is the reactant (Fig 4.1d), Fe/Fe + Mg content increases in both minerals.

In the event of the biotite producing reaction;

Biotite + aluminosilicates + plagioclase + quartz↔ k-feldspar + garnet + melt (Le Breton and Thompsom, 1988), biotite integrates the Fe released by garnet leading to a scenario where retrograde biotite records a higher Fe content than peak metamorphism biotite. Where such biotite crystals are used in a calibration with a core garnet, the calculated temperature is too

high (Spear and Florence, 1992). However, since the sample under consideration does not contain aluminosilicates, this problem is not encountered.

The GASP geobarometer is based in part, on the Ca content in garnet and plagioclase and for it to be applicable; the rock must have produced or consumed plagioclase and garnet (Spear and Florence, 1992). Since the GBPQ geothermobarometer is calibrated based on the GASP barometer, this must also hold for samples to which the GBPQ geothermobarometer is applied to.

Plagioclase does not re-equilibrate by diffusion since the intracrystalline diffusion in NaSi – CaAl in plagioclase at temperatures below 900˚C is very slow, and would therefore re-equilibrate with a coexisting garnet by recrystallizing to a mew composition (Spear and Florence, 1992).

The X_{gr} content in garnet rims decreases whiles X_{an} increases in plagioclase during retrogression, thus, the recyrstallized plagioclase will only be in equilibrium with the garnet rims. Consequently, plagioclase composition in a rock is commonly heterogeneous at both amphibolite and granulite facies (Spear and Florence, 1992). Peak metamorphism conditions determined by recyrstallized plagioclase and garnet cores are therefore erroneous.

4.5 Electron Microprobe analyses and results

Sample NA 09-3

The garnets in this sample are 300 - 700µm across. The primary end members are grossular and almandine. Some crystals show increasing grossular from core to rim (X_{gr} = 0.34 – 0.46) whiles almandine is fairly constant (X_{alm} = 0.15 – 0.16) for one equilibrated assemblage and for another equilibrated cluster, X_{gr} =0.38 – 0.61 and X_{alm} = 0.12 – 0.14.

Plagioclase has a range of composition X_{an} = 0.49 – 0.51; X_{al} = 0.68 – 0.70. One potassium feldspar crystal shows a composition of X_{san} = 0.93; X_{ab} = 0.507

The amount of titanium in present in individual biotite crystals is fairly constant although there are some variations between different crystals.

The presence of the sanidine end-member in K – feldspar and the relatively high amounts of Mn in garnet suggest high temperatures and pressures respectively.

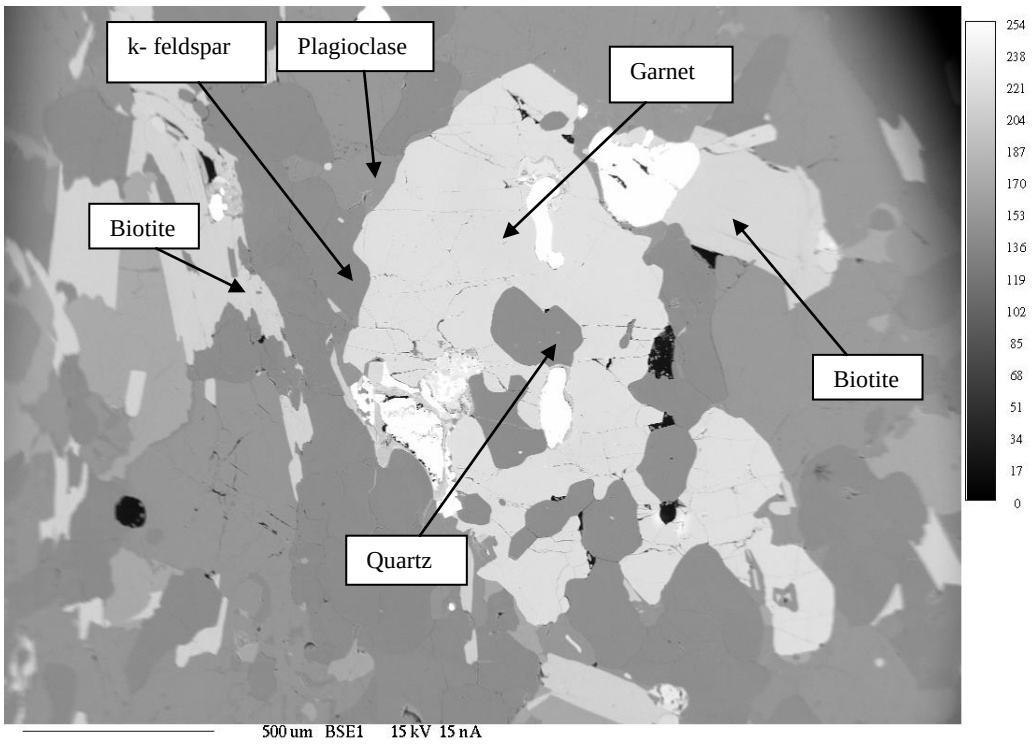

Fig 4.3 Electron backscatter image showing equilibrated mineral assemblage

The GBPQ geothermobarometer is applied to this sample.

The reactions used to estimate P and T are;

- py + ann = alm + phl
- 2gr + 3alm + 3east + 6q = 2py + 3ann + 6an

Table 3 Estimated P – T values for sample NA 09-3

P	1	3	5	7	9	11	13	15	17	19		
av T (˚C)	212	312	412	512	612	712	812	912	1011	1110		
SD	267	229	192	154	115	76	41	42	46	86		
Sig Fit	6.8	5.8	4.8	3.8	2.8	1.9	0.9	0.1	1.1	2		
T	100	200	300	400	500	600	700	800	900	1000	1100	1200
av P(kbar)	1.6	3	4.6	6.2	7.9	9.6	11.3	13	14.8	16.5	18.2	
SD	5.54	4.82	4.12	3.44	2.75	2.07	1.39	0.88	0.98	1.07	1.41	2.13
Sigma Fit	16.6	11.9	8.6	6.2	4.4	2.9	1.7	0.8	0	0.7	1.2	1.7

SD =Standard deviation

From the results, the pressure is estimated to be between 11.3kbars – 18.2 kbars, whiles temperatures are estimated to be between 812˚C - 1011˚C.

Sample NA 09 -15

The garnets are mainly composed of grossular and almandine with spessartine, pyrope and andradite being minor components. Grossular decreases from the core to the rim (X_{gr} = 0.077 – 0.058); whiles X_{alm} does not show a clear trend.

Plagioclase, amphibole, plagioclase and scapolite do not show any significant variation. Although scapolite is not necessary for the application of the Hornblende – garnet – plagioclase - quartz geothermobarometer, it is analyzed due to the fact that it is Ca-bearing and this may be exchanged with garnet as is the case in plagioclase.

Reactions used to estimate P and T are;

- 2py + 4gr + 3ts + 12q = 3tr + 12an
- 6tr + 21an = 10py + 11gr + 27q + 6H2O
- 6fact + 21an = 11gr + 10alm + 27q + 6H2O
- 4py + 8gr + 9ts + 6ab = 3tr + 6parg + 24an

The results obtained are;

T = 750˚C, sd = 116,

P = 8.1 kbars, sd = 1.2, cor = 0.480, sigfit = 2.24

The complete dataset obtained from the microprobe analyses is presented in Appendix 1.

4.6 Discussion

In the orthogneiss, the a temperature of 712˚C is estimated for a 95% confidence and a sigma fit of 1.9 and a pressure of 11.3kbars, whiles the calculated temperature and pressure in the Bodø Group metasediments are 750˚C and 8.1 kbars.

This makes the temperature in the Bodø Group higher than that in the Pre – Caledonian gneisses. The current interpretation by Nicholson and Rutland (1969) and Gustavson (1991) that the gneisses are deep seated rocks which have been thrust onto the Bodø Group suggests that the temperatures recorded in the gneisses to be higher than that in the Bodø Group unless of course the calculated values do not represent peak metamorphic conditions.

Higher values of T (812˚C - 1011˚C) with a corresponding sigma fit values of 0.9 – 1.1 are quite considering that the sigma fit values are much closer to 1. Further, the presence of the sanidine end member in k – feldspar increases the likelihood of temperatures higher than 712˚C.

The lower temperatures calculated may be due to some disequilibrium in the mineral assemblage. Also, the anhydrous nature of the rock makes it quite possible that even at temperatures of about 812˚C - 900˚C, melting would not have taken place. A temperature of about 800˚C for the recording peak metamorphism of the gneiss is therefore considered more likely.

If this is so, the metamorphic grade decreases from granulite facies in the Pre – Caledonian gneisses to amphibolite facies in the Bodø Group supracrustals.

5. Geochronology

5.1 Introduction

Studied samples were taken from key units for U –Pb zircon dating. magmatic zircons from the Heggmovatn area were dated by thermal ionization mass spectrometry (TIMS) whiles clastic zircons and magmatic zircons from the Bratten area were dated by laser ablation - induced coupled plasma mass spectrometry (LA - ICPMS). Samples were taken from the supposed basement unit in Western Bodø and its intrusive units. The Heggmovatn metasediments were also sampled for provenance studies. Two generations of intrusives from the Heggmovatn dome were also sampled for TIMS dating. The TIMS dating was done by Lars Augland Eivind although sample preparation was done by me.

5.2 Analytical Procedure for TIMS

Sample processing was done at the University of Oslo. The samples were crushed and separated by standard mineral separation methods (wilfley table, heavy liquid and magnetic separation) and zircons were handpicked and discriminated on the basis of morphology, transparency, colour and internal textures. Air-abrasion (Krogh, 1982) was conducted, and grains were washed in dilute HNO_3, ionized water and acetone using an ultrasonic bath, before weighing and spiking (^{202}Pb - ^{205}Pb – ^{235}U tracer). The zircons were dissolved in HF and a drop of HNO_3 in Teflon bombs at c. 190° C for 5 days. U/Pb-solutions were dried down and loaded on degassed single Re filaments with silica gel and measured on a Finnigan MAT 262 mass spectrometer, using either Faraday cups in static mode or, for low-intensity samples, a Secondary Electron Multiplier (SEM) in peak jumping mode. $^{207}Pb/2^{04}Pb$ ratios were measured on SEM for all samples. SEM data were corrected for non-linearity based on measurements of the standard NBS 982-Pb + U500 (Corfu, 2004). Measurements were corrected for a 0.1 pg U and 2 pg Pb blank, with Pb blank compositions: $^{206}Pb/^{204}Pb$ = 18.3, $^{207}Pb/^{206}Pb$ = 0.85 and $^{207}Pb/^{204}Pb$ = 15.555 (Corfu, 2004). As the analyzed rocks have a juvenile character (refs.) common Pb corrections were employed using the depleted mantle Pb-evolution (ref) at the age in question. U source fractionation was estimated to be 0.12 % / a.m.u. Pb source fractionation was corrected for using the measured $^{205}Pb/^{202}Pb$ tracer ratio, normalized to the certified value of 0.44050. A standard fractionation error of 0.06 % /a.m.u.

is incorporated in the calculations if the $^{205}Pb/2^{02}Pb$ ratio is determined very precisely and the fractionation corrections become unrealistically precise. If $^{205}Pb/^{202}Pb$-ratio is not determined, or the measured $^{205}Pb/^{202}Pb$-ratio is far of from 0.44050, Pb fractionation is set at 0.1 % /a.m.u. Pb fractionation values between 0.06 - 0.1 % / a.m.u. are generated by this procedure. The analytical errors and corrections were then incorporated and propagated using the ROMAGE 6.3 program, originally developed by T. E. Krogh. Graphic presentations and age-calculations were performed using the ISOPLOT program of Ludwig (2003). All errors are reported at the 2-sigma confidence interval.

5.3 Analytical procedure for LA – ICPMS

Sample processing was done at the University of Oslo. The samples were crushed and separated by magnetic and heavy liquid separation methods and zircons were handpicked and discriminated on the basis of morphology, transparency, colour and internal textures. Selected zircons were mounted in epoxy and polished. Zircons were imaged on a JEOL JSM 6460LV scanning electron microscope prior to analysis using a combination of backscattered electron and cathodoluminescence imaging.

U–Pb dating was performed by ICPMS using a Nu Plasma HR multicollector system with a U–Pb collector block and a New Wave/Merchantek LUV-213 laser microprobe at the Department of Geosciences, University of Oslo. The mass spectrometer is equipped with a specially designed U–Pb collector block, which allows simultaneous detection of masses 204, 206 and 207 in ion counters and mass 238 in a Faraday detector. Ablations were made in helium, which was mixed with argon prior to entering the ICP. Laser conditions were: 40 μm beam diameter, 10 Hz repetition rate, energy density ≤0.10 J/cm2. Ablations were static, and measurements were made in time-resolved mode. The contribution of 204Hg from the plasma was eliminated by on-mass background measurement prior to each analysis. At the low laser power used, no excess ionization of Hg during ablations was observed.

A single measurement included 30s of on-mass background measurement, followed by 60s of ablation in helium with a 55-*l*m stationary beam. Raw data from the instrument were corrected for background and calibrated against zircon 91500, applying a sample-standard bracketing protocol similar to that of Jackson et al. (2004), in an interactive Excel spreadsheet program. Common lead was corrected using mass 204 as a monitor for 204Pb, and corrections were

applied where needed using the Stacey–Kramers common-lead composition for the appropriate age (Stacey and Kramers 1975). Only zircons which showed less than 10% discordant are used.

5.4 Heggmovatn units

The rocks of the Heggmovatn have been considered by several workers to represent a major basement culmination comparable to the Rishaugfjellet and Glomfjord culminations (Rutland and Nicholson, 1965; Rutland and Nicholson, 1969; Gustavson 1991). However, the rocks of the Heggmovatn are atypical of the Baltic basement as described in other basement windows. Whereas orthogneisses dominate the Rishaugfjellet dome comparable with basement rocks exposed in the Tysfjord and Glomfjord culminations, the Heggmovatn area dominated by alternating metapsammites and metapelites. Cross-bedding is locally observed in the meta-psammites. The Heggmovatn metasediments are intruded by both pre-, syn- and post-tectonic granitoids

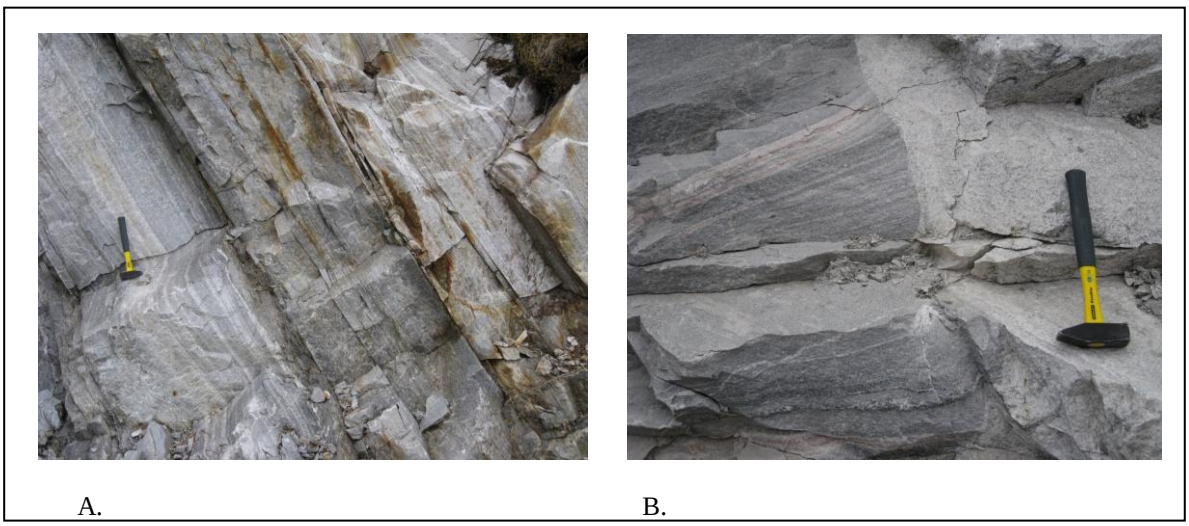

A. B.

Fig 5.1 A. Quartzitic metapsammite (AA 09 - 8 sampled for zircon provenance studies)

B. Arkosic metapsammite cut by granite (Granite AA 09 - 10 sampled for U – Pb dating)

A B

Fig 5.2 Foliated and folded orthogneiss (AA 09 - 11) sampled for ID-TIMS dating.

B is a close up picture of A (bottom left) showing folding of the primary foliation

5.4.1 Cross – cutting Granite (AA 09-10)

This is an undeformed granite that cuts across a metapsammite. There were few zircons in this sample, but the ones that are there can be divided in two main groups:

1. clear colourless to slightly yellowish prisms dominated by {100} shapes. The zircons have few inclusions and aspect ratios of 1:4 – 1:5;

2. slightly yellowish, metamict or altered zircons also dominated by {100} shapes. These zircons contain some inclusions. Aspect ratios range between 1:4 – 1:7.

The fractions that gave almost concordant Caledonian ages were from group 2 (pictured below).

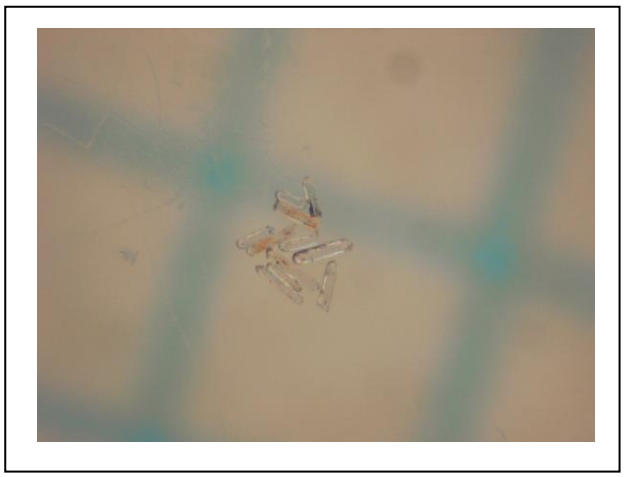

Fig 5.3 Zircons from group 2 that yielded near concordant ages

Table 4. Analytical U- Pb data from cross cutting granite (AA 09 -10)

Fraction Analysed	Weight	U	Th/U	Pbcom	206/204	207/235	2 sigma	206/238	2 sigma	rho	207/206	2 sigma	206/238	2 sigma	207/235	2 sigma	207/206	2 sigma	Disc.
	[ug]	[ppm]		[pg]			[abs]		[abs]			[abs]		[abs]		[abs]		[abs]	[%]
AA09-10_241/12	1	359	0.81	1.1	3195	1.98679	0.00708	0.15584	0.00049	0.85	0.09246	0.00017	933.6	2.7	1111.0	2.4	1476.9	3.5	39.5
AA09-10_241/10	6	91	0.37	2.8	869	0.52586	0.00374	0.06926	0.00019	0.53	0.05507	0.00034	431.7	1.1	429.1	2.5	415.0	13.6	-4.1
AA09-10_241/11	3	4014	0.16	4.9	12311	0.77217	0.00328	0.07986	0.00031	0.96	0.07013	0.00009	495.3	1.8	581.0	1.9	932.2	2.5	48.7
AA09-10_246/4	1	317	0.81	0.9	1503	0.52729	0.00331	0.06916	0.00030	0.68	0.05530	0.00026	431.1	1.8	430.0	2.2	424.3	10.3	-1.6

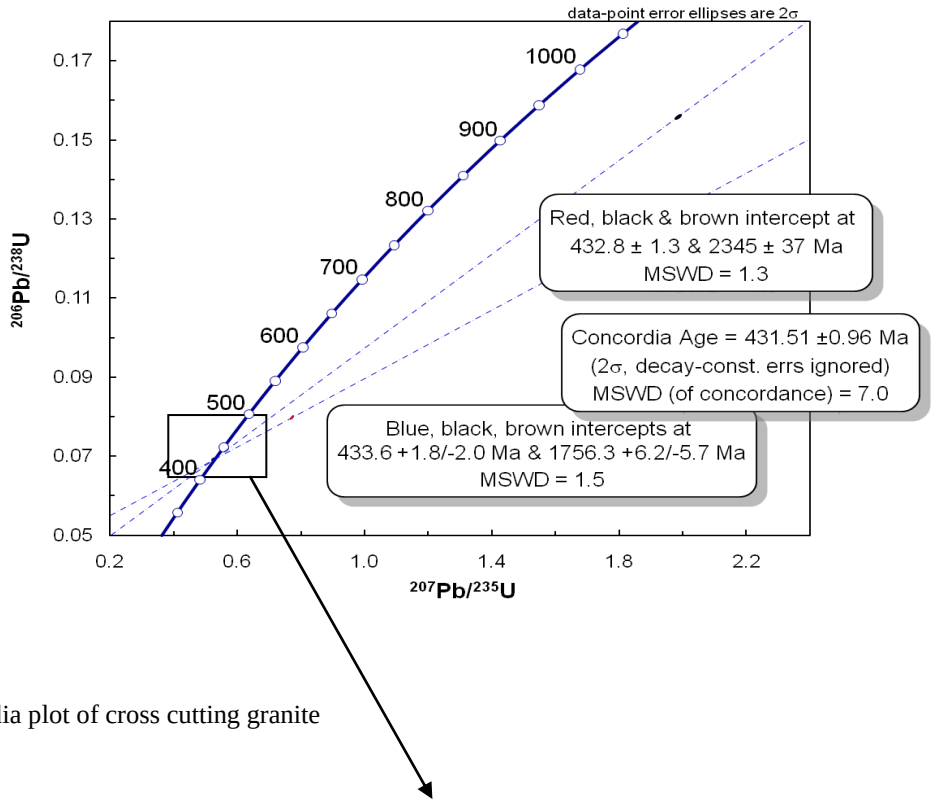

Fig 5.4 Concordia plot of cross cutting granite

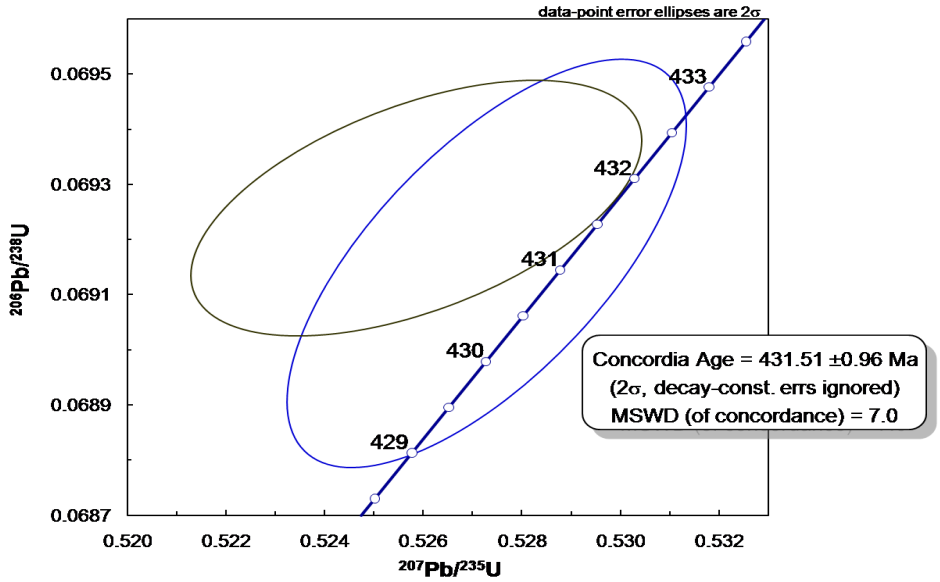

Fig 5.5 Close up image of 5.3 showing concordia age

The older discordant grains are inherited zircons from the host rock which how lead loss. They define 2 discordia lines which intercept the concordia at 432.8 ± 1.3 and 433.6 ± 2.0 Ma. This intercept coincides with two concordant zircons. The age obtained from these

concordant points is 431.5 ± 1 Ma (2σ, MSWD=7.0), and is interpreted to be the emplacement age of the granite.

5.4.2 Deformed orthogneiss (AA 09 – 11)

Zircons were abundant in this sample. The zircon grains can be divided in four main groups:

1. small, clear colourless, euhedral prisms dominated by {100} shapes. Few inclusions and aspect ratios between 1:2 and 1:4.

2. clear, slightly yellowish, euhedral grains with high aspect ratios between 1:4 and 1:7.Most grains dominated by {100}, but some by {110}, crystal shapes. Few inclusions.

3. yellow, stubby prism shaped grains. The grains are metamict and dominated by {100} crystal faces. Aspect ratios from 1:2 -1:4.

4. clear, colourless grains with flat terminations dominated by {100} shapes. These grains contain few inclusions.

The least discordant point was from group 2 (pictured below).

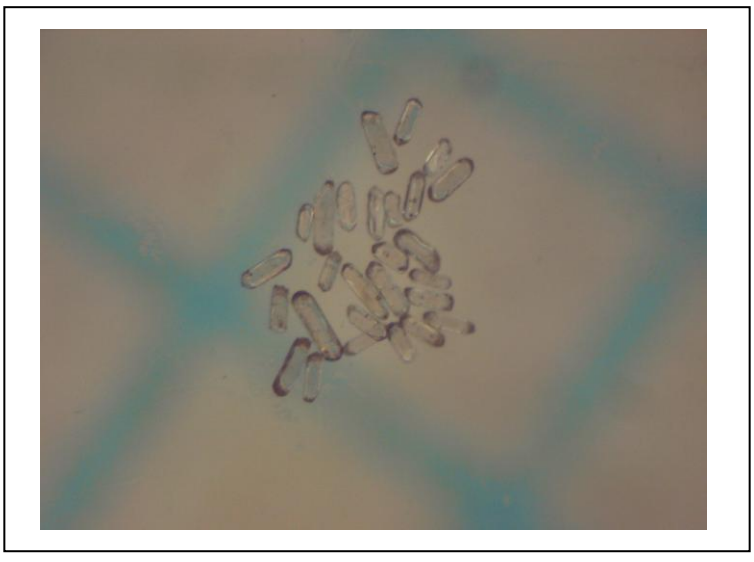

Fig 5.6 Clear euhedral zircons from group 2

Table 5. Analytical U - Pb data from folded orthogneiss (AA 09 – 11)

Fraction Analysed	Weight	U	Th/U	Pbcom	206/204	207/235	2 sigma	206/238	2 sigma	rho	207/206	2 sigma	206/238	2 sigma	207/235	2 sigma	207/206	2 sigma	Disc.
	[ug]	[ppm]		[pg]			[abs]		[abs]			[abs]		[abs]		[abs]		[abs]	[%]
AA09-11_241/2	4	260	0.40	1.8	5809	1.69438	0.00424	0.16381	0.00036	0.86	0.07502	0.00010	977.9	2.0	1006.4	1.6	1069.0	2.5	9.2
AA09-11_246/5	10	134	0.45	2.4	5123	1.42956	0.00420	0.14867	0.00039	0.83	0.06974	0.00011	893.5	2.2	901.4	1.8	920.7	3.3	3.2
AA09-11_246/6	8	471	0.44	2.6	12803	1.33653	0.00328	0.13983	0.00030	0.91	0.06932	0.00007	843.7	1.7	861.7	1.4	908.3	2.1	7.6
AA09-11_246/7	1	518	0.32	5.9	840	1.28314	0.02875	0.15019	0.00077	0.43	0.06196	0.00128	902.0	4.3	838.3	12.7	672.8	43.7	-36.5
AA09-11_246/12	1	1207	0.36	2.0	5589	1.42510	0.00580	0.14695	0.00055	0.92	0.07034	0.00011	883.8	3.1	899.5	2.4	938.2	3.2	6.2

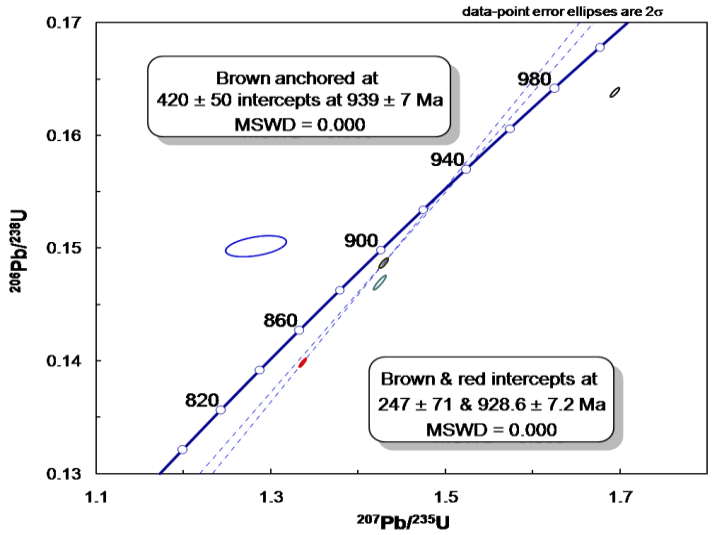

Fig 5.7 Concordia plot of deformed orthogneiss

The zircons, as can be seen from the plot above have suffered progressive lead loss that define a discordia line with an upper intercept age of 928 ± 7.2 Ma (2σ, MSWD = 0.000), which is considered to represent the crystallization age of the protolith.

5.4.3 Quartzitic metapsammite (AA 09 – 8)

The analytical results for this sample are presented in appendix 2

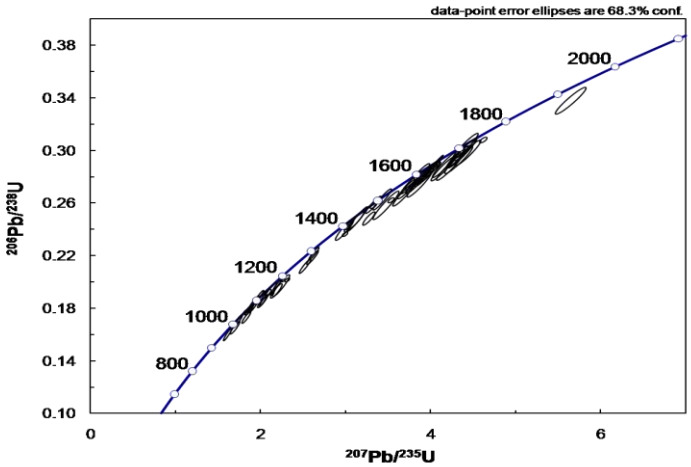

Fig 5.8 Concordia plot of Quartzitic metapsammite showing all data points

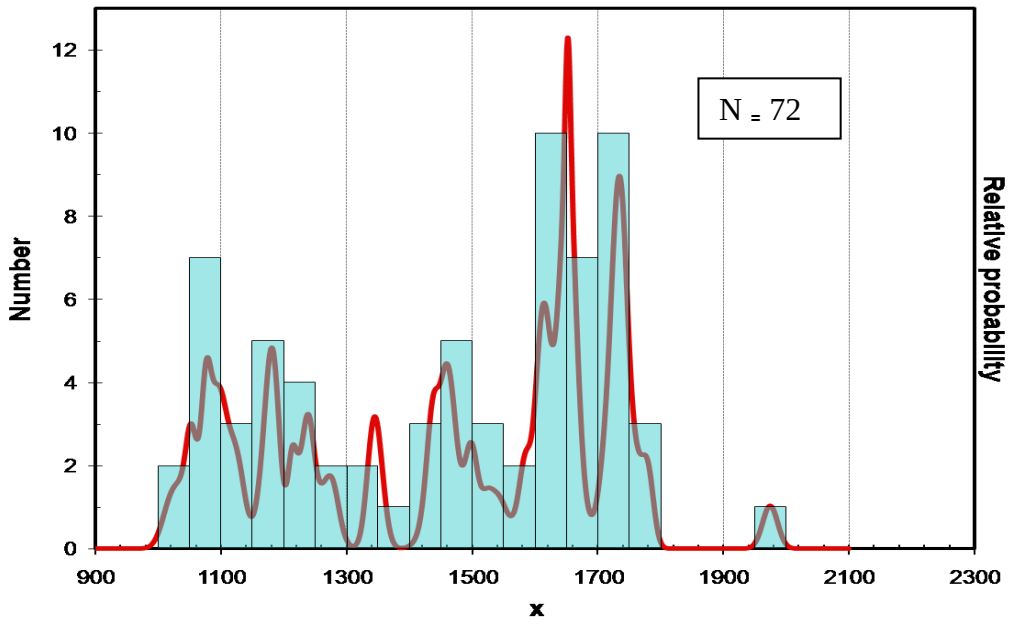

Fig 5.9 Graph showing age distribution of zircon populations in Quartzitic metapsammite

5.5 Western gneissic area (Bratten)

The granitic gneisses and oryhogneisses at the western part of Bodø (at Bratten) as well as their associated intrusives are analyzed here.

5.5.1 Megacrystic granite (NA 09 – 5)

After the selected zircons had been handpicked, they were imaged by a JEOL JSM 6460LV scanning electron microscope (SEM) prior to analysis using a combination of backscattered electron and cathodoluminescence imaging. This was to check for homogeneity of the zircon crystals. Most zircon crystals in the sample are moderately elongated euhedral to subhedral prisms with terminal pyramid faces.

Some crystals show low-wavelength–moderate-amplitude oscillatory zoning on cathodoluminescence (CL) images (Fig 5.8C), which is characteristic of primary magmatic zircon (Corfu et al. 2003).The zircons which showed zoning were duly noted. Some of the xenocrystic cores show oscillatory magmatic zoning and are relatively bright in CL (Fig.

5.8H), whereas others are metamict, turbid in transmitted light, darker in CL than the rims and without, or with only weak oscillatory zoning (Fig 5.8G).

The cores and rims of these zoned zircons were analyzed separately. Those zircons which were not zoned were fairly uniform in appearance and size. They were well formed and did not show any fracturing or deformation.

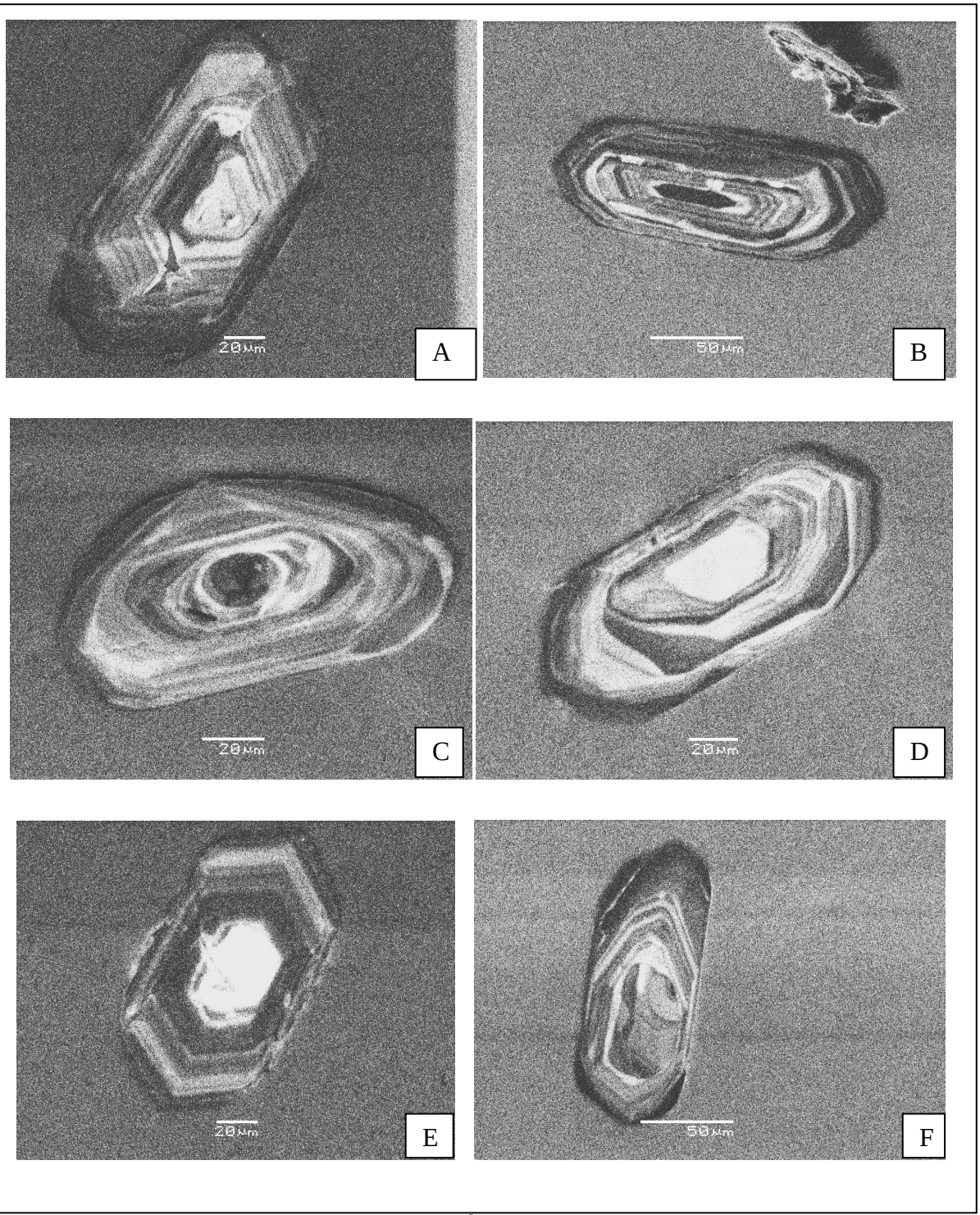

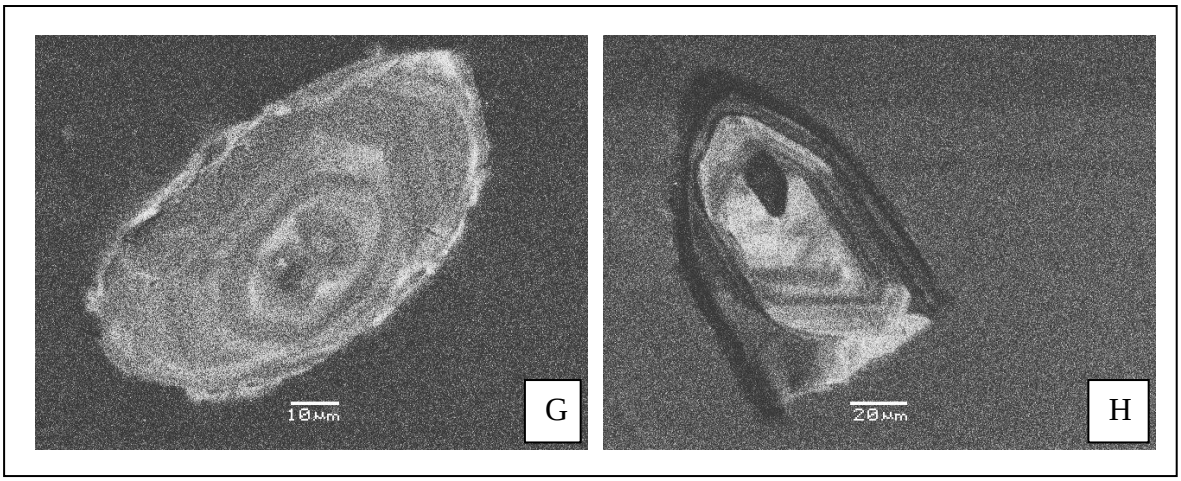

Fig 5.10 Cathodoluminescence images of zircons showing zoning

Table 6. Analytical U – Pb data from NA 09 - 5

	ppm				*Ratios*							*Discordance*		*Ages*					
Sample No	U	^{206}Pb	$^{206}Pb_c$(%)	206/204	$^{207}Pb^*/^{206}Pb^*$	1SE	$^{207}Pb^*/^{235}U$	1SE	$^{206}Pb^*/^{238}U$	1SE	Rho	Central (%)	Min. rim(%)	207/206	1σ	207/235	1σ	206/238	1σ
NA09-05-18	325	100.9	0.00E+00	17124	0.069	0.00069	1.41769	0.03895	0.14902	0.00382	0.932	-0.4	.	899	20	896	16	895	21
NA09-05-19innerrim	196	43.2	0.00E+00	30947	0.06391	0.00075	0.97118	0.02597	0.1102	0.00265	0.898	-9.2	-1.1	739	25	689	13	674	15
NA09-05-23	99	66.5	0.00E+00	18673	0.11308	0.00139	4.83066	0.1554	0.30983	0.00921	0.924	-6.8	-2.4	1849	22	1790	27	1740	45
NA09-05-26	229	105.6	0.00E+00	9244	0.08502	0.00098	2.52491	0.07355	0.2154	0.00577	0.919	-4.9	.	1316	21	1279	21	1258	31
NA09-05-26rim	276	93.4	0.00E+00	13944	0.07001	0.00074	1.5522	0.04105	0.1608	0.0039	0.917	3.8	.	929	21	951	16	961	22
NA09-05-30	86	33.1	0.00E+00	6259	0.07743	0.00085	1.95922	0.0568	0.18353	0.00492	0.925	-4.4	.	1132	21	1102	19	1086	27
NA09-05-30rim	194	76.2	0.00E+00	14972	0.07639	0.00083	1.95522	0.05679	0.18564	0.005	0.927	-0.7	.	1105	20	1100	20	1098	27
NA09-05-33rim	431	145.3	0.00E+00	22361	0.07018	0.00075	1.57166	0.04286	0.16242	0.00407	0.919	4.2	.	934	21	959	17	970	23
NA-09-5-01	228	77	0.00E+00	9567	0.0704	0.00071	1.54093	0.04239	0.15875	0.00406	0.930	1.1	.	940	20	947	17	950	23
NA-09-5-01b	449	154.4	0.00E+00	29114	0.07003	0.0007	1.56107	0.04299	0.16166	0.00415	0.931	4.2	.	929	20	955	17	966	23
NA-09-5-02	424	142.3	0.00E+00	24583	0.06943	0.0007	1.51074	0.04144	0.1578	0.00403	0.931	3.9	.	912	19	935	17	945	22
NA-09-5-03	83	27.2	0.00E+00	6586264	0.0701	0.00073	1.49147	0.04093	0.15431	0.00392	0.926	-0.7	.	931	20	927	17	925	22
NA-09-5-04	260	87.1	0.00E+00	16542	0.07028	0.00071	1.52863	0.04198	0.15775	0.00403	0.930	0.9	.	937	20	942	17	944	22
NA-09-5-05	410	137	0.00E+00	38131	0.06932	0.00069	1.4958	0.04125	0.15651	0.00402	0.932	3.4	.	908	21	929	17	937	22
NA-09-5-06	262	87.9	0.00E+00	131001	0.06958	0.0007	1.51172	0.04165	0.15758	0.00404	0.931	3.2	.	916	20	935	17	943	23
NA-09-5-09	133	43.5	0.00E+00	9865	0.06983	0.00071	1.49033	0.04088	0.15478	0.00394	0.928	0.5	.	923	20	926	17	928	22
NA-09-5-11	341	114.6	0.00E+00	15971	0.06957	0.0007	1.5178	0.04197	0.15822	0.00408	0.932	3.6	.	916	20	938	17	947	23
NA-09-5-14	142	45	0.00E+00	7692	0.07098	0.00073	1.50201	0.04011	0.15348	0.00378	0.922	-4.1	.	957	20	931	16	920	21
NA09-05-28	125	42.5	0.00E+00	10830	0.06934	0.00071	1.47853	0.04119	0.15465	0.004	0.929	2.1	.	909	21	922	17	927	22
NA09-05-29	234	78.9	0.00E+00	11379	0.07019	0.00075	1.54847	0.04356	0.15999	0.00417	0.926	2.6	.	934	21	950	17	957	23

NA09-05-31	210	67	0.00E+00	30639	0.06994	0.00075	1.48862	0.04018	0.15436	0.00382	0.917	-0.2	.		927	21	926	16	925	21
NA-09-5-10	282	89.7	0.00E+00	11858	0.06919	0.0007	1.44376	0.0399	0.15133	0.00389	0.931	0.5	.		904	20	907	17	908	22
NA09-05-33core	106	56	0.00E+00	10675	0.09218	0.001	3.1681	0.09922	0.24928	0.00733	0.938	-2.8	.		1471	19	1449	24	1435	38
NA09-05-22core	97	52.1	0.00E+00	14402	0.09171	0.00102	3.12058	0.09514	0.24677	0.00701	0.931	-3	.		1461	20	1438	23	1422	36
NA09-05-26core	365	200.3	0.00E+00	230499	0.09146	0.00103	3.21645	0.09546	0.25507	0.007	0.925	0.6	.		1456	21	1461	23	1465	36
NA09-05-30core	233	125.7	0.00E+00	21507	0.09551	0.00109	3.30645	0.09752	0.25108	0.00682	0.921	-6.8		-2.2	1538	21	1483	23	1444	35
NA-09-5-07	346	107.3	0.00E+00	16253	0.06847	0.00069	1.38731	0.0379	0.14694	0.00373	0.93	0.1	.		883	19	884	16	884	21
NA-09-5-08	347	108.7	0.00E+00	113977	0.06879	0.00069	1.40691	0.03822	0.14834	0.00375	0.93	-0.1	.		892	21	892	16	892	21
NA-09-5-15	616	212.5	0.00E+00	23218	0.06933	0.00069	1.57077	0.04267	0.16432	0.00415	0.93	8.6		1.1	909	19	959	17	981	23

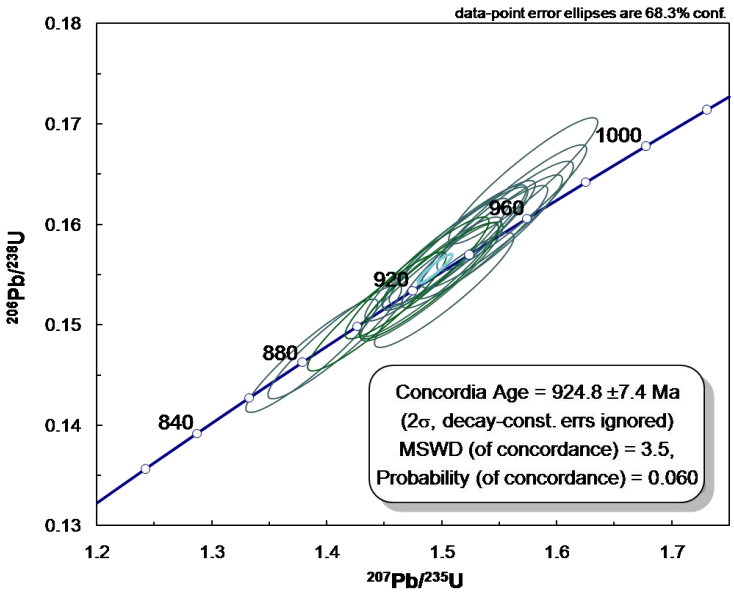

Fig 5.11A Concordia plot of homogeneous zircons and rims of zoned zircons (Green ellipse shows overall statistical concordia age determined by Isoplot and is not an analyzed zircon)

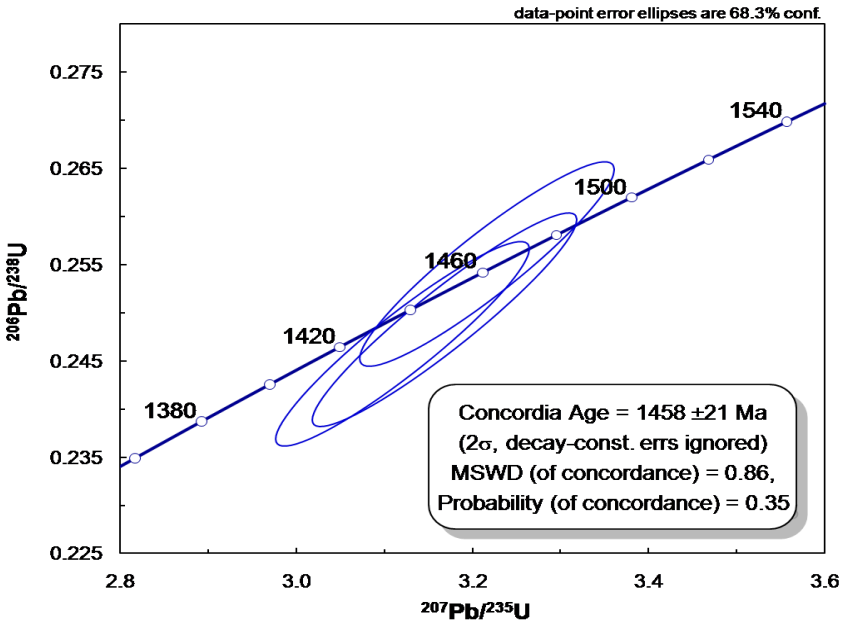

Fig 5.11B Concordia plot of xenocrystic cores of zoned zircons

The ages derived from the megacrystic granite in the Bratten area fall into two populations. The dominant age population represents generally homogeneous zircons and rims of large zoned zircons with a Neoproterozoic concordia age of 924 ± 7.4 Ma (1σ, MSWD=3.5), and population II (3 zircon grains, a fourth grain with an age of 1538 Ma and a central discordance of -6.8% was not plotted) representing the cores of the zoned zircons with an a concordia age of 1458 ± 21 Ma (1σ, MSWD=3.5) Ma (1σ, MSWD=0.86) (Figs. 5.9A, 5.9B respectively). Ages ranging from 1105 – 1316 Ma are considered to be inherited zircons. The 924 ±7.4 Ma zircons record emplacement ages for the rocks whiles the older 1458 ± 21 Ma zircons are xenocrysts from an earlier emplaced pluton. This scenario is considered more likely because the zoning patterns shown in Fig 5.8 are oscillatory which is typical for magmatic zircons. Recrystallized zircons are not expected to show this feature.

5.5.2 Diorite (NA 09 – 1)

The diorite is deformed together with the megacrystic granite (which it intrudes). This sample has very few zircons as compared to the megacrystic granite. Electron backscatter images of the zircons were made by use of an SEM. Most of the zircons are subhedral and show some fracturing. They were mostly uniform and showed weak zoning. CL images showed fairly uniform crystals whereas backscatter images show some weak zoning. Fractured areas were avoided during the analysis.

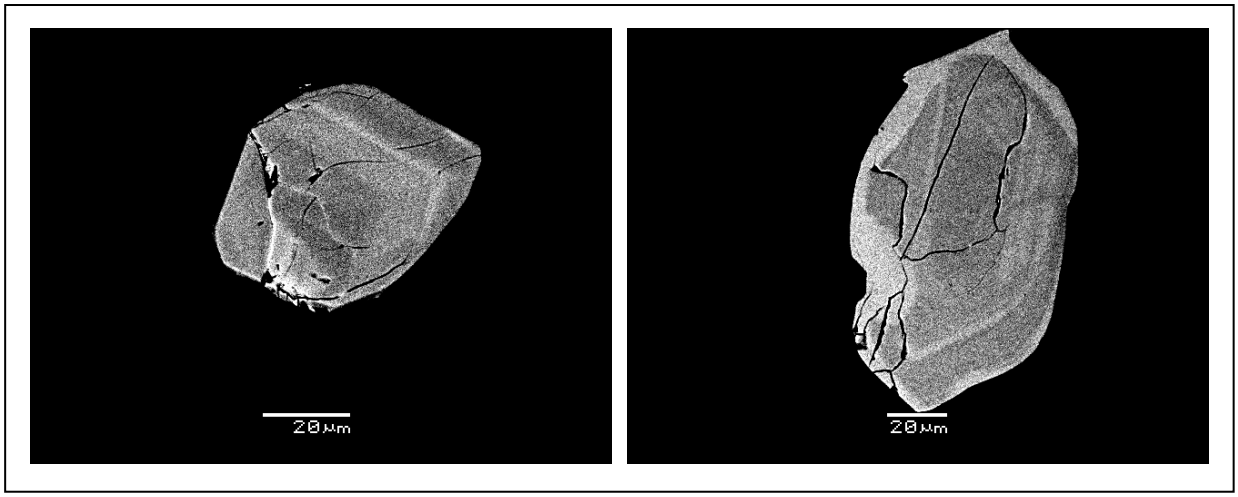

Fig 5.12 Electron backscatter images of zircons from diorite

Table 7 Analytical U – Pb data from diorite (NA 09 -1)

	ppm				*Ratios*							*Discordance*		*Ages*					
Sample No.	U	^{206}Pb	$^{206}Pb_c$(%)	206/204	$^{207}Pb/^{206}Pb^*$	1SE	$^{207}Pb/^{235}U^*$	1SE	$^{206}Pb/^{238}U^*$	1SE	Rho	Central (%)	Min. rim (%)	207/206	1σ	207/235	1σ	206/238	1σ
NA09-01-5	146	72.4	0.00E+00	16164	0.08176	0.00073	2.06928	0.03738	0.18355	0.00288	0.868	-13.5	-9.7	1240	17	1139	12	1086	16
NA09-01-13	271	110	0.00E+00	35106	0.06796	0.00055	1.31587	0.02064	0.14043	0.00189	0.857	-2.5	.	867	16	853	9	847	11
NA09-01-14	264	97.9	0.00E+00	24456	0.06719	0.00058	1.21968	0.02647	0.13165	0.00262	0.919	-5.9	-0.4	844	17	810	12	797	15
NA09-01-11rim	815	193.5	0.00E+00	53600	0.05902	0.0005	0.68213	0.01264	0.08383	0.00138	0.888	-9	-1.7	568	17	528	8	519	8
NA09-01-19short	250	47.4	0.00E+00	26243	0.05905	0.00054	0.67829	0.01327	0.08332	0.00144	0.886	-9.7	-1.9	569	19	526	8	516	9
NA09-01-8	219	98.9	0.00E+00	30523	0.06977	0.00049	1.44671	0.02005	0.15039	0.00179	0.860	-2.1	.	922	14	909	8	903	10
NA09-01-20	360	186.2	0.00E+00	43099	0.06968	0.00062	1.51048	0.02634	0.15723	0.00236	0.861	2.6	.	919	18	935	11	941	13
NA09-01-18	304	139.1	0.00E+00	31873	0.06995	0.00053	1.56237	0.02302	0.162	0.00204	0.857	4.8	0.3	927	15	955	9	968	11
NA09-01-01	184	88.8	0.00E+00	12922	0.07018	0.00073	1.54599	0.0245	0.15978	0.00191	0.754	2.5	.	933	20	949	10	956	11
NA09-01-11core	127	54.3	0.00E+00	19371	0.06961	0.0005	1.37682	0.01902	0.14346	0.00169	0.854	-6.1	-2.1	917	14	879	8	864	10
NA09-01-16	502	191.6	0.00E+00	65342	0.06957	0.00042	1.53591	0.02346	0.16011	0.00225	0.918	4.9	0.7	916	13	945	9	957	12
NA09-01-17	326	150.2	0.00E+00	97555	0.0695	0.00051	1.55752	0.0227	0.16254	0.00204	0.862	6.7	2.2	914	14	953	9	971	11
NA09-01-17b	413	209.4	0.00E+00	1358104	0.06944	0.00071	1.60321	0.0255	0.16746	0.00203	0.762	10.2	4.6	912	20	971	10	998	11

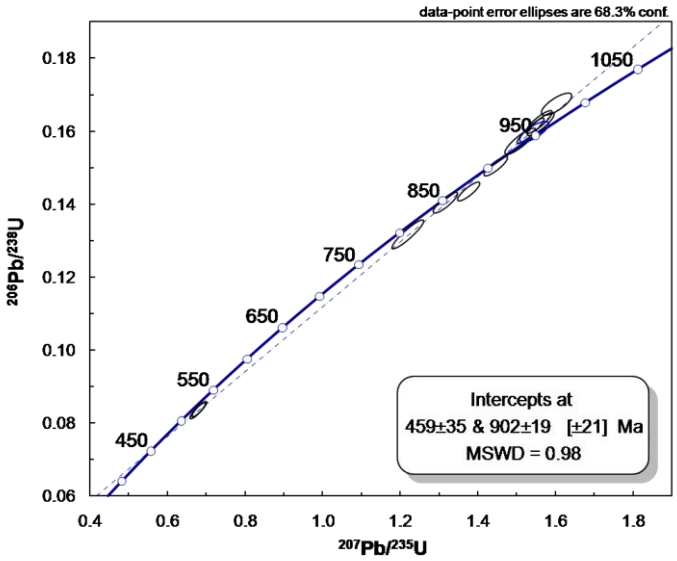

Fig 5.13A Plot of Diorite zircons showing intercepts. A close-up image of the concordant zircon cluster is shown below

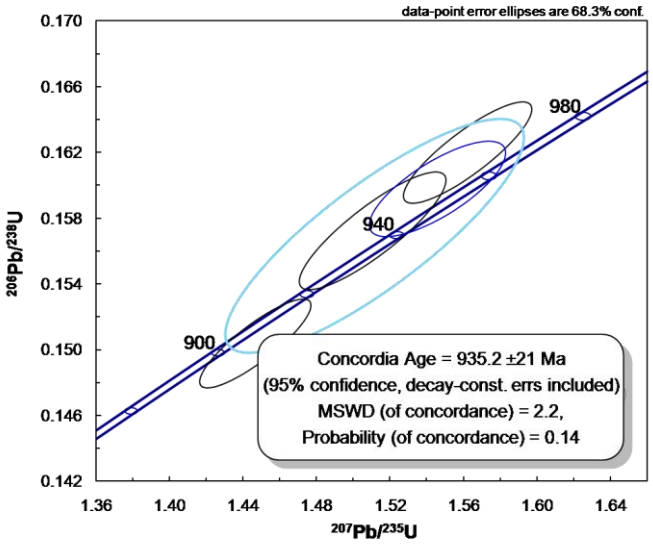

Fig 5.13B Close up plot of Fig 5.11A showing concordia age (Green ellipse shows overall statistical concordia age determined by programme and is not an analyzed zircon)

The zircons have ages ranging between 844 – 1240 Ma and show a progressive lead loss which defines a discordia that intercepts the concordia at an upper intercept of 902 ± 19 Ma and a lower intercept at 459 ± 35 Ma. The lower intercept of 459 ± 35 Ma is considered to

record a Caledonian event that lead to the lead loss, whiles the emplacement age of the diorite is calculated to be a concordia age of 935 ± 21 Ma (1σ, MSWD=2.2). Ideally, the upper intercept age should be expected to determine the emplacement age, however, in this case, it can be seen from the plot that the discordia line is defined by only two points. It is also clear that most of the points cluster around the concordia age. The lower age of the defined by the upper intercept is most likely due to analytical scatter of the points. The oldest zircon is aged 1240 Ma, and is interpreted to be an inherited zircon

5.5.3 Pegmatite (NA 09 – 2)

NA 09-2 is a deformed pegmatite that intrudes both the megacrystic granite and the diorite. The zircons in this sample are elongated euhedral to subhedral crystals. Most of the crystals have a dark brown colour, have several inclusions, and are very uranium rich and fractured. Metamict zircons are also observed. These metamict brownish zircons were avoided as much as was possible resulting in very few zircons being analyzed for this sample. They were generally homogeneous or very weakly zoned.

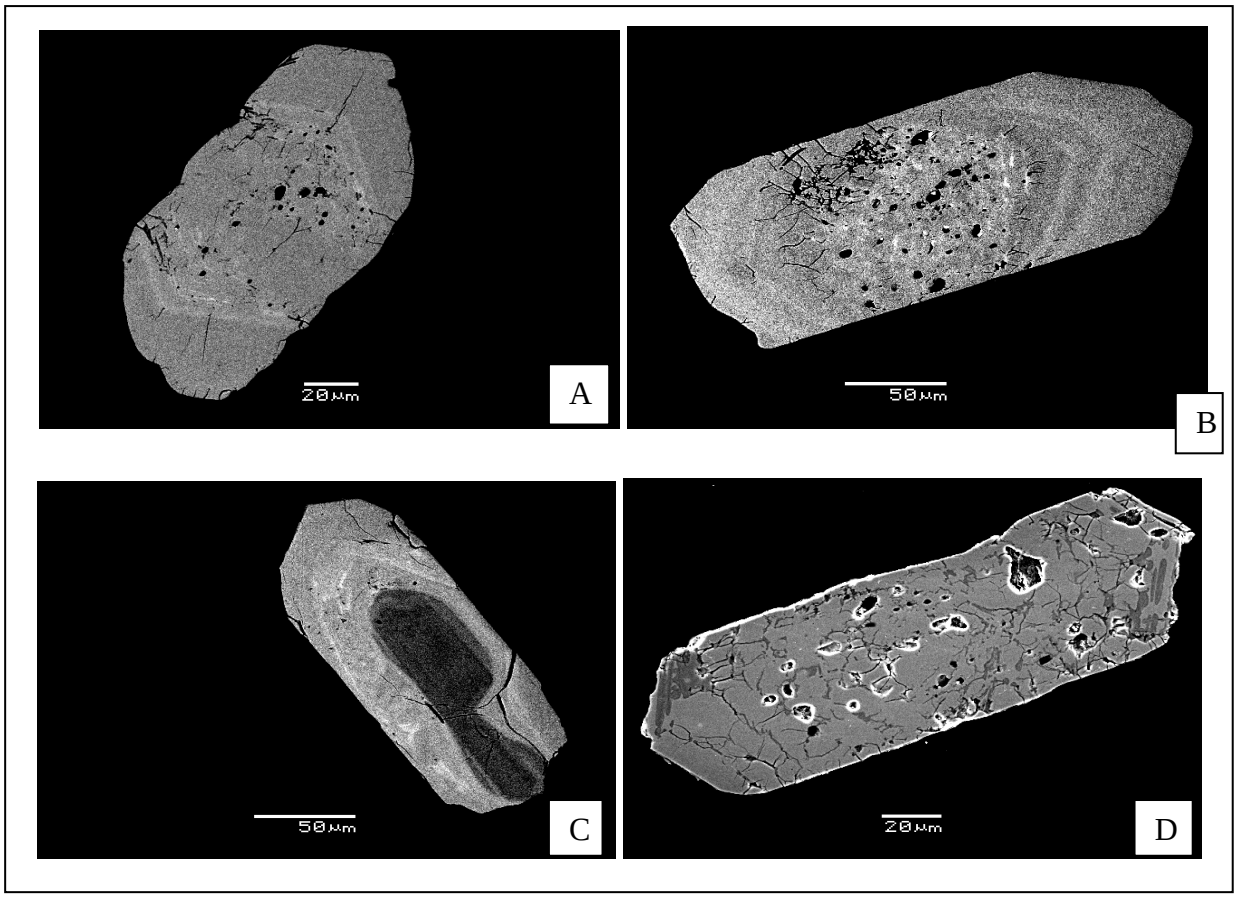

Fig 5.14 Electron backscatter (A, B and C) and secondary electron (D) images showing variably deformed zircons from pegmatite

Table 8 Analytical U – Pb data from pegmatite (NA 09 – 2)

	ppm				*Ratios*							*Discordance*		*Ages*					
Name	U	^{206}Pb	$^{206}Pb_c$(%)	206/204	$^{207}Pb^*/^{206}Pb^*$	1SE	$^{207}Pb^*/^{235}U$	1SE	$^{206}Pb^*/^{238}U$	1SE	Rho	Central (%)	Mini. rim (%)	207/206	1σ	207/235	1σ	206/238	1σ
NA09-02-15	3972	223.2	0.00	23366	0.0552	0.0006	0.5113	0.0077	0.0672	0.0007	0.725	-0.3	.	420	23	419	5	419	4
NA09-02-8	2055	134.7	0.00	26205	0.0548	0.0006	0.5135	0.0067	0.068	0.0006	0.634	5.7	.	402	22	421	4	424	3
NA09-02-3	2656	184.8	0.31	6372	0.0559	0.0006	0.555	0.0077	0.072	0.0007	0.648	-0.1	.	449	23	448	5	448	4
NA09-02-4	2403	174.8	0.00	23007	0.0556	0.0006	0.5646	0.0082	0.0737	0.0007	0.687	5.3	.	436	23	455	5	458	4
NA09-02-17	3768	232.6	0.00	20009	0.0559	0.0007	0.5709	0.0094	0.0741	0.0009	0.692	3	.	448	25	459	6	461	5
NA09-02-6rim	3739	269.5	0.00	35906	0.0558	0.0006	0.5711	0.0075	0.0743	0.0006	0.662	4.4	.	443	20	459	5	462	4
NA09-02-20	3811	236.4	0.00	20323	0.0568	0.0008	0.5832	0.0107	0.0745	0.0009	0.66	-4	.	482	29	466	7	463	5
NA09-02-2	2981	214.7	0.72	2263	0.0564	0.0008	0.5845	0.0102	0.0751	0.0007	0.539	-0.5	.	469	31	467	7	467	4
NA09-02-6core	153	21.3	0.00	3190	0.069	0.0008	1.3176	0.023	0.1384	0.0018	0.761	-7.6	-1.6	900	22	853	10	836	10
NA09-02-1	782	118.5	6.90	228	0.0663	0.0021	1.3053	0.0428	0.1427	0.0013	0.282	5.6	.	817	64	848	19	860	7

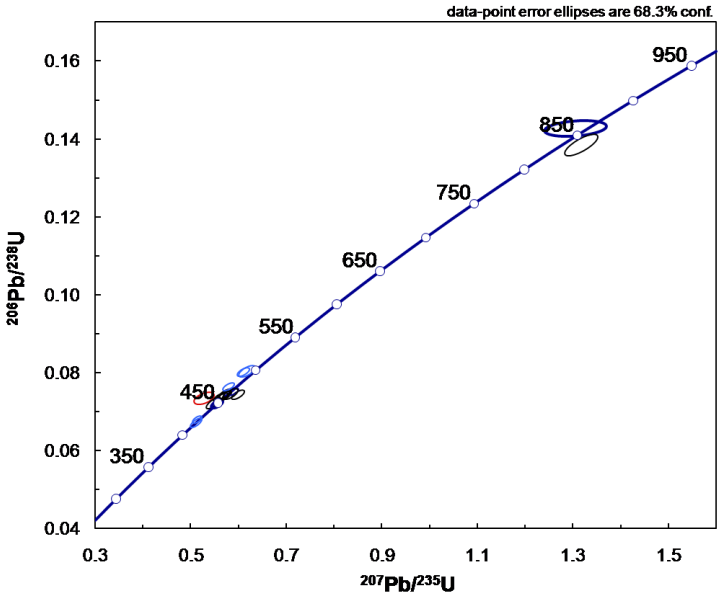

Fig 5.15A Concordia plot showing all analyzed zircon grains from pegmatite.

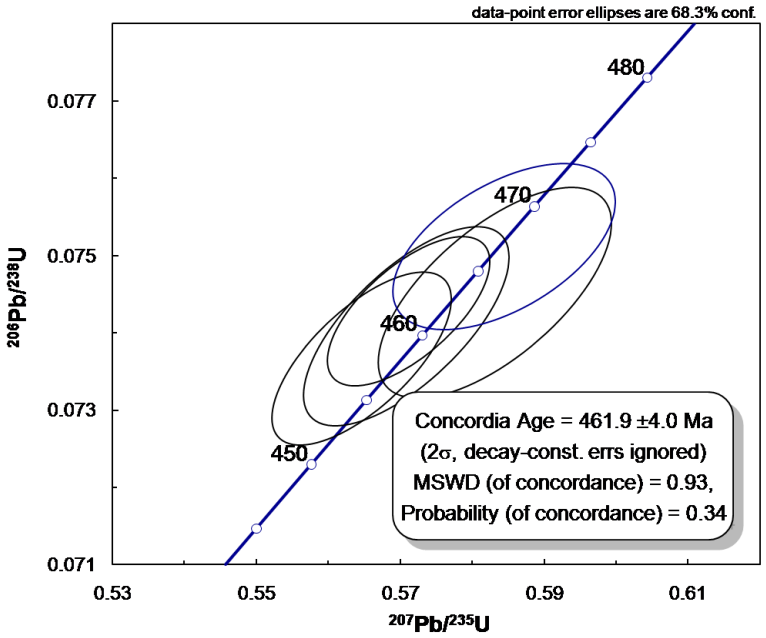

Fig 5.15B Concordia plot showing early Caledonian magmatic event in the Bodø area

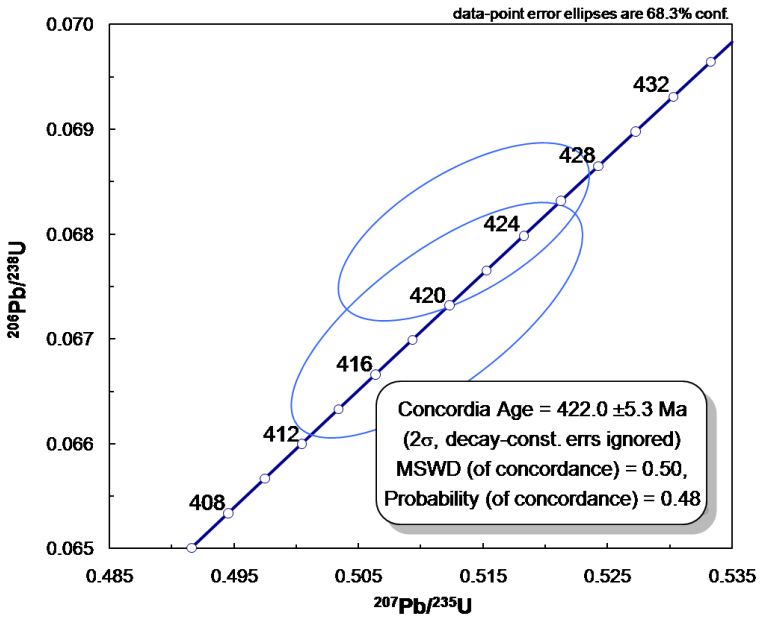

Fig 5.15C Concordia plot showing ages of fluid induced recrystallized zircons in the pegmatite

Zircons from the pegmatite yields three age clusters;

- a minor inherited population of two grains with age of ~ 850 Ma
- a dominant population with a concordia age of 461 ± 4.0 Ma
- a minor population of two grains with a concordia age of 422 ±5.3 Ma.

Most of the zircons showed significant lead loss and were discordant. As described in the previous chapter, the zircons are dark brown in colour, very uranium rich, deformed and had several inclusions (Figs 5.12B, D). However, both concordia ages calculated from the few "good" zircons show a relatively high level of precision.

These ages can be interpreted in one of two ways;

1. the 422 ±5.3 Ma age is the age of crystallization/emplacement whiles the older population are inherited grains or

2. the older 461 ± 4.0 Ma is the age of emplacement whiles the younger age records a later magmatic and/or metamorphic event that recrystallizes (to a small extent) the older population.

The latter scenario would appear to be unlikely given the fact that the zircons do not show any distinct zoning. The event that caused the lead loss in the diorite described above (NA 09-1 is interpreted to be 459 ± 35 Ma and may be used to constrain the emplacement age of the pegmatite if it is assumed that the tectonothermal event that emplaced the pegmatite triggered the lead loss in the diorite which it intrudes. However, age range for the lower intercept in the diorite, 459 ± 35 Ma is rather wide. As such, both ages calculated for the pegmatite populations (422 ±5.3 Ma and 461 ± 4.0 Ma) overlap with lower age defined by the lower intercept in the diorite (459 ± 35 Ma) and cannot therefore, reliably constrain the emplacement age of the pegmatite.

As the pegmatite is deformed (and apparently of a different generation than the presumed undeformed Caledonian pegmatites in the Bodø Group), with metamict zircons, it is likely to be older and the emplacement age of the pegmatite is considered to be 461 ± 4.0 Ma whiles the 422 ±5.3 Ma age may be considered to record a Caledonian tectonothermal and magmatic event.

A more likely scenario is that the older 461 ±4.0 Ma zircons record the emplacement age whiles the 422 ± 5.3 Ma zircons could be related to fluid induced recrystallization. This is considered more likely because, if the younger age represents a metamorphic event, the older grains would most likely not have yielded such concordant and precise ages. Moreover, fluid induced recrystallization may be local which would explain why only very few zircons were affected by it.

An attempt was made to date the metasedimentary (paragneiss) “cover sequence” of the Pre – Caledonian rocks to compare the time of sedimentation to that of the Heggmovatn metasediments. After crushing and magnetic separation methods had been applied, as with the other samples, no zircons were found after heavy liquid separation. X-ray mapping for silica and zirconium on the scanning electron microscope did not yield any positive results either. This could be attributed to either of two reasons; that the zircons were lost during the sample preparation (although there were no accidents or mistakes as far as I know during the

preparation) or that the clastic zircons were very small in size and population, and were somehow, washed out during sedimentation.

The significance of these ages is discussed in the next chapter.

6. Discussion and Conclusion

6.1 Introduction

The results of geochronological investigations in the Heggmovatn units, as well the rocks in the western "basement" region of Bodø and their associated intrusives are discussed in this chapter. All ages reported in this thesis are $^{207}Pb/^{206}Pb$ unless otherwise stated.

6.2 The Heggmovatn and "Basement" rocks in Bodø; a Fennoscandian, Laurentian or suspect terrane?

As has been stated in Chapter 2, both the Heggmovatn rocks and the gneisses in the Bodø area have been interpreted as being part of the autochthonous Baltic basement (Gustavson, 1991). This interpretation is re-examined in light of the new data presented in this thesis.

6.2.1 The case for/against a Fennoscandia origin.

With source rocks easily available (from north to south, east of the study area): in northernmost Norway (Archean terranes, ≥ 2Ga), Paleoproterozoic Svecofennian terranes (1.9 - ~ 1.7 Ga), TIBS (1.85 – 1.65 Ga), Gothian terranes (1.75– 1.50 Ga) and rocks ranging in age from 1500 – 920 Ma in southern Norway, the zircon age population in the Heggmovatn could be linked to a Baltic source. However, since no Archean zircons are found in the Heggmovatn metapsammites, the Archean terranes in northernmost Norway can be effectively ruled out as a source for the sediments.

Furthermore, lithologically similar rocks with Neoproterozoic ages comparable to the Heggmovatn orthogneiss and the Bodø granite are present in Southern Norway and have been reported by several workers. Andersen et al., (2002) confirm the existence of an event of granitic magmatism across Southern Norway caused by deep crustal melting associated with mafic underplating; an event (920 to 950 Ma) involving the emplacement of juvenile, mantle-derived material into the crust in this period demonstrated by the 940 Ma Tovdal granite.

Andersen et al., (2002) also report distinct, mantle-derived components in other granites associated with this event which possibly started as early as ~1030 Ma west of the Mandal-Ustaoset shear zone, and was of longer duration.

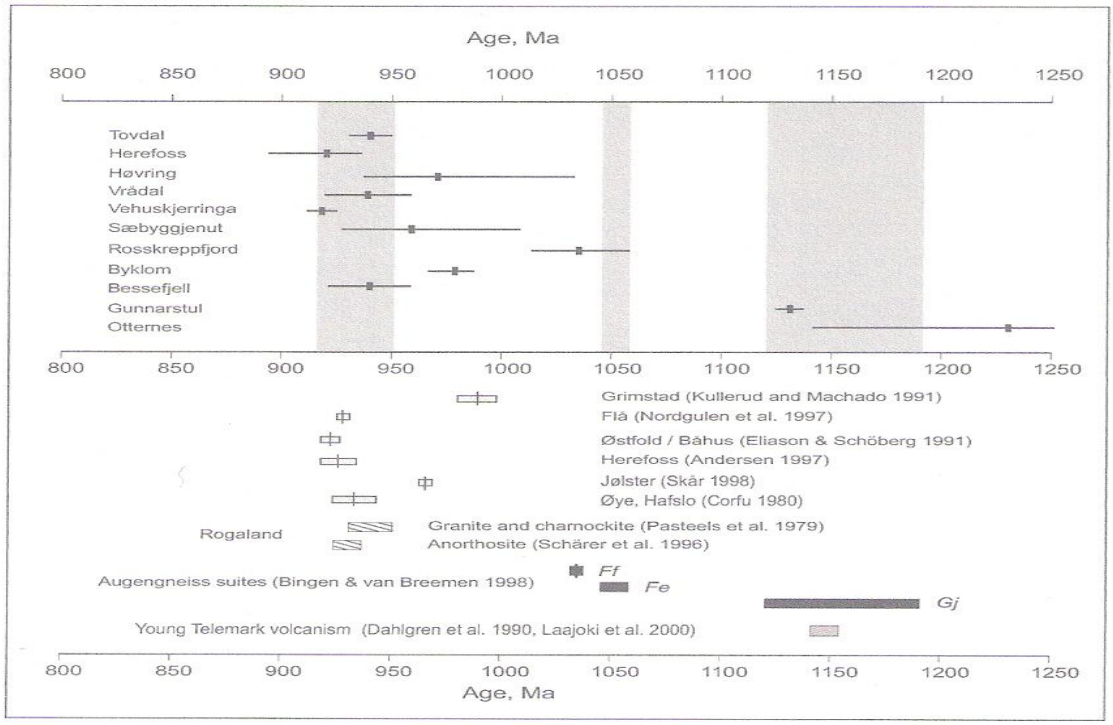

Fig 6.2 Summary of geochronologic data from South Norway and some basement windows in from the Western Gneiss Region. Bars indicate total duration of magmatic activity. Abbreviations: *Ff:* Fennefoss augen gneiss (Telemark sector), *Fe:* Feda suite augen gneiss, and *Gj:* Gjerstad suite augen gneiss.

Reproduced from Andersen et al., (2002)

Although the 1458 ± 21 Ma age (in the xenocrystic zircons from the Bodø megacrystic granite) is well documented in Fennoscandian terranes where it records the second main crust – forming period in Southwest Norway, including the Western Gneiss Region, which range from 1550Ma - 1400 Ma (Kullerud et al., 1986; Tucker et al., 1990b; Koenemann, 1993; Tucker et al., 2004), such ages have not been reported in northern Norway.

If the Bodø granites and the protolith to the Heggmovatn orthogneisses were to have originated from Southern Norway, the most likely mechanism would be via right lateral strike – slip movement during the oblique Caledonian collision. However, most models for

the oblique Caledonian continent-continent collision invoke left-lateral displacement. Furthermore; the orientation of stretching lineations in the Caledonides does not support this (Fossen et al., 2008). Generally, the Caledonian nappes were transported in an easterly to south-easterly direction and a more south-southeasterly direction in the southernmost areas. Although there was additional movement in the longitudinal direction of the orogenic belt in the westernmost nappes, this movement is not recorded as far north as the Bodø area.

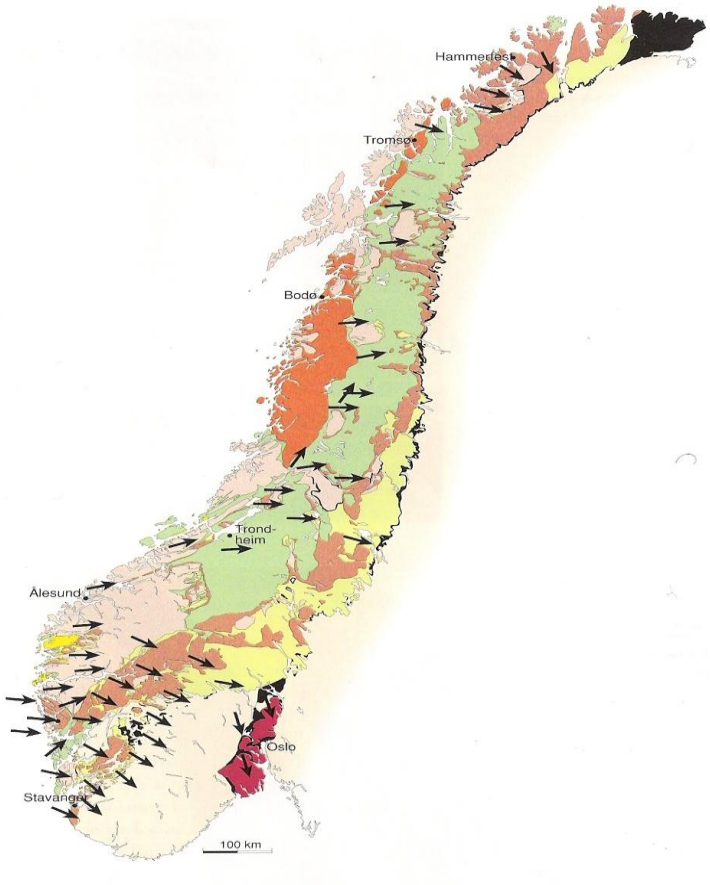

Fig 6.3 The main Caledonian lineation direction (shown by arrows) showing predominantly SSE transport direction of the rocks. Reproduced from Fossen et al. (2008)

This effectively rules out, or minimizes the likelihood that the Neoproterozoic rocks found in Bodø and the Heggmovatn areas originated from the Fennoscandian terrenes in southern Norway.

Also, whereas orthogneisses dominate the Rishaugfjellet dome, comparable with basement rocks exposed in the Tysfjord and Glomfjord culminations, the Heggmovatn area is dominated by alternating metapsammites and metapelites. Apart from the lithologic differences between the Heggmovatn supracrustals and related intrusives, the Neoproterozoic ages reported in this thesis for both the Heggmovatn orthogneisses and the granites in the area west of Bodø (928.6 ± 7.2 Ma and 924 ± 7.4 Ma respectively) are remarkably different from ages (1860-1790 Ma) reported from the Lofoten (Corfu, 2004) and basement tectonic windows in Nordland (c. 1800 Ma) (Skår 2002).

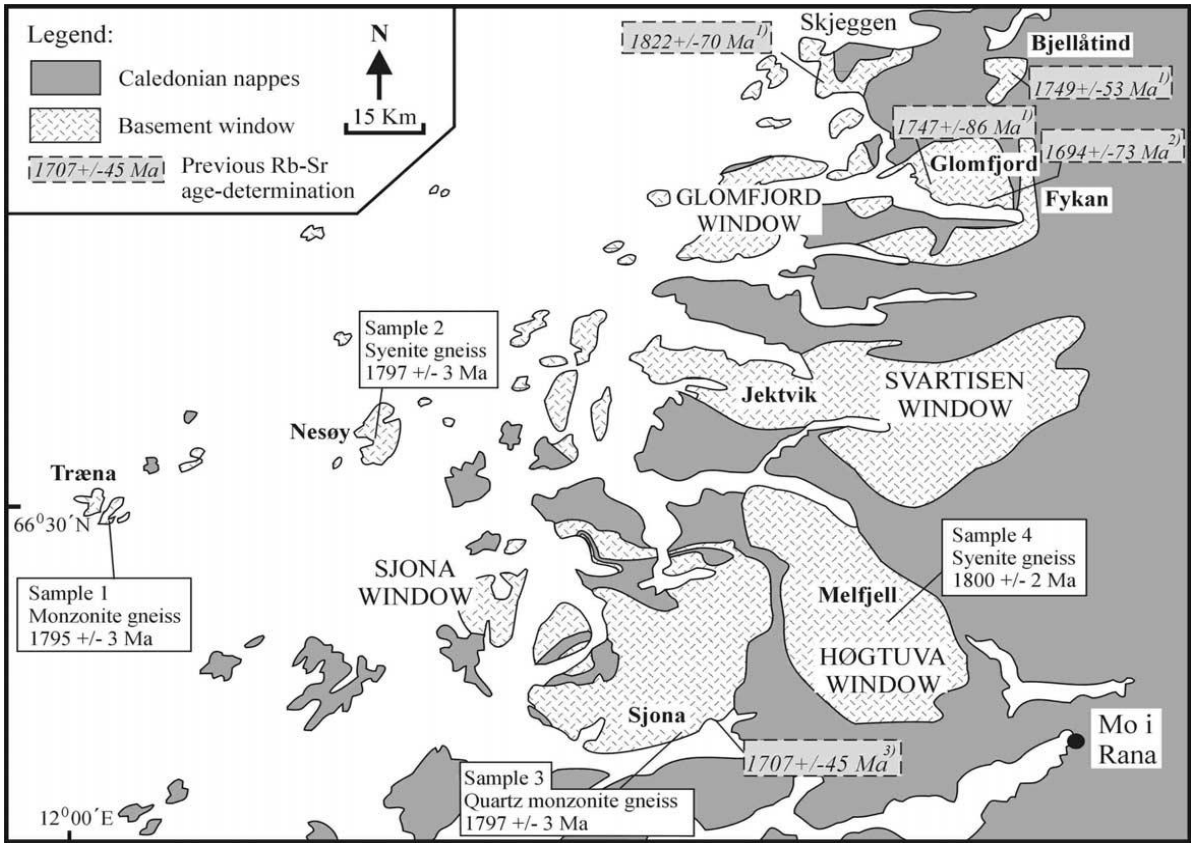

Fig 6.4 Map showing ages of Central Nordland Basement Windows by Skår and some previous age determinations; (1) Cribb (1981); (2) Wilson and Nicholson (1973); (3) Wilberg (1987). Reproduced from Skår (2002)

The lithologic differences between the Heggmovatn supracrustals and related intrusives (as well as the Bodø granite and its related intrusives), and the nearby basement culminations, coupled with the obtained radiometric ages indicate that the former represent an exotic terrane/thrust sheet, and not a culmination/dome exposing Baltic basement.

6.2.2 The case for/against a Laurentian origin

The Uppermost Allochthon has traditionally been considered to be of Laurentian or peri-Laurentian ancestry (Roberts, 2003). In this section, the geology of the "western basement region" in Bodø and the Heggmovatn area is compared to the eastern extremity of Laurentia, i.e. East Greenland (as it was the portion of Laurentia involved in the Scandian collision with Baltica). The provenance data from the arkosic metapsammite in the Heggmovatn units is also compared with provenance data from Scotland and Ireland. This is because Scotland and Ireland make up the southern continuation of Laurentia's eastern margin when the tectonic plates are reconstructed.

6.2.2.1 East Greenland

The Heggmovatn units are lithologically comparable to the Krummedal Sequence of the Niggli – Hagar thrust sheet in NE Greenland. Whiles the Krummedal Sequence is composed of psammites, semi – pelites, pelites and mica schists with minor quartzites, marbles and amphibolites, the Heggmovatn units are composed of alternating metapsammites (which are cross bedded) and metapelites.

The Krummedal Sequence is intruded by two generations of leucogranitic plutons and dykes dated to c. 940–910 Ma (Kalsbeek et al., 2000; Watt et al., 2000; Higgins et al., 2004), and around 435–420 Ma (Andresen et al., 1998b; Hartz et al., 2001).

In the study area, the rocks of the Heggmovatn are also intruded by orthogneisses and granites which are dated to be 928.6 ± 7.2 Ma and 431.5 ±1.0 Ma respectively. Furthermore, the Bodø granite and diorite intrusions both record Neoproterozoic ages of 924 ± 7.4 Ma and 935 ±21Ma respectively, all of which fall in the range of ages reported by workers in NE Greenland.

The metasedimentary succession in the Krummedal Sequence is generally accepted to have been deposited between 1100 – 930Ma (Kalsbeek et al., 2000) whiles the timing of sedimentation of the Heggmovatn supracrustals have been constrained in this study to be between1038 – 928 Ma.

6.2.2.2 Sediment Provenance

Siliciclastic-dominated sequences of largely Neoproterozoic age are widespread along the eastern continental margin of Laurentia, stretching from the southern Appalachians to northern Greenland (Watt and Thrane, 2001). These rocks are generally related to a protracted history of rifting and ocean formation associated with the break-up of Laurentia from the supercontinent Rodinia (Cawood et al., 2003). These supracrustal sequences include: the high grade Krummedal Sequence and the Eleonore Bay Supergroup of NE Greenland, and the Torridonian, Moinian and Dalradian successions in Scotland.

The age data obtained from the clastic zircons in the arkosic metapsammites in the Heggmovatn supracrustals are compared to the sediment populations in the Krummedal Sequence, Eleonore Bay Supergroup, Moine and Dalradian Supergroups.

The Moine succession in NW Scotland was deposited after about 900 Ma (Cawood et al., 2004) and underwent several tectonomagmatic events, including deformation and metamorphism at 870-800 Ma, the Knoydartian orogeny (Rogers et al., 2001), about 740 Ma (Tanner and Evans, 2003), 670 Ma (Storey et al., 2004) and 600 Ma (Kinny et al., 2003). Besides the younger age of deposition and lack of Grenvillian intrusions, the Moine has been affected by Ordovician (470-460 Ma) tectonomagmatic activity, which may be comparable to the 461 ± 4.0 Ma ages recorded by the pegmatite intruding the Bodø granite.

The Krummedal sequence, however, has no record of intrusive activity between 900 and 450 Ma.

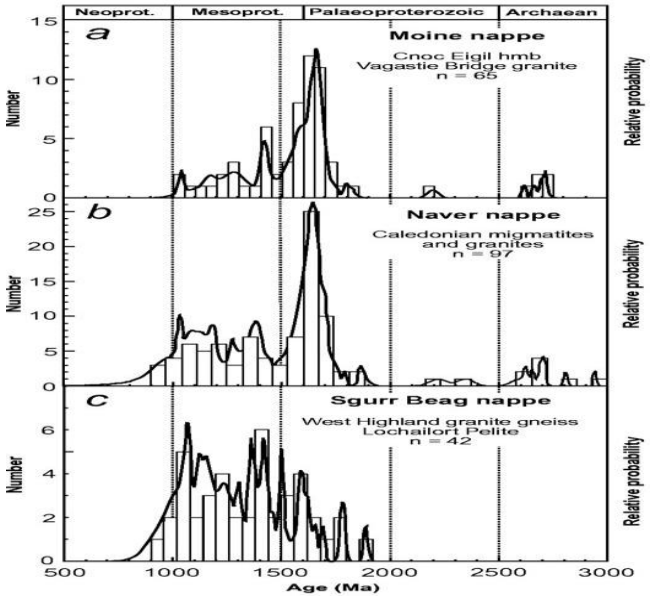

Moine Supergroup. From Friend et al. (2003)

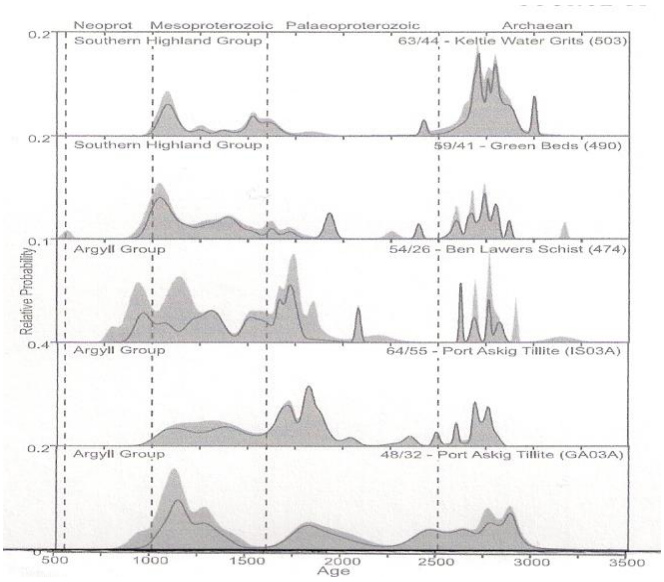

Dalradian Supergroup. From Cawood et al. (2003)

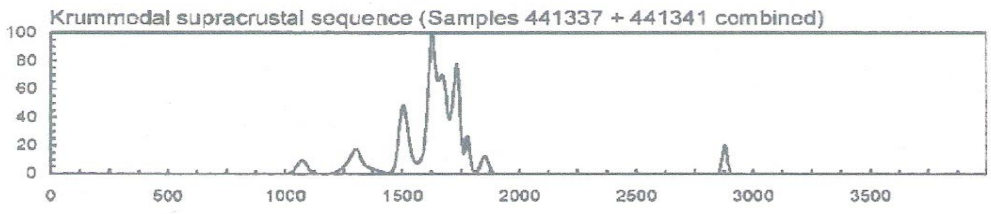

Krummedal sequence. From Watt et al (2000)

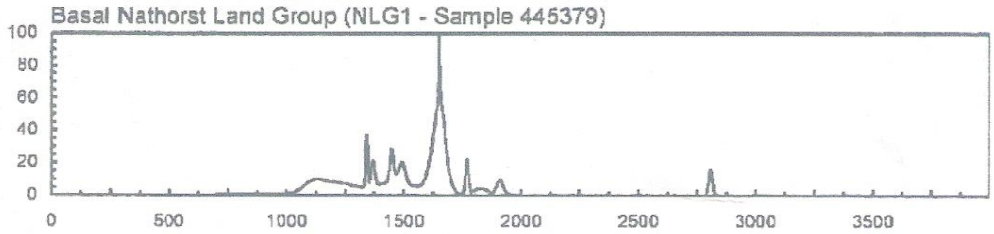

Eleonore Bay Supergroup. From Watt et al (2000)

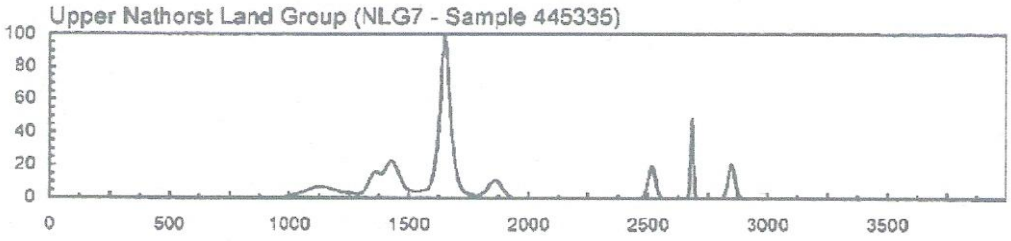

Eleonore Bay Supergroup. From Watt et al (2000)

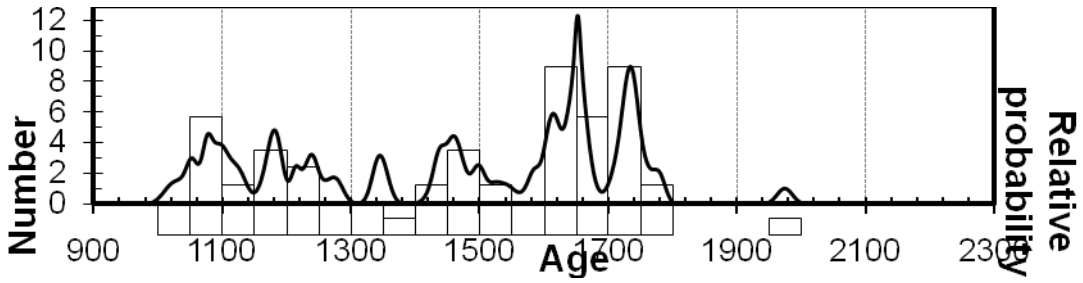

Heggmovatn metasediments

Fig 6.5 Comparison of the concordant data from the Heggmovatn metapsammites with the Moine Supergroup of NW Scotland, the Krummedal Supergroup and the Eleonore Bay Supergroup.

From the comparison (Fig. 6.5), it is observed that the Heggmovatn sediments have a close resemblance to the Krummedal and Moine Supergroups. However, whiles the Krummedal Sequence and the Heggmovatn sediments do not have any Archean zircons, the Moine Supergroup and Dalradian Supergroup (especially), have a considerable Archean zircon population.

6.2.2.3 Magmatism in the Heggmovatn area

The emplacement age of the protolith to the Heggmovatn orthogneiss, 928.6 ± 7.2 Ma is in good agreement with the 940–910 Ma Grenvillian ages of leucocratic plutons in the Krummedal Sequence.

Ca. 445 – 420 Ma

Ages in this range are generally thought to record Caledonian deformation, metamorphism and magmatism. The age 431 ± 1.0 Ma of the Heggmovatn granite is interpreted to be the emplacement age due to its undeformed nature. The older discordant zircons are considered to represent inherited zircons. The Krummedal Sequence and the Eleonore Bay Supergroup are also intruded by ca 435-425 Ma leucogranites, interpreted to be derived from partial melting of the Krummedal Sequence metasediments (e.g. Andresen et al., 2007; Kalsbeek et al., 2008).

Considering the lithologic similarities between the Heggmovatn and the Krummedal Sequence, the similarities in age of the intrusive rocks in both units and the similarities in the ages of their clastic zircon populations, the Heggmovatn units are considered to be more closely related to the Krummedal Sequence than to other siliciclastic-dominated sequences of largely Neoproterozoic age along the eastern continental margin of Laurentia.

6.2.2.4 Magmatism in the Bodø area

Whiles the Heggmovatn units seem to be correlative to the Krummedal Sequence in NE Greenland, the same cannot be easily said of the Bodø granites, although the Bodø granites and diorite both record Neoproterozoic magmatism which is comparable to the Grenvillian aged plutons in the Krummedal.

Pre – Grenvillian magmatism

The Bodø megacrystic granite records evidence for a magmatic event prior to its emplacement in the Neoproterozoic (the 1458 ±21 Ma xenocrystic zircon cores). For the same reasons as in section 6.2.1, this earlier magmatism is not considered to be of Fennoscandian origin.

Whiles these (xenocrystic cores ranging from 1456 – 1538 Ma) ages are not found in NE Greenland, they have been recorded elsewhere in Laurentia; further south along the eastern Grenvillian province in Labrador.

In Labrador, the Pinware terrane was first identified as a separate tectonic unit by Gower (1988) and the Pinwarian orogeny is used to refer to rocks having ages between 1520 and 1460 Ma as well as deformation and metamorphic events during that time period (Gower and Krogh, 2001) thought to have been emplaced in a continental – margin arc tectonic setting.

A unique feature of the Pinwarian orogeny is that both large plutonic bodies and minor intrusions have a granitic (sensu stricto) character (Gower and Krogh, 2001).

Post – Grenvillian magmatism

Post-Grenvillian/Sveconorwegian magmatism in the study area is recorded by the 461 ± 4.0 Ma and 422 ± 5.3 Ma ages found in the pegmatites intruding the Bodø granite and the 431.5 ±1 Ma age of cross cutting undeformed granites in the Heggmovatn supracrustals.

Ca. 470 - 455 Ma (Grampian event)

Although the Krummedal sequence has no record of intrusive activity between 900 and 450 Ma, other parts of the Caledonides record this activity. In the Helgeland Nappe, further south of the study area, minor mafic magmatism is recorded by the Hortavaear igneous complex and the Svarthopen pluton at ~ 465 Ma (Barnes et al., 2007). The 470 - 455 Ma age range is also common in the Upper Allochthon (Meyer et al., 2003).

In Laurentia, ages in this range are found in the East Greenland and the Irish Caledonides. In East Greenland, south of 72°N, Caledonian granitoid rocks are present that are very different from the leucogranites further north. The calc-alkaline Korridoren granodiorite consisting of granodioritic and quartzdioritic rocks which is an intrusion in east Milne Land yield U –Pb SHRIMP ages of 466 ± 9 Ma and are interpreted to be derived from a volcanic arc related to subduction of the Iapetus Ocean beneath that part of Laurentia (Kalsbeek et al., 2008).

Friedrich et al., (1999) also report U – Pb ages of 467 ± 2 Ma for a calc-alkaline pegmatite and 468 ± 2 Ma for a leucosome in metapelites in the Connemara region of the Irish

Caledonides interpreted to have been emplaced during syn – deformational continental arc magmatism.

It is interesting to note that these ages are all recorded in rocks with a calc-alkaline character. If geochemical analysis of the Bodø pegmatite also reveals a calc alkaline character, then they may be inferred to be related to these rocks emplaced during the Grampian event.

The obtained data strongly reinforces the interpretation that the Uppermost Allochthon in the Scandinavian Caledonides represents a fragment of Laurentian continental crust.

6.3 Correlation between Bodø and Heggmovatn units, and contact relationships

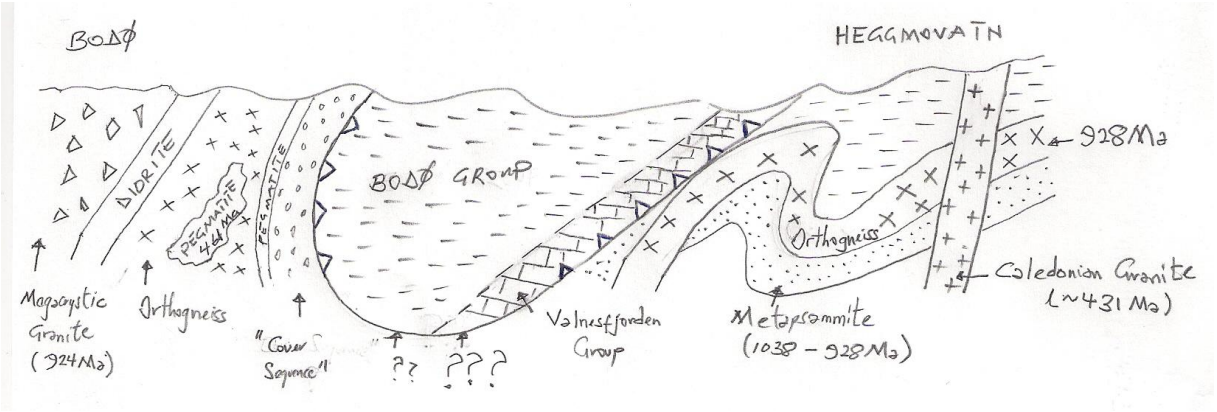

Fig 6.6 Simplified section from Bodø to the Heggmovatn area illustrating possible correlation between Bodø and Heggmovatn units

Whiles both the Bodø granites (and diorite) and Heggmovatn orthogneisses record Grenvillian magmatism, a straightforward correlation of the two units is perhaps, over simplistic for several reasons.

Firstly, as has been previously discussed, the Bodø granites were most likely intruded into a previously emplaced pluton of Pinwarian age possibly derived from terranes in the eastern Grenville province in Labrador (further south along the eastern Laurentian margin). No such evidence is found in the Heggmovatn Grenvillian intrusions.

The 461 Ma pegmatite emplacement ages in the Bodø granite are some 30 m.y. older than the undeformed granitic intrusions in the Heggmovatn area. Considering the fact that 461 Ma ages are distinctly absent from the Krummedal Sequence (to which the Heggmovatn metasediments are most closely related) and the fact that similar 461 Ma ages are rather common south of 72˚N in eastern Greenland, and in the Irish Caledonides, it is fair to assume that the Bodø and Heggmovatn terranes developed in different crustal settings before being juxtaposed during the Scandian collision of Laurentia and Baltica.

Also, the inability to find zircons in the metapsammite of the "cover sequence" to the Bodø orthogneisses does not permit a comparison between the deposition of the cover sequence and the Heggmovatn metapsammites.

Contact relationships

As has been previously stated, the nature of the contact between the Bodø orthogneisses and the "cover sequence" could not be determined from the available data. The possibilities for the contact are

1. a purely tectonic contact
2. a tectonically disturbed
    - depositional contact
    - intrusive contact

This contact is interpreted by Gustavson (1991) to be a depositional contact. The only thing that was positively determined from the field was that the contact is overturned, as the orthogneisses overlie the cover sequence. In the absence of further data (clastic zircon ages) from the cover sequence, it is difficult to tell the exact nature of this contact as the contact is intruded by a pegmatite (see Fig 3.4). Re-sampling and dating of the cover sequence is therefore imperative.

If the contact is an intrusive contact, then none of the clastic zircons from the cover sequence are expected to be younger than ~924 Ma (the age of the granitic protolith to the

orthogneiss). A considerably younger (relative to the granitic protolith/orthogneiss) of the cover sequence might suggest a purely tectonic contact, or in the very least, an unconformity between the two prior to the overturning of the contact.

The contact between the orthogneisses (with cover sequence) and the Bodø Group is interpreted by Rutland and Nicholson (1969) and Gustavson (1991) to be a thrust which runs all towards the north and "swings" around to separate the Valnesfjorden Group from the Heggmovatn rocks. No evidence for such a thrust was found in the Bodø area. Hopefully, traverses in the area just east of Steigtindvatnet, and in the valley between Finnkonnaken and Bagnesfjellet should yield information about this thrust if it is present.

In the absence of any such information, and from the field observations, it appears that there is no such thrust and the cover sequence to the Bodø orthogneiss grades into the metapelitic units of the Bodø Group.

6.4 Conclusions

The high grade gneissic rocks outcropping on the western part of the Bodø peninsula, previously thought to represent exposed Baltic basement comparable to the basement rocks of the Lofoten area (Rutland and Nicholson, 1969; Gustavson, 1991), are considerably younger than nearby Baltic basement rocks.

The "basement rocks" in the Bodø area record an earlier magmatic activity at ~ 1458 Ma, with emplacement of the megacrystic granite followed by more recent Grenvillian magmatic activity at 924 ± 7.4 Ma. Dioritic and mafic intrusions occurred almost concurrently with this event

The rocks of Heggmovatn area, considered to be a major basement culmination exposing Baltic basement rocks comparable to the Rishaugfjell and Glomfjord basement domes (Rutland and Nicholson, 1969; Gustavson, 1991) are composed of lithologies that are atypical of Baltic basement.

The metasediments of the Heggmovatn were deposited between 1100 – 930 Ma. The granitic protolith of the orthogneisses of the Heggmovatn were emplaced at 928.6 ± 7.2 Ma.

Both of the Bodø gneisses and Heggmovatn rocks are interpreted to be exotic with respect to Baltica.

The lithologies in the Heggmovatn are similar to those of the Krummedal supracrustal sequence in the East Greenland Caledonides. Both are composed of alternating metapsammites and metapelites and intruded by Grenvillian/Sveconorwegian rocks, as well as Caledonian granites. The zircons populations of the Heggmovatn supracrustals are more similar to the Krummedal Sequence than it is to other supracrustal sequences of similar depositional age elsewhere along the eastern margin of Laurentia.

It is therefore concluded that the Heggmovatn supracrustals are most likely to be genetically related to the Krummedal Sequence of NE Greenland.

Although the Heggmovatn rocks are here, linked to the Krummedal sequence in NE Greenland, the absence of the ~461 Ma ages in the Krummedal, as well as the presence of a relicts of a 1458 Ma event in the Bodø granites (which are also absent in the Krummedal) make it entirely possible that the Bodø granites and orthogneisses could be derived from other sources part from the Krummedal.

In either scenario, it is quite clear that both the Bodø granites and orthogneisses and the Heggmovatn supracrustals are not Baltic basement rocks but represent an exotic terrane/thrust sheet of Laurentian affinity.

This further strengthens the widely held view that the Uppermost Allochthon of the Scandinavian Caledonides is of Laurentian affinity.

Thoughts on further work

Apart from the need to date the "cover sequence" of the Bodø orthogneisses, it is also necessary to extend this to the granitic gneisses outcropping on Hjartøya and Landegode, as these units were considered together with the granitic gneisses at Bratten to be Baltic basement.

Much more regional work is required to see how the “Heggmovatn and Bodø thrust sheet” correlate with other thrust sheets in the Uppermost Allochthon (e.g. the Helgeland Nappe Complex, Rødingfjell Nappe Complex and the Allochthon in the Ofoten -Troms area).

No geochemical investigation has been carried out in this study. Geochemical character of the various units might prove insightful on their possible sources whiles a more concerted effort is required to obtain data on the metamorphic evolution of the area.

References

Andersen, T. 1997: Radiogenic isotope systematics of the Herefoss granite, South Norway: an indicator of Sveconorwegian (Grenvillian) crustal evolution in the Baltic Shield. *Chemical Geology* 135, 139-158.

Andersen, T., 2005: Terrane analysis, regional nomenclature and crustal evolution in the Southwest Scandinavian Domain of the Fennoscandian Shield. *GFF*, Vol. 127 (Pt. 2, June), pp. 159–168. Stockholm. ISSN 1103-5897.

Andersen, T., Graham, S. & Sylvester A. G., 2007: Timing and tectonic significance of Sveconorwegian A-type granitic magmatism in Telemark, southern Norway: New results from laser-ablation ICPMS U-Pb dating of zircon. *NGU*-BULL 447, pp17-31

Andresen, A., Hartz, E.H. & Vold, J., 1998a: A late orogenic extensional origin for the infracrustal gneiss domes of the East Greenland Caledonides (728– 748N). *Tectonophysics*, 285, 353–369.

Andresen, A. & Steltenpohl, M.G., 1994: Evidence for ophiolite obduction, terrane accretion and polyorogenic evolution of the north Scandinavian Caledonides. *Tectonophysics 231*, 59-70.

Andresen, A., Rehnström, E.F. and Holte M., 2007: Evidence for simultaneous contraction and extension at different crustal levels during the Caledonian orogeny in NE Greenland. *Journal of the Geological Society*; v. 164; p. 869-880

Augland, L. E., 2010: The Caledonian Liverpool Land eclogite terrane, East Greenland: a Baltic orphan in a Laurentian allochthon. *Journal of the Geological Society* (in press)

Barnes, C. G., Prestvik, T., Nordgulen, Ø. & Barnes, M. A. 1992: Geology of three dioritic plutons in Velfjord, Nordland. *Norges Geologiske Undersokelse* Bulletin 423, 41-54.

Barnes, C.G., Frost, C.D., Yoshinobu, A.S., McArthur, K., Barnes, M.A., Allen, C.M., Nordgulen, O. & Prestvik, T. 2007: Timing of sedimentation, metamorphism, and plutonism in the Helgeland Nappe Complex, north-central Norwegian Caledonides. *Geosphere 3*, 683-703.

Berman, R.G., Aranovich, L.Y., 1996: Optimized standard state and solution properties of minerals. I. Calibration for olivine, orthopyroxene, cordierite, garnet, and ilmenite in the system FeO–MgO– CaO–Al2O3–TiO2–SiO2. *Contributions to Mineralogy and Petrology* 126, 1 – 24.

Bingen, B. and van Breemen, O., 1998: Tectonic regimes and terrane boundaries in the high-grade Sveconorwegian belt of SW Norway, inferred from U-Pb zircon geochronology and geochemical signature of augen gneiss suites. *Journal of the Geological Society, London 155*, 143-154.

Bingen, B., Nordgulen, O. and Solli, A., 2002: U-Pb geochronology of Paleozoic events in the Mid Scandinavian Caledonides, in Eide , E.A.,coord., BATLAS – Mid Norway Plate Reconstruction Atlas with Global and Atlantic Perspectives: Trondheim, *Geological Survey of Norway*, p.66-67

Bingen, B. and Solli, A., 2009: Geochronology of magmatism in the Caledonian and Sveconorwegian belts of Baltica: synopsis for detrital zircon provenance studies. *Norwegian Journal of Geology*, vol. 89, pp. 267-290. Trondheim 2009. ISSN 029-196X.

Birkeland, A., Nordgulen, Ø., Cumming, G.L., and Bjorlykke, A., 1993: Pb-Nd-Sr isotopic constraints on the origin of the Caledonian Bindal Batholith, central Norway: *Lithos*, v. 29, p. 257–271, doi: 10.1016/0024- 4937(93)90020-D.

Bjerkard, T., Larsen, R.B. and Marker, M., 1997, Regional setting of the Bleisvassli Zn-Pb deposit in Nordland, Norway (extended abstracts) *Norges Geologiske Undersokelse Bulletin 433*, 34 – 35

Björklund L., 1987: Basement-cover relationships and regional correlations of the Caledonian nappes, eastern Hinnøy N. Norway, *Nor. Geol. Tidsskr.* **67**, pp. 3–14.

Bugge J.A.W., 1948: Rana Gruber. Geologisk beskrivelse av jernmalmfeltene I Dunderlandsdalen. (Geological description of the iron ore fields in Dunderlandsdal. *Norges Geologiske Undersokelse Bulletin* 171, 149 pp

Cawood, P.A., Nemchin, A.A., Smith, M., Loewy, S., 2003: Source of the Dalradian supergroup constrained by U–Pb dating of detrital zircon and implications for the East Laurentian margin. *Journal of the Geological Society of London* 160, 231–246.

Cawood, P.A., Nemchin, A.A., Strachan, R.A., Kinny, P.D., Loewy, S., 2004:Laurentian provenance and an intracratonic tectonic setting for the Moine Supergroup, Scotland, constrained by detrital zircons from the Loch Eil and Glen Urquhart successions. *Journal of the Geological Society of London* 161 (5), 861–874.

Cocks, L.R.M. and Torsvik, T.H., 2002: Earth geography from 500 to 400 million years ago. A faunal and palaeomagnetic review. *Journal of the Geological Society of London*, 159:631-644.

Corfu, F., 1980: U-Pb and Rb-Sr systematics in a polyorogenic segment of the Precambrian shield, central southern Norway. *Lithos 13*, 305- 323.

Corfu, F., Armitage, P.E.B., Kullerud, K. & Bergh, S.G. 2003a: Preliminary U-Pb geochronology in the West Troms Basement Complex, North Norway: Archaean and Palaeoproterozoic events and younger overprints. *Norges Geologiske Undersokelse Bulletin441*, 61-72.

Corfu, F., Ravna, E.J.K. & Kullerud, K. 2003b: A Late Ordovician U-Pb age for the Tromso Nappe eclogites, Uppermost Allochthon of the Scandinavian Caledonides. *Contributions to Mineralogy and Petrology 145*, 502-513.

Corfu, F., 2004a: U-Pb age, setting and tectonic significance of the anorthosite-mangerite-charnockite-granite suite, Lofoten-Vesteralen, Norway. *Journal of Petrology 45*, 1799-1819

Corfu, F., Torsvik, T.H., Andersen, T.B., Ashwal, L.D., Ramsay, D.M. & Roberts, R.J. 2006: Early Silurian mafic-ultramafic and granitic plutonism in contemporaneous

flysch, Mageroy, northern Norway: U-Pb ages and regional significance. Journal of the Geological Society, *London 163*, 291-301

Corfu, F., 2007: Multistage metamorphic evolution and nature of the amphibolite-granulite facies transition in Lofoten-Vesteralen, Norway, revealed by U-Pb in accessory minerals. *Chemical Geology 241*, 108-128.

Cribb, S.J. 1981: Rb-Sr geochronological evidence suggesting a reinterpretation of part of the north Norwegian Caledonides. *Nor. Geol. Tidsskr* 61,97-110.

Dahl, O., 1969: Irregular distribution of iron and magnesium among coexisting biotite and garnet. *Lithos* 2, 311– 322.

Dahlgren, S., Heaman, L.M. & Krogh, T., 1990a: Abstract. Geological evolution and U - Pb geochronology of the Proterozoic Central Telemark area, Norway. *Geonytt 17*, 38-3

Dahlgren, S., Heaman, L.M. & Krogh, T. 1990b: Abstract. Precise U-Pb zircon and baddeleyite age of the Hesjabutind gabbro, central Telemark area, Southern Norway. *Geonytt 17*, 38.

Dale, J., Holland, J., Powell,R. (2000) Hornblende-garnet-plagioclase thermobarometry: a natural assemblage calibration of the thermodynamics of hornblende. *Contributions to Mineralogy and Petrology* 140, 353 – 362

Dallmeyer, R.D., 1974. The role of crystal structure in controlling the partitioning of Mg and Fe^{2+} between coexisting garnet and biotite. *American Minera*logist 59, 201–203.

Dunning, G.R., and Pedersen, R.B., 1988: U/Pb ages of ophiolites and arc-related plutons of the Norwegian Caledonides: Implications for the development of Iapetus: *Contributions to Mineralogy and Petrology*, v. 98, p. 13–23, doi: 10.1007/BF00371904

Eliasson, T. and Schöberg, H., 1991: U-Pb dating of the post-kinematic Sveconorwegian (Grenvillian) Bohus granite, SW Sweden: Evidence of restitic zircon. *Precambrian Research 51*, 337-350.

Escher, J.C., 2001: Kong Oscar Fjord, sheet no. 11, Geological map of Greenland. 1: 500 000. *Geological Survey of Denmark and Greenland, Copenhagen*

Ferry, J.M. and Spear, F.S., 1978: Experimental calibration of the partitioning of Fe and Mg between biotite and garnet. *Contributions to Mineralogy and Petrology* 66, 113–117.

Fossen, H., Pedersen, RB., Bergh, S. and Andresen, A., 2008: Creation of a mountain chain. In: Ramberg, I.B., Bryhni, I., Nottvedt, A. and Rangnes, K. (eds.) 2008, The Making of a Land – Geology of Norway. Trondheim, *Norsk Geologisk Forening*, 178 – 231

Friend, C.R.L., Strachan, R.A., Kinny, P.D. & Watt, G.R., 2003: Provenance of the Moine Supergroup of NW Scotland: evidence from geochronology of detrital and inherited zircons from sediments, granites and migmatites. *Journal of the Geological Society, London*, 160, 247–258

Friedrich, A.M., Hodges, K.V., Bowring, S.A. and Martin, M.W., 1999: Geochronological constraints on the magmatic, metamorphic, and thermal evolution of the Connemara Caledonides, western Ireland. *Journal of the Geological Society, London* 156, pp. 1217–1230

Friderichsen, D.N., Henriksen, N. and Stracharn, A. 1994: Basement-cover relationships and regional structure in the Grandjean Fjord-Bessel Fjord region (75-76"N), North-East Greenland Caledonides. *Rapport Gronlands geologiske UndersQgelse***,** 162, 17-23.

Frost, M.J., 1962: Metamorphic grade and iron–magnesium distribution between coexisting garnet–biotite and garnet–hornblende. *Mineralogical Magazine* 99, 427–438

Fuhrman, M.L., Lindsley, D.H., 1988: Ternary-feldspar modeling and thermometry. *American Mineralogist* 73, 201– 215.

Furnes, H., Skjerlie, K.P., Pedersen, R.B., Andersen, T.B., Stillman, C.J., Suthren, R.J., Tysseland, M., Garmann, L.B., 1990: The Solund –Stavfjord Ophiolite Complex

and associated rocks, west Norwegian Caledonides: geology and tectonic environment. *Geol. Mag*. 127, 209– 224.

Furnes, H. & Pedersen, R. B. 1995: The Lyngen Magmatic Complex: geology and geochemistry. *Geonytt* 22, 30.

Ganguly, J., Kennedy, G.C., 1974: The energetics of natural garnet solid solution I. Mixing of the aluminosilicate end-members. *Contributions to Mineralogy and Petrology* 48, 137-148

Ganguly, J., Cheng, W., Tirone, M., 1996: Thermodynamics of aluminosilicate garnet solid solution: new experimental data, an optimized model, and thermodynamic applications. *Contributions to Mineralogy and Petrology* 126, 137– 151.

Gee DG and Sturt BA (eds.) 1985: The Caledonides Orogen – Scandinavia and Related Areas. Chichester: Wiley.

Gee, D.G., 1975: A tectonic model for the central part of the Scandinavian Caledonides. *American Journal of Science* 275A, 468– 515.

Gee, D. G., 1978: Nappe displacement in the Scandinavian Caledonides. *Tectonophysics* **47**, 393–419.

Gee, D.G. 2005: Scandinavian Caledonides (with Greenland). *In* Selley, R.C., Cocks, L.R.M. & Plimer, I.R. (eds), *Encyclopedia of Geology*. Elsevier, Amsterdam, 64 -74

Gower, C.F., Krogh, T.E., 2002. A U–Pb geochronological review of the Proterozoic history of the eastern Grenville Province. *Canadian Journal of Earth Science*. 39 (5), 795–829.

Graham, C.M., and Powell, R., 1984: A garnet - hornblende geothermometer: Calibration, testing, and application to the Pelona Schist, southern California. *Journal of Metamorphic Geology*, 2, 13-21.

Grenne, T., Ihlen, P.M. & Vokes, F.M., 1999: Scandinavian Caledonide metallogeny in a plate tectonic perspective. *Mineralium Deposita 34*, 422-471.

Griffin, W. L. & Taylor, P. N., 1978: Geology and age relations on Vaerøy, Lofoten, North Norway. *Norges Geologiske Undersøkelse* 338, 71–82.

Gustavson, M. 1966. The Caledonian mountain chain of the southern Troms and Ofoten areas: Part I: Basement rocks and Caledonian metasediments. *Norges Geologiske Undersøkelse*, 239, 1–162.

Gustavson, M. 1981: Geologisk kart over Norge, berggrunnSkårt MOSJØEN – M 1:250 000.*Norges Geologiske Undersokelse*

Gustavson, M. and Blystad, P., 1995: Geologisk kart over Norge, berggrunnSkårt BODØ, M 1:250 000. *Norges geologiske undersøkelse*.

Gustavson, M. 1991:, BODØ 2029 IV, berggrunnSkårt M 1: 50 000. *Norges geologiske undersøkelse*.

Gustavson, M., Gjelle, S.T., 1991. Geologisk kart over Norge. BerggrunnSkårt MO I RANA, M 1:250 000. *Norges geologiske undersøkels*

Gustavson, M., 1996: Geologisk kart over Norge. BerggrunnSkårt SULITJELMA, M 1:250 000. *Norges Geologiske Undersokelse*

Gustavson, M., Cooper, M. A., Kollung, S. and Tragheim, D. G., 1999: BerggrunnSkårt Fauske 2129 IV, M 1:50 000. *Norges Geologiske Undersokelse.*

Haller, J. 1971: Geology of the East Greenland Caledonides. *Interscience*. London.

Hambrey, M.J. & Spencer, A.M. 1987: Late Precambrian Glaciation of Central East Greenland. Meddelelser om Grønland, *Geoscience*. 19, 1–50.

Heldal, T., 2001: Ordovician stratigraphy in the western Helgeland Nappe Complex in the Brønnøysund area, north-central Norway: *Norges Geologiske Undersøkelse* Bulletin, v. 438, p. 47–61.

Henriksen, N. 2003: Caledonian Orogen, East Greenland 708–808N, Geologic Map 1:1000 000. *Geological Survey of Denmark and Greenland, Copenhagen.*

Hietanen, A., 1969: Distribution of Fe and Mg between garnet, staurolite, and biotite in aluminum-rich schist in various metamorphic zones north of the Idaho batholith. *American Journal of Science* 267, 422– 456.

Higgins, A.K., 1988: The Krummedal supracrustal sequence in East Greenland. In: Winchester, J.A. (ed.): *Later Proterozoic stratigraphy of the northern Atlantic regions*, 86–96. Glasgow & London: Blackie and Son Ltd.

Higgins, A.K., Elvevold, S. & Escher, J.C. et al. 2004: The foreland propagating architecture of the East Greenland Caledonides 728–758N. *Journal of the Geological Society, London*, 161, 1009–1026.

Hodges, K.V., Spear, F.S., 1982: Geothermometry, geobarometry and the Al2SiO5 triple point at Mt Moosilauke, New Hampshire. *American Mineralogist* 67, 1118–1134.

Holdaway, M.J., 2000: Application of new experimental and garnet Margules data to the garnet–biotite geothermometer, *American Mineralogist* 85, pp. 881–892.

Holdaway, M.J. Optimization of some key geothermobarometers for pelitic metamorphic rocks, *Mineralogical Magazine* 68 (2004), pp. 1–14

Holland, T. and Blundy, J., 1994: Non-ideal interactions in calcic amphiboles and their bearing on amphibole-plagioclase thermometry. *Contributions to Mineralogy and Petrology*, 116: 433-447.

Holmquist, P.J., 1900: En geologisk profil ofver fjallomradena emellan kvikkjokk och norska kutsen. *GFF*. Bd. 22

Indares, A., Martignole, J., 1985: Biotite–garnet geothermometry in the granulite facies: the influences of Ti and Al in biotite. *American Mineralogist* 70, 272– 278.

Jackson S.E., Pearson, N.J. Griffin, W.L. and Belousova, E.A. The application of laser ablation-inductively coupled plasma-mass spectrometry to in situ U–Pb zircon geochronology *Chem. Geol.* 211 (2004), pp. 47–69

Kalsbeek, F., Nutman, A.P., and Taylor, P.N., 1993: Palaeoproterozoic basement province in the Caledonian fold belt of North-East Greenland: *Precambrian Research*, v. 63, p. 163–178, doi: 10.1016/0301-9268(93) 90010-Y.

Kalsbeek, F., Thrane, K., Nutman, A.P., and Jepsen, H.F., 2000: Late Mesoproterozoic to early Neoproterozoic history of the East Greenland Caledonides: Evidence for Grenvillian orogenesis?: *Journal of the Geological Society of London*, v. 157, p. 1215–1225.

Kalsbeek, F. Higgins, A.K., Jepsen H. F., Frei, R. and Nutman, A.P., 2008: Granites and granites in the East Greenland Caledonides. *The Geological Society of America Memoir* 202 pp227 – 249

Kautsky, G., 1953: Der geologische Bau des Sulitelma-Salojauregebietes in den nordskandinavischen Kaledoniden. *Sver. Geol. Unders*., No. C528, 233 pp.

Kinny, P.D., Strachan, R.A., Friend, C.R.L., Kocks, H., Rogers, G. & Paterson, B., 2003: U–Pb geochronology of deformed metagranites in central Sutherland, Scotland: evidence for widespread late Silurian metamorphism and ductile deformation of the Moine Supergroup during the Caledonian orogeny. *Journal of the Geological Society, London*, 160, 259–269

Kretz, R., 1964: Analysis of equilibrium in garnet–biotite–sillimanite gneisses from Quebec. *Journal of Petrology* 5, 1 –20.

Kohn, M.J. and Spear, F.S., 1989: Empirical calibration of geobarometers for the assemblage garnet + hornblende + plagioclase + quartz. *American Mineralogist*, 74, 77-84.

Koenemann, F. H., 1993: Tectonics of the Scandian Orogeny and the Western Gneiss Region in southern Norway. *Geologische Rundschau* 82, 696–717.

Kohn, M.J. and Spear, F.S., 1990: Two new barometers for garnet amphibolites with applications to southeastern Vermont. *American Mineralogist*, 75, 89-96

Krogh, T.E., 1982: Improved accuracy of U-Pb zircon ages by the creation of more concordant systems using an air abrasion technique: *Geochimica et Cosmochimica Acta*, v. 46, p. 637–649.

Kullerud, L., Torudbakken, B. O. & Ilebekk, S., 1986: A compilation of radiometric age determinations from the Western Gneiss Region. South Norway. *Norges Geologiske Undersokelse*., 406, 17-42

Kullerud, L. & Machado, N., 1991: Abstract. End of a controversy: U-Pb geochronological evidence for significant Grenvillian activity in the Bamble area, Norway. *Terra Abstracts, supplement to Terra Nova 3*, 504.

Laajoki, K., Corfu, F. & Andersen, T., 2000: U-Pb zircon dating of the Mesoproterozoic Brunkeberg Formation and its bearing on the stratigraphy of Telemark Supracrustals, South Norway. *Goldschmidt 2000, Oxford UK, Journal of Conference Abstracts 5(2)*, 611.

Leslie, A.G., and Nutman, A.P., 2003: Evidence for Neoproterozoic orogenesis and early high temperature Scandian deformation events in the southern East Greenland Caledonides: *Geological Magazine*, v. 140, p. 309–333, doi: 10.1017/S0016756803007593

Ludwig, K.R., 2003: User's Manual for Isoplot 3.00 a Geochronological Toolkit for Microsoft Excel

Lyons, J.B., Morse, S.A., 1970: Mg/Fe partitioning in garnet and biotite from some granitic, pelitic, and calcic rocks. *American Mineralogist* 55, 231–245.

Melezhik V.A., Gorokhov I.M., Fallick A.E. and Gjelle S., 2001a: Strontium and carbon isotope geochemistry applied to dating of carbonate sedimentation: an example from high-grade rocks of the Norwegian Caledonides, *Precambrian Research* 108, pp. 267–292

Melezhik, V. A., Roberts, D., Gorokhov, I. M., Fallick, A.E., Zwaan, K.B., Kuznetsov, A.B. & Pokrovsky, B.G. 2002a: Isotopic evidence for a complex Neoproterozoic to

Silurian rock assemblage in the North-Central Norwegian Caledonides. *Precambrian Research*, 114, 55–86.

Melezhik V.A., Gorokhov I.M., Fallick A.E., Roberts D., Kuznetsov A.B. and Zwaan K.B. , 2002b: Isotopic stratigraphy suggests Neoproterozoic ages and Laurentian ancestry for high-grade marbles from the North-Central Norwegian Caledonides, *Geol. Mag.* 139 pp. 375–393.

Melezhik V.A., Filippov M.M. and Romashkin A.E., 2003: Shunga Event—was it a case of Palaeoproterozoic mass extinction? *Geochim. Cosmochim. Acta* 67S 286.

Meyer, G. B., Grenne, T., & Pedersen, R. B., 2003: Age and tectonic setting of the Nesåa Batholith: implications for Ordovician arc development in the Caledonides of central Norway. *Geological Magazine* 140, 573–594.

Newton, R.C., Charlu, T.V., Kleppa, O.J., 1977: Thermochemistry of high pressure garnets and clinopyroxenes in the system $CaO–MgO–Al_2O_3–SiO_2$. *Geochimica et Cosmochimica Acta* 41,369–377.

Nicholsen, R. & Rutland, R.W.R. 1969: A section across the Norwegian Caledonides; Bodø to Sulitjelma. *Norges Geologiske Undersøkelse* 260, pp. 86.

Nordgulen, Ø., Bickford, M.E., Nissen, A.l. and Wortman, G.L. 1993: U/Pb zircon ages from the Bindal Batholith and the tectonic history of the Helgeland Nappe Complex, Scandinavian Caledonides. *Journal of the Geological Society, London* 150, 771-783.

Nordgulen, Ø.,Tucker, R.D., Sundvoll, B., Solli, A., Nissen, A. L., Zwaan, K. B., Birkeland, A. & Sigmond, E. M. O. 1997: Palaeo- to Mesoproterozoic intrusive rocks in the area between Numedal and Mjøsa, SE Norway. *In* Nordgulen, Ø., Padget, P., Robinson, P. & McEnroe, S. (eds.), *Copena Conference*, 97.131, 69-70. *Norges Geologiske Undersøkelse*, Trondheim

Nystuen, J.P., Andresen, A., Kumpulainen, R. and Siedlecka, A., 2008: Neoproterozoic basin evolution in Fennoscandia, East Greenland and Svalbard. *Norwegian Journal of Geology* Episodes, *31(1),* 35-43.

Oliver, G.J.H. & Krogh, T.E. 1995: U-Pb zircon age of 469 ±5 Ma for a metatonalite from the Kjosen Unit of the Lyngen Magmatic Complex, northern Norway. *Norges Geologiske Undersokelse Bulletin 428*, 27-32.

Pasteels, P., Demaiffe, D. & Michot, J. 1979: U-Pb and Rb-Sr geochronology of the eastern part of the south Rogaland igneous complex, southern Norway. *Lithos 12*, 199-208.

Pedersen, R.B., Furnes, H., Dunning, G., 1991: A U/Pb age for the Sulitjelma Gabbro, north Norway: further evidence for the development of a Caledonian marginal basin in Ashgill– Llandovery time. *Geol. Mag*. 128, 141–153.

Perchuk, L.L., 1967: Biotite–garnet geothermometer. *Dokalady Geoscience* Section 177, 411 –414.

Perchuk, L.L., 1970: Equilibrium of biotite with garnet in metamorphic rocks. *Geochemistry International* 7, 157– 179.

Perchuk, L.L., Lavrent'eva, I.V., 1983: Experimental investigation of exchange equilibria in the system cordierite–garnet–biotite. In: Saxena, S.K. (Ed.), *Kinetics and Equilibrium in Mineral Reactions*. Springer-Verlag, New York, pp. 199–239

Ramberg, I. B., 1967:Kongsfjell-omrhdets geologi, en petrografisk og strukturell undersokelse i Helgeland, Nord-Norge. *Norges Geologiske. Undersøkelse*. 240, 152 pp

Rex, D.C. & Gledhill, A.R. 1981: Isotopic studies in the East Greenland Caledonides (72°–74°N) – Precambrian and Caledonian ages. *Rapport Grønlands Geologiske Undersøgelse 104, 47–72.*

Roberts, D. Nordgulen, O. Melezhik, V., 2007: The Uppermost Allochthon in the Scandinavian Caledonides: From a Laurentian ancestry through Taconian orogeny to Scandian crustal growth on Baltica. MEMOIRS- *Geological Society of America*, NUMB 200, pages 357-378

Roberts, D., Gee, D.G., 1985: An introduction to the structure of the Scandinavian Caledonides. In: Gee, D.G., Sturt, B.A. (Eds.), *The Caledonide Orogen—Scandinavia and Related Areas. Wiley, Chichester,* pp. 55– 68.

Roberts R.J., Corfu F, Torsvik T.H., Ashwal L.D. and Ramsay D.M. 2006: Short-lived mafic magmatism at 560-570 Ma in the northern Norwegian Caledonides: U/Pb zircon ages from the Seiland Igneous Province. *Geological Magazine* 143**:** *887-903.*

Roberts, D., 2003: The Scandinavian Caledonides: event chronology, palaeogeographic settings and likely modern analogues. *Tectonophysics* 365 (1–4), 283–299.

Rogers, G., Kinny, P.D., Strachan, R.A., Friend, C.R.L. & Paterson, B.A., 2001: U–Pb geochronology of the Fort Augustus granite gneiss: constraints on the timing of Neoproterozoic and Palaeozoic tectonothermal events in the NW Highlands of Scotland. *Journal of the Geological Society, London,* 158, 7–14.

Rutland, R. W. R. 1959: Structural geology of the Sokumvatn area, North Norway .Norsk *geol.Tidsskr.* 39, PP. 287-337

Rutland, RW.R. & Nicholsen, R., 1965: Tectonics of the Caledonides of part of Nordland, Norway. Quarterly Journal of the Geological Society 121, 73-109.

Sandøy, R. 2003: Geological variations in marble deposits. The geometry, internal structure and geochemical variations of the industrial mineral marble deposits in the Velfjord area. *PhD thesis, Norwegian University of Science and Technology, Trondheim.*

Saxena, S.K., 1969: Silicate solid solutions and geothermometry: 3. Distribution of Fe and Mg between coexisting garnet and biotite. *Contributions to Mineralogy and Petrology* 22, 259– 267.

Schärer, U., Wilmart, E. & Duchesne, J.-C. 1996: The short duration and anorogenic character of anorthosite magmatism: U-Pb dating of the Rogaland complex, Norway. *Earth and Planetary Science Letters 139,* 335-350.

Sen, S.K. and Chakraborty, K.R., 1968: Magnesium–iron equilibrium in garnet–biotite and metamorphic grade. *Neues Jahrbuch fu¨ r Mineralogie. Abhandlungen* 108, 181– 207.

Selbekk, R. S., Skjerlie, K. P. & Pedersen, R. B., 2000: Generation of anorthositic magma by H_2O-fluxed anatexis of silica - undersaturated gabbro: an example from the north Norwegian Caledonides.

Skår, Ø. 1998: The Proterozoic and Early Paleozoic evolution of the southern parts of the Western Gneiss Complex, Norway. *PhD thesis, University of Bergen*

Skår, Ø., 2002: U–Pb geochronology and geochemistry of early Proterozoic rocks of the tectonic basement windows in central Nordland, Caledonides of north–central Norway. *Precambrian Research* 116, 265–283.

Smith, M.P. & Bjerreskov, M., 1994: The Ordovician System in Greenland; correlation chart and stratigraphic lexicon. In: Williams, S.H. (ed.) The Ordovician System in Greenland and South Africa. *International Union of Geological Sciences*, Publication, 29A, 1–46.

Solli, A and Nordgulen,O. 2008: Bedrock map of Norway and the Caledonides in Sweden and Finland- 1: 2000 000. *Geological Survey of Norway*.

Sønderholm, M., and Tirsgaard, H., 1993: Lithostratigraphic framework of the Upper Proterozoic Eleonore Bay Supergroup of East and North-East Greenland: *Grønlands Geologiske Undersøkelse* Bulletin, v. 167, pp. 1–38.

Spear, F.S., 1991: On the interpretation of peak metamorphic temperatures in light of garnet diffusion during cooling. *Journal of Metamorphic Geology*, 9, 379-388.

Spear, F.S. and Florence, F.P., 1992: Thermobarometry in granulites: Pitfalls and new approaches. *Journal of Precambrian Research*, 55, 209-241.

Spear, F.S., 1993: Metamorphic Phase Equilibria and Pressure-temperature-Time Paths. *Mineralogical Society of America*. Monograph 1. MSA, Washington DC

Stacey, J.S., Kramers, J.D., 1975: Approximation of terrestrial lead isotope evolution by a two-stage model. Earth Planet. *Sci. Lett*. 26, 207– 221

Steiger; R.H, Harnik-Soptrajanova, G., Zimmermann, E. and Henriksen, N., 1976: Isotopic age and metamorphic history of' the banded gneiss at Danmarkshavn, East Green1and.- *Contributions to Mineralogy and Petrology*, 57: 1-24

Steiger, R.H., Hansen, B.T., Schuler, C., Bär, M.T. & Henriksen, N. 1979: Polyorogenic nature of the southern Caledonian fold belt in East Greenland. *Journal of Geology* 87, 475–495.

Steltenpohl, M.G., Andresen, A. & Tull, J.M. 1990: Lithostratigraphic correlation of the Salangen (Ofoten) and Balsfjord (Troms) Groups: evidence for post-Finnmarkian unconformity, North Norwegian Caledonides. *Norges Geologiske Undersøkelse Bulletin*, 418, 61–77.

Steltenpohl M.G. and Andresen A., 1991: Nappe sequences in the Ofoten Region: Implication for terrane accretion, ophiolite obduction and polyorogenic evolution. In: A. Andresen and M.G. Steltenpohl, Editors, *A Geotraverse Excursion through the Scandinavian Caledonides: Tornetrask-Ofoten-Tromsø*, pp. 1–19.

Steltenpohl, M., Hames, W., Andresen, A. & Markl, G. 2003: New Caledonian eclogite province in Norway and potential Laurentian (Taconic) and Baltic links. *Geology 31*, 985-988.

Stephens, M.B., Gee, D.G., 1985: A tectonic model for the evolution of the eugeoclinal terranes in the central Scandinavian Caledonides. In: Gee, D.G., Sturt, B.A. (Eds.), *The Caledonide Orogen—Scandinavia and Related Areas.* Wiley, Chichester, pp. 953–970.

Stephens, M.B., Gee, D.G., 1989: Terranes and polyphase accretionary history in the Scandinavian Caledonides. *Geological Society of America*. Special Paper 230, 17– 30.

Stephens, M.B., Gustavson, M., Ramberg, I.B., Zachrisson, E., 1985: The Caledonides of central-north Scandinavia? A tectonostratigraphic overview. In: Gee, D.G., Sturt, B.A. (Eds.), *The Caledonide Orogen—Scandinavia and Related Areas*. John Wiley and Sons, Chichester. pp. 135–162.

Stephens, M.B., Kullerud, K. & Claesson, S., 1993a: Early evolution in outboard terranes, central Scandinavian Caledonides: new constraints from U-Pb zircon dates. *Journal of the Geological Society, London 150*, 51-56.

Storey, C.D., Brewer, T.S., and Parrish, R.R., 2004: Late Proterozoic tectonics in northwestScotland: one contractional orogeny or several. *Precambrian Research*, v. 134, p. 227- 247

Sturt, D. A. & Austrheim, H. 1985: Age of gneissic rocks in the Caledonian nappes of the Alta district, northern Norway. *Norges Geologiske Undersøkelse, Bulletin,* 403, 179–181.

Tanner, P.W.G. & Evans, J.A. 2003: Late Precambrian U–Pb titanite age for peak regional metamorphism and deformation (Knoydartian orogeny) in the western Moine, Scotland. *Journal of the Geological Society, London*, 160, 555–564

Tørudbakken, B. & Brattli, B. 1985: Ages of metamorphic and deformational events in the Beiarn Nappe Complex, Nordland, Norway. *Norges Geologiske Undersøkelse* 399, 27-39.

Tucker, R.D., Krogh, T.E. & Raheim, A., 1990b: Proterozoic evolution and age – province boundaries in the central part of the Western Gneiss Region, Norway: results of U-Pb dating of accessory minerals from Trondheimsfjord to Geiranger. *In:* C.F. Gower, T. Rivers & B.

Tucker, R.D., Robinson, P., Solli, A., Gee, D.G., Thorsnes, T., Krogh, T.E., Nordgulen, O. & Bickford, M.E., 2004: Thrusting and extension in the Scandian hinterland, Norway: new U-Pb ages and tectonostratigraphic evidence. *American Journal of Science 304*, 477-532.

Watt, G.R., Kinny, P.D., and Friderichsen, J.D., 2000: U-Pb geochronology of Neoproterozoic and Caledonian tectonothermal events in the East Greenland Caledonides: *Journal of the Geological Society of London*, v. 157, p. 1031–1048.

Watt, G. R., and Thrane, K. 2001: Early Neoproterozoic events in east Greenland. *Precambrian Research*. 110:165– 184.

Wilberg, R., 1987: Rekognoserende Rb–Sr aldersbestemmelser av granittiske gneiser fra grunnfjellsvinduene Høgtuva og Sjona i Nordland. *Norges Geologiske Undersokelse* Rapport 87.074, 21 pp

Williams, M.L., Grambling, J.A., 1990: Manganese, ferric iron, and the equilibrium between garnet and biotite. *American Mineralogist* 75, 886–908

Wilson, M.R., 1971: The timing of orogenic activity in the Bodø-Sulitjelma area. Norges *Geologiske Undersøkelse* 269, 184-190

Wilson, M.R., 1973: The geological setting of the Sulitjelma ore bodies, Central Norwegian Caledonides. *Economic Geology* 68, 307-316.

Wilson, M.R. & Nicholson, R. 1973: The structural setting and geochronology of basal granitic gneisses in the Caledonides of part of Nordland, Norway. *Journal of the Geological Society, London*. 129, 365-387.

Wu, C.M., Zhang, J. and Ren, L.D., 2004a: Empirical garnet–biotite–plagioclase–quartz (GBPQ) geobarometry in medium- to high-grade metapelites, *Journal of Petrology* 45, pp. 1907–1921

Yoshinobu, A.S., Barnes, C.G., Nordgulen, Ø., Prestvik, T., Fanning, M., and Pedersen, R.B., 2002: Ordovician magmatism, deformation, and exhumation in the Caledonides of central Norway: An orphan of the Taconic orogeny?: *Geology*, v. 30, p. 883– 886, doi: 10.1130/0091-7613(2002)030<0883:

Appendix 1- Electron microprobe Analysis

Garnet in NA 09-3 Orthogneiss (Pre – Caledonian rocks)

	Core	Core	Core	Core	Core	Core	Rim	Rim	Rim	Rim	Rim
SiO2	37.386	37.891	37.932	37.331	37.882	37.761	37.202	37.793	37.121	37.461	36.383
TiO2	0.02	0.128	0.015	0.083	0.067	0.08	0.088	0.142	0.095	0.105	0.03
Al2O3	20.867	21.135	21.154	20.99	21.163	21.383	21.033	21.273	21.007	21.318	20.988
Cr2O3	0	0.05	0	0	0.031	0	0.022	0.031	0.019	0.013	0.054
Fe2O3	0	0	0	0	0	0	0	0	0	0	0
FeO	26.024	24.421	25.31	25.507	24.679	23.968	25.966	24.578	24.86	24.291	26.876
MnO	2.863	3.338	2.185	2.919	2.856	2.601	2.936	2.901	2.814	3.364	2.727
MgO	1.363	1.089	1.195	1.194	1.109	1.083	1.267	1.192	1.22	1.055	1.378
CaO	11.518	12.544	12.297	11.792	12.437	13.544	11.775	12.639	12.847	12.832	10.909
Na2O	0.049	0.022	0.022	0.035	0.026	0.007	0.059	0.018	0.012	0.004	0.044
K2O	0.006	0.007	0	0.008	0	0	0.007	0.005	0.014	0.001	0
Total	100.1	100.63	100.11	99.863	100.25	100.43	100.36	100.57	100.01	100.45	99.393
				Cations based on 12 oxygens atoms							
Si	2.971	2.992	3.007	2.973	3.001	2.979	2.949	2.982	2.947	2.962	2.916
Ti	0.001	0.008	0.001	0.005	0.004	0.005	0.005	0.008	0.006	0.006	0.002
Al2	1.955	1.968	1.977	1.971	1.976	1.989	1.966	1.979	1.966	1.987	1.983
Cr	0	0.003	0	0	0.002	0	0.001	0.002	0.001	0.001	0.003
Fe3+	0.109	0.034	0.009	0.078	0.016	0.046	0.134	0.041	0.131	0.076	0.184
Fe2+	1.621	1.579	1.669	1.621	1.619	1.535	1.588	1.581	1.52	1.53	1.618
Mn	0.193	0.223	0.147	0.197	0.192	0.174	0.197	0.194	0.189	0.225	0.185
Mg	0.161	0.128	0.141	0.142	0.131	0.127	0.15	0.14	0.144	0.124	0.165
Ca	0.981	1.061	1.045	1.006	1.056	1.145	1	1.069	1.093	1.087	0.937
Na	0.008	0.003	0.003	0.005	0.004	0.001	0.009	0.003	0.002	0.001	0.007
K	0.001	0.001	0	0.001	0	0	0.001	0.001	0.001	0	0
Total	8	8	7.999	7.999	8.001	8.001	8	8	8	7.999	8

Appendix 1- Electron microprobe Analysis

Biotite in NA 09-3 Orthogneiss (Pre – Caledonian rocks)

	Core	Core	Core	Core	Rim	Rim	Rim	Rim	Rim
SiO2	35.632	35.506	36.212	35.268	35.283	35.705	35.221	35.491	35.484
TiO2	3.555	2.607	3.698	3.553	3.404	3.531	2.522	2.54	3.424
Al2O3	16.674	16.746	16.678	16.517	16.353	16.5	16.714	17.201	16.351
Cr2O3	0	0.032	0.029	0.035	0.096	0.067	0.001	0.006	0.009
Fe2O3	0	0	0	0	0	0	0	0	0
FeO	23.579	25.592	23.365	23.966	24.502	23.777	25.278	24.981	23.838
MnO	0.118	0.216	0.17	0.146	0.174	0.163	0.187	0.187	0.155
MgO	6.578	6.032	6.574	6.675	6.685	6.732	6.112	6.113	6.881
CaO	0	0	0.011	0.003	0	0.001	0	0	0
Na2O	0.042	0.057	0.042	0.061	0.031	0.032	0.03	0.043	0.012
K2O	9.55	9.55	9.762	9.722	9.867	9.823	9.638	9.679	9.776
Total	95.73	96.341	96.544	95.95	96.4	96.335	95.705	96.246	95.935
				Cations based on 11 oxygen atoms					
Si	2.763	2.764	2.78	2.742	2.74	2.759	2.76	2.757	2.756
Ti	0.207	0.153	0.214	0.208	0.199	0.205	0.149	0.148	0.2
Al2	1.524	1.537	1.51	1.514	1.497	1.503	1.544	1.575	1.497
Cr	0	0.002	0.002	0.002	0.006	0.004	0	0	0.001
Fe3+	0	0	0	0	0	0	0	0	0
Fe2+	1.529	1.666	1.5	1.558	1.591	1.537	1.657	1.623	1.549
Mn	0.008	0.014	0.011	0.01	0.011	0.011	0.012	0.012	0.01
Mg	0.76	0.7	0.752	0.773	0.774	0.775	0.714	0.708	0.797
Ca	0	0	0.001	0	0	0	0	0	0
Na	0.006	0.009	0.006	0.009	0.005	0.005	0.005	0.006	0.002
K	0.945	0.948	0.956	0.964	0.978	0.969	0.964	0.959	0.969
Total	7.744	7.793	7.732	7.78	7.801	7.768	7.804	7.79	7.781

Appendix 1- Electron microprobe Analysis

Plagioclase in NA 09-3 Orthogneiss (Pre – Caledonian rocks)

	Core	Core	Rim	Rim
SiO2	61.164	60.63	61.328	60.67
TiO2	0	0.015	0	0.013
Al2O3	24.512	24.422	23.824	24.436
Cr2O3	0	0	0	0
Fe2O3	0	0	0	0
FeO	0.033	0.04	0.046	0.03
MnO	0	0	0	0
MgO	0	0	0	0
CaO	6.313	6.714	6.431	6.638
Na2O	8.132	7.87	8.296	7.879
K2O	0.253	0.223	0.359	0.214
Total	100.411	99.914	100.284	99.883
	Cations based on 8 oxygen atoms			
Si	2.71	2.702	2.726	2.704
Ti	0	0.001	0	0
Al2	1.281	1.283	1.248	1.284
Cr	0	0	0	0
Fe3+	0.001	0.001	0.002	0.001
Fe2+	0	0	0	0
Mn	0	0	0	0
Mg	0	0	0	0
Ca	0.3	0.321	0.306	0.317
Na	0.699	0.68	0.715	0.681
K	0.014	0.013	0.02	0.012
Total	5.005	5.001	5.017	5

Appendix 1- Electron microprobe Analysis

Garnet in NA 09 – 15 Garnetiferous schist (Bodø Group)

	Core	Core	Core	Core	Core	Core	Rim	Rim	Rim	Rim	Rim
SiO2	37.767	37.979	38.464	37.842	38.171	38.028	38.443	38.088	38.334	37.816	38.143
FeO	20.546	20.865	21.062	20.207	19.664	18.996	20.05	20.335	21.175	21.738	21.583
Al2O3	20.965	20.946	21.419	21.762	21.609	21.351	21.611	21.419	21.521	21.589	21.496
Cr2O3	0.186	0.167	0.139	0.083	0.041	0.174	0.118	0.124	0.13	0.086	0
TiO2	0.254	0.23	0.033	0.025	0.055	0.038	0.035	0.065	0.063	0.043	0.047
MnO	3.313	3.049	2.868	2.959	2.745	3.29	2.879	2.736	2.601	3.018	3.027
MgO	2.083	2.071	2.723	2.394	2.5	1.925	2.756	2.857	2.766	2.477	2.905
CaO	15.022	14.75	14.058	14.873	15.643	16.684	14.529	14.217	14.102	13.743	13.207
Na2O	0	0	0	0	0	0.007	0	0.008	0.005	0.015	0
K2O	0	0.011	0	0.01	0.008	0	0.005	0	0	0.006	0.006
Total	100.14	100.07	100.77	100.16	100.44	100.5	100.43	99.852	100.7	100.53	100.42
				Cations based on 12 oxygens atoms							
Si	2.962	2.953	2.958	2.928	2.94	2.937	2.956	2.949	2.949	2.927	2.947
Ti	0.015	0.013	0.002	0.001	0.003	0.002	0.002	0.004	0.004	0.003	0.003
Al2	1.938	1.92	1.942	1.985	1.962	1.944	1.959	1.955	1.952	1.97	1.958
Cr	0.012	0.01	0.008	0.005	0.002	0.011	0.007	0.008	0.008	0.005	0
Fe3+	0.097	0.097	0.096	0.097	0.096	0.096	0.096	0.097	0.096	0.097	0.096
Fe2+	1.251	1.357	1.354	1.308	1.266	1.227	1.289	1.317	1.362	1.407	1.394
Mn	0.22	0.201	0.187	0.194	0.179	0.215	0.188	0.179	0.169	0.198	0.198
Mg	0.243	0.24	0.312	0.276	0.287	0.222	0.316	0.33	0.317	0.286	0.334
Ca	1.262	1.229	1.158	1.233	1.291	1.381	1.197	1.179	1.162	1.14	1.093
Na	0	0	0	0	0	0.001	0	0.001	0.001	0.002	0
K	0	0.001	0	0.001	0.001	0	0	0	0	0.001	0.001
Total	8	8.021	8.018	8.028	8.027	8.036	8.011	8.018	8.02	8.036	8.024

Appendix 1- Electron microprobe Analysis

Amphibole in NA 09 – 15 Garnetiferous schist (Bodø Group)

	Inclusion	Inclusion	Inclusion	Core	Core	Rim	Rim	Rim
SiO2	44.737	46.429	43.582	49.826	51.57	48.795	48.506	48.519
TiO2	0.53	0.515	0.519	0.329	0.235	0.367	0.344	0.38
Al2O3	13.687	11.535	15.578	8.33	7.099	9.438	10.545	9.591
Cr2O3	0.247	0.076	0.162	0.08	0.022	0.009	0.06	0.034
Fe203	0	0	0	0	0	0	0	0
FeO	13.482	12.519	13.755	10.869	10.601	11.454	11.904	11.339
MnO	0.283	0.258	0.236	0.26	0.226	0.283	0.265	0.235
MgO	11.034	12.043	9.834	14.573	15.321	13.775	13.127	13.981
CaO	11.775	12.011	12.33	12.409	12.527	12.381	12.342	12.566
Na2O	1.131	0.929	1.266	0.682	0.553	0.764	0.829	0.793
K2O	0.205	0.204	0.279	0.133	0.089	0.152	0.147	0.167
Total	97.117	96.523	97.545	97.496	98.246	97.421	98.072	97.61
			Cations based on 23 oxygens atoms					
Si	6.538	6.711	6.3	7.052	7.213	6.938	6.863	6.892
Ti	0.058	0.056	0.056	0.035	0.025	0.039	0.037	0.041
Al2	2.358	1.966	2.655	1.39	1.171	1.582	1.759	1.606
Cr	0.029	0.009	0.019	0.009	0.002	0.001	0.007	0.004
Fe3+	0.239	0.236	0.236	0.231	0.229	0.233	0.231	0.232
Fe2+	1.409	1.513	1.663	1.287	1.24	1.362	1.409	1.347
Mn	0.035	0.032	0.029	0.031	0.027	0.034	0.032	0.028
Mg	2.403	2.594	2.119	3.074	3.194	2.919	2.768	2.96
Ca	1.844	1.86	1.91	1.882	1.878	1.886	1.871	1.913
Na	0.32	0.26	0.355	0.187	0.15	0.211	0.227	0.218
K	0.038	0.038	0.051	0.024	0.016	0.028	0.027	0.03
Total	15.35	15.276	15.392	15.203	15.144	15.234	15.229	15.271

Appendix 1- Electron microprobe Analysis

Pagioclase in NA 09 – 15 Garnetiferous schist (Bodø Group)

	Core	Core	Core	Core	Rim	Rim	Rim
SiO2	45.92	60.64	51.473	59.472	60.02	51.195	45.903
TiO2	0	0	0	0	0	0	0
Al2O3	33.464	24.844	30.9	25.628	25.175	30.535	33.252
Cr2O3	0.016	0.016	0.009	0.009	0	0	0
Fe203	0	0	0	0	0	0	0
FeO	0.027	0.094	0.019	0.124	0.091	0.039	0.062
MnO	0.032	0.008	0	0.04	0	0.004	0
MgO	0	0	0	0	0	0	0
CaO	17.999	6.864	14.157	7.735	6.776	13.655	17.638
Na2O	1.514	7.929	3.846	7.407	7.759	3.761	1.657
K2O	0.013	0.037	0.012	0.039	0.03	0.02	0.011
Total	98.989	100.436	100.419	100.456	99.855	99.211	98.525
			Cations based on 8 oxygen atoms				
Si	2.138	2.689	2.333	2.645	2.676	2.344	2.145
Ti	0	0	0	0	0	0	0
Al2	1.836	1.299	1.651	1.344	1.323	1.648	1.832
Cr	0.001	0.001	0	0	0	0	0
Fe3+	0.001	0	0	0	0	0	0.001
Fe2+	0	0.003	0.001	0.005	0.003	0.001	0.002
Mn	0.001	0	0	0.002	0	0	0
Mg	0	0	0	0	0	0	0
Ca	0.898	0.326	0.687	0.369	0.324	0.67	0.883
Na	0.137	0.682	0.338	0.639	0.671	0.334	0.15
K	0.001	0.002	0.001	0.002	0.002	0.001	0.001
Total	5.012	5.002	5.011	5.002	4.997	4.999	5.013

Appendix 1- Electron microprobe Analysis

Scapolite in NA 09 – 15 Garnetiferous schist (Bodø Group)

	Core	Core	Core	Rim	Rim	Rim
SiO2	45.426	45.323	45.541	45.834	44.822	45.284
TiO2	0	0	0.002	0	0.003	0
Al2O3	27.595	27.629	27.701	27.739	26.958	27.519
Cr2O3	0	0	0.006	0.05	0	0
Fe203	0	0	0	0	0	0
FeO	0.08	0.077	0.033	0.095	0.06	0.049
MnO	0	0.027	0.021	0.031	0.032	0.025
MgO	0	0	0	0	0	0
CaO	18.766	19.116	19.156	18.913	18.946	19.212
Na2O	2.929	2.89	3.001	3.033	3.102	2.999
K2O	0.01	0.018	0.016	0.007	0.019	0.016
Total	94.807	95.083	95.478	95.705	93.946	95.108
			Cations based on 24 oxygens atoms			
Si	6.998	6.967	6.963	6.993	6.961	6.95
Ti	0	0	0	0	0	0
Al2	5.012	5.007	4.993	4.989	4.936	4.979
Cr	0	0	0.001	0.006	0	0
Fe3+	0.005	0	0.005	0.005	0	0.005
Fe2+	0.01	0.01	0.004	0.012	0.008	0.006
Mn	0	0.004	0.003	0.004	0.004	0.003
Mg	0	0	0	0	0	0
Ca	3.098	3.148	3.138	3.092	3.153	3.16
Na	0.875	0.861	0.89	0.897	0.934	0.893
K	0.002	0.004	0.003	0.001	0.004	0.003
Total	16	16	16	16	16	16

Appendix 2 U – Pb data for Quarzitic metapsammite in Heggmovatn

	ppm				*Ratios*							*Discordance*		*Ages*					
Name	U	^{206}Pb	$^{206}Pb_c$(%)	206/204	$^{207}Pb_*/^{206}Pb$	1SE	$^{207}Pb_*/^{235}U$	1SE	$^{206}Pb_*/^{238}U$	1SE	Rho	Central(%)	Min. rim(%)	207/206	1σ	207/235	1σ	206/238	1σ
AA09-08-74	4	2	0.00E+00	575	0.08207	0.00075	2.18638	0.0457	0.19321	0.00363	0.9	-9.5	-5.4	1247	17	1177	15	1139	20
AA09-08-87	21	17.4	0.00E+00	6767	0.08127	0.00042	2.14029	0.01442	0.191	0.00084	0.650	-9	-7.1	1228	10	1162	5	1127	5
AA09-08-64	172	73.7	0.00E+00	18624	0.07695	0.00053	1.83606	0.03316	0.17305	0.00289	0.923	-8.8	-5.4	1120	13	1058	12	1029	16
AA09-08-78	96	46.5	0.00E+00	12508	0.0863	0.00052	2.52217	0.04499	0.21197	0.00356	0.941	-8.6	-6	1345	11	1278	13	1239	19
AA09-08-29	143	142.4	0.00E+00	44289	0.08258	0.0009	2.24657	0.06637	0.19731	0.00542	0.929	-8.5	-3.5	1259	20	1196	21	1161	29
AA09-08-91	61	64.4	0.00E+00	14399	0.09574	0.00063	3.27703	0.04766	0.24825	0.00323	0.893	-8.2	-5.7	1543	12	1476	11	1429	17
AA09-08-96	10	8.8	0.00E+00	8095	0.08334	0.00049	2.31746	0.01793	0.20169	0.001	0.643	-7.9	-5.9	1277	11	1218	5	1184	5
AA09-08-65	11	4.8	0.00E+00	1329	0.07916	0.00057	2.01439	0.03295	0.18457	0.00271	0.896	-7.8	-4.4	1176	14	1120	11	1092	15
AA09-08-62	157	67.4	0.00E+00	28631	0.07945	0.00043	2.03782	0.03208	0.18603	0.00275	0.940	-7.7	-5.1	1183	10	1128	11	1100	15
AA09-08-68	157	67.4	0.00E+00	28631	0.07945	0.00043	2.03782	0.03208	0.18603	0.00275	0.940	-7.7	-5.1	1183	10	1128	11	1100	15
AA09-08-84	16	16.2	0.00E+00	6745	0.09198	0.00048	2.99497	0.02084	0.23615	0.00109	0.663	-7.6	-5.9	1467	9	1406	5	1367	6
AA09-08-16	55	77.1	0.00E+00	16231	0.1066	0.00077	4.21706	0.09838	0.28692	0.00636	0.950	-7.5	-4.9	1742	13	1677	19	1626	32
AA09-08-3	112	103.6	0.00E+00	43258	0.07459	0.00065	1.70009	0.03736	0.1653	0.00334	0.919	-7.3	-2.7	1058	17	1009	14	986	18
AA09-08-34	15	20.9	0.00E+00	13599	0.1024	0.00081	3.87111	0.09593	0.27419	0.00644	0.948	-7.2	-4.1	1668	14	1608	20	1562	33
AA09-08-41	44	58.6	0.00E+00	19213	0.10026	0.00076	3.69087	0.09001	0.26699	0.00619	0.951	-7.1	-4.2	1629	13	1569	19	1525	31
AA09-08-50	18	23.7	0.00E+00	7635	0.0976	0.00088	3.47569	0.10117	0.25828	0.00715	0.951	-6.9	-3.4	1579	16	1522	23	1481	37
AA09-08-43	38	29.2	0.00E+00	8475	0.07317	0.0005	1.61424	0.03317	0.16001	0.0031	0.942	-6.5	-2.7	1019	14	976	13	957	17
AA09-08-15	45	63.4	0.00E+00	20054	0.10521	0.00075	4.15138	0.09525	0.28619	0.00624	0.951	-6.3	-3.6	1718	12	1664	19	1622	31
AA09-08-32	7	10.3	0.00E+00	3030	0.10725	0.00085	4.33273	0.10742	0.293	0.00688	0.947	-6.3	-3.3	1753	14	1700	20	1657	34
AA09-08-63	44	22.2	0.00E+00	9886	0.08657	0.00053	2.61009	0.04542	0.21867	0.00356	0.935	-6.2	-3.5	1351	11	1303	13	1275	19
AA09-08-106	59	66.1	0.00E+00	20821	0.0979	0.00046	3.53896	0.02302	0.26216	0.00119	0.699	-5.9	-4.5	1585	9	1536	5	1501	6
AA09-08-73	45	36.1	0.00E+00	9408	0.12121	0.00082	5.64825	0.11803	0.33795	0.00668	0.946	-5.7	-3.3	1974	12	1923	18	1877	32
AA09-08-85	19	19.6	0.00E+00	4094	0.09145	0.00042	3.01871	0.01906	0.2394	0.00104	0.689	-5.5	-4	1456	8	1412	5	1384	5
AA09-08-47	17	25.1	0.00E+00	6148	0.10803	0.00079	4.43983	0.10114	0.29808	0.00643	0.947	-5.4	-2.7	1766	13	1720	19	1682	32
AA09-08-55	35	23.8	0.00E+00	11074	0.09975	0.00069	3.72081	0.07226	0.27055	0.00491	0.934	-5.3	-2.5	1619	13	1576	16	1544	25
AA09-08-82	62	53.5	0.00E+00	37579	0.08178	0.00035	2.26882	0.01355	0.20122	0.00084	0.696	-5.1	-3.5	1240	8	1203	4	1182	4

AA09-08-92	53	63	0.00E+00	34775	0.10085	0.00045	3.83065	0.02481	0.2755	0.00129	0.72	-4.9	-3.5	1640	8	1599	5	1569	6
AA09-08-45	29	39.6	0.00E+00	12179	0.10091	0.00074	3.84579	0.09001	0.2764	0.00615	0.95	-4.7	-1.8	1641	13	1602	19	1573	31
AA09-08-46	89	126.6	0.00E+00	20584	0.1047	0.00077	4.17738	0.10048	0.28938	0.00663	0.952	-4.7	-1.9	1709	13	1670	20	1638	33
AA09-08-5	137	169.4	0.00E+00	39559	0.08064	0.0003	2.20015	0.02965	0.19788	0.00256	0.961	-4.4	-2.6	1213	7	1181	9	1164	14
AA09-08-104	216	261.4	0.00E+00	164657	0.10136	0.00046	3.90588	0.0261	0.27948	0.00137	0.736	-4.1	-2.7	1649	8	1615	5	1589	7
AA09-08-53	85	44.5	0.00E+00	11838	0.08609	0.00045	2.63087	0.04106	0.22163	0.00326	0.942	-4.1	-1.7	1340	10	1309	11	1290	17
AA09-08-57	56	38.5	0.00E+00	58945	0.10595	0.00068	4.31339	0.083	0.29527	0.00536	0.943	-4.1	-1.7	1731	11	1696	16	1668	27
AA09-08-81	56	36.5	0.00E+00	11211	0.10161	0.00067	3.92918	0.07609	0.28046	0.00511	0.94	-4.1	-1.5	1654	12	1620	16	1594	26
AA09-08-12	2	2.4	0.00E+00	1478	0.09047	0.00079	2.98866	0.07146	0.23959	0.00533	0.930	-3.9	-0.1	1435	16	1405	18	1385	28
AA09-08-42	35	51.4	0.00E+00	20677	0.10638	0.00082	4.364	0.11037	0.29752	0.00717	0.952	-3.9	-0.9	1738	14	1706	21	1679	36
AA09-08-98	21	25.4	0.00E+00	7976	0.10182	0.0005	3.95481	0.02653	0.28169	0.0013	0.685	-3.9	-2.4	1658	9	1625	5	1600	7
AA09-08-102	4	3.3	0.00E+00	963	0.07895	0.00055	2.08878	0.02284	0.19189	0.00162	0.774	-3.7	-0.6	1171	13	1145	8	1132	9
AA09-08-44	6	5.5	0.00E+00	2048	0.07938	0.00062	2.12199	0.04499	0.19388	0.00382	0.93	-3.6	.	1182	14	1156	15	1142	21
AA09-08-95	66	84.9	0.00E+00	48139	0.10571	0.00049	4.31781	0.02759	0.29625	0.00129	0.683	-3.5	-2.2	1727	8	1697	5	1673	6
AA09-08-56	15	9.6	0.00E+00	3873	0.10105	0.00069	3.90705	0.07086	0.28041	0.00471	0.925	-3.4	-0.7	1644	12	1615	15	1593	24
AA09-08-67	88	59	0.00E+00	86303	0.10204	0.00062	3.99458	0.0738	0.28391	0.00496	0.945	-3.4	-1.1	1662	10	1633	15	1611	25
AA09-08-79	150	95.7	0.00E+00	30799	0.09937	0.00061	3.76052	0.07117	0.27447	0.00491	0.946	-3.4	-0.9	1612	11	1584	15	1563	25
AA09-08-93	112	145.6	0.00E+00	42939	0.10619	0.00048	4.37023	0.0288	0.29847	0.00143	0.727	-3.4	-2	1735	8	1707	5	1684	7
AA09-08-101	5	3.4	0.00E+00	1544	0.07557	0.0006	1.84367	0.02017	0.17695	0.00134	0.694	-3.3	.	1084	15	1061	7	1050	7
AA09-08-108	44	58.4	0.00E+00	20552	0.10884	0.00053	4.62076	0.03141	0.30791	0.00147	0.701	-3.2	-1.7	1780	9	1753	6	1730	7
AA09-08-112	13	13.8	0.00E+00	5195	0.09046	0.00049	3.01316	0.02226	0.24159	0.00121	0.675	-3.1	-1.3	1435	10	1411	6	1395	6
AA09-08-30	26	22.6	0.00E+00	6520	0.07654	0.00052	1.92046	0.0389	0.18198	0.00347	0.943	-3.1	.	1109	13	1088	14	1078	19
AA09-08-4-	94	132.4	0.00E+00	41370	0.09176	0.00078	3.12911	0.06197	0.24731	0.00443	0.904	-2.9	.	1463	15	1440	15	1425	23
AA09-08-80	106	74.9	0.00E+00	78071	0.10639	0.00067	4.41301	0.08726	0.30083	0.00564	0.948	-2.8	-0.4	1738	12	1715	16	1695	28
AA09-08-99	56	73.9	0.00E+00	13445	0.10651	0.00049	4.426	0.02921	0.30138	0.00142	0.711	-2.8	-1.3	1741	8	1717	5	1698	7
AA09-08-33	12	9.7	0.00E+00	5357	0.07387	0.00053	1.73349	0.03642	0.1702	0.00336	0.939	-2.6	.	1038	15	1021	14	1013	19
AA09-08-89	21	21.7	0.00E+00	7686	0.0907	0.00046	3.0501	0.0203	0.24391	0.00105	0.647	-2.6	-0.9	1440	9	1420	5	1407	5
AA09-08-66	9	3.8	0.00E+00	1454	0.07561	0.00058	1.86704	0.0315	0.17908	0.00269	0.892	-2.3	.	1085	14	1069	11	1062	15
AA09-08-86	149	113.3	0.00E+00	31728	0.0753	0.00029	1.84264	0.00994	0.17748	0.00066	0.688	-2.3	-0.6	1076	7	1061	4	1053	4
AA09-08-88	4	5	0.00E+00	1573	0.10204	0.00074	4.05066	0.04614	0.28792	0.00253	0.772	-2.1	.	1662	13	1644	9	1631	13
AA09-08-14	77	70.1	0.00E+00	20158	0.07729	0.00049	2.00168	0.03893	0.18784	0.00345	0.945	-1.8	.	1129	12	1116	13	1110	19

AA09-08-105	210	254.2	0.00E+00	60520	0.09956	0.00044	3.84403	0.02587	0.28002	0.00141	0.748	-1.7	-0.2	1616	8	1602	5	1591	7
AA09-08-40	109	151.2	0.00E+00	36025	0.09952	0.00075	3.84195	0.09566	0.28	0.00665	0.953	-1.7	.	1615	14	1602	20	1591	33
AA09-08-107	29	32.3	0.00E+00	8662	0.0936	0.00045	3.32709	0.0222	0.25779	0.00119	0.69	-1.6	.	1500	9	1487	5	1479	6
AA09-08-111	27	32.9	0.00E+00	9874	0.10161	0.0005	4.03587	0.02917	0.28807	0.00152	0.729	-1.5	.	1654	8	1641	6	1632	8
AA09-08-27	43	55.8	0.00E+00	14696	0.09467	0.00063	3.42941	0.07246	0.26272	0.00527	0.949	-1.3	.	1522	11	1511	17	1504	27
AA09-08-7	114	170.1	0.00E+00	45610	0.10552	0.00074	4.40858	0.10134	0.30301	0.00663	0.952	-1.1	.	1723	12	1714	19	1706	33
AA09-08-60	69	41.9	0.00E+00	20854	0.09326	0.00056	3.32703	0.05886	0.25875	0.00431	0.942	-0.7	.	1493	11	1487	14	1483	22
AA09-08-1	48	89.2	0.00E+00	38952	0.10152	0.00023	4.06623	0.05566	0.29049	0.00392	0.986	-0.6	.	1652	4	1648	11	1644	20
AA09-08-97	73	89.6	0.00E+00	25670	0.09896	0.00044	3.84855	0.02403	0.28206	0.00124	0.702	-0.2	.	1605	8	1603	5	1602	6
AA09-08-11	13	11.2	0.00E+00	6124	0.07563	0.00051	1.92264	0.03769	0.18438	0.00339	0.938	0.6	.	1085	14	1089	13	1091	18
AA09-08-54	78	34.7	0.00E+00	10460	0.07614	0.00039	1.99062	0.0299	0.18961	0.00268	0.94	2	.	1099	10	1112	10	1119	15
AA09-08-90	136	102.5	0.00E+00	25615	0.07438	0.0003	1.81719	0.0097	0.17719	0.00063	0.668	.	.	1052	8	1052	3	1052	3